

CEMENTATION PROCESSES OF NATURALLY AGED
HAWAIIAN CALCAREROUS SANDS

A THESIS SUBMITTED TO THE GRADUATE DIVISION OF THE
UNIVERSITY OF HAWAI'I IN PARTIAL FULFILLMENT
OF THE REQUIREMENTS FOR THE DEGREE OF

MASTER OF SCIENCE

IN

CIVIL ENGINEERING

DECEMBER 2002

DISTRIBUTION STATEMENT A
Approved for Public Release
Distribution Unlimited

By
Thomas B. McLemore

Thesis Committee:

Peter Nicholson, Chairperson
Horst Brandes
Phillip Ooi

20030701 110

MAY-23-2003 13:05

DTIC-OC

703 767 9244

P. 02/02

**DEFENSE TECHNICAL INFORMATION CENTER
REQUEST FOR SCIENTIFIC AND TECHNICAL REPORTS**

Title

*CEMENTATION PROCESSES OF NATURALLY AGED
HAWAIIAN CALCAREOUS SANDS***1. Report Availability (Please check one box)**

- ☐ This report is available. Complete sections 2a - 2f
- ☐ This report is not available. Complete section 3.

**2a. Number of
Copies Forwarded****2b. Forwarding Date****2c. Distribution Statement (Please check ONE box)**

DoD Directive 5230.24, "Distribution Statements on Technical Documents," 18 Mar 87, contains seven distribution statements, as described briefly below. Technical documents **MUST** be assigned a distribution statement.

- ☒ DISTRIBUTION STATEMENT A: Approved for public release. Distribution is unlimited.
- ☐ DISTRIBUTION STATEMENT B: Distribution authorized to U.S. Government Agencies only.
- ☐ DISTRIBUTION STATEMENT C: Distribution authorized to U.S. Government Agencies and their contractors.
- ☐ DISTRIBUTION STATEMENT D: Distribution authorized to U.S. Department of Defense (DoD) and U.S. DoD contractors only.
- ☐ DISTRIBUTION STATEMENT E: Distribution authorized to U.S. Department of Defense (DoD) components only.
- ☐ DISTRIBUTION STATEMENT F: Further dissemination only as directed by the controlling DoD office indicated below or by higher authority.
- ☐ DISTRIBUTION STATEMENT X: Distribution authorized to U.S. Government agencies and private individuals or enterprises eligible to obtain export-controlled technical data in accordance with DoD Directive 5230.25, Withholding of Unclassified Technical Data from Public Disclosure, 6 Nov 84.

2d. Reason For the Above Distribution Statement (in accordance with DoD Directive 5230.24)**2e. Controlling Office****2f. Date of Distribution Statement
Determination****3. This report is NOT forwarded for the following reasons. (Please check appropriate box)**

- ☐ It was previously forwarded to DTIC on _____ (date) and the AD number is _____
- ☐ It will be published at a later date. Enter approximate date if known. _____
- ☐ In accordance with the provisions of DoD Directive 3200.12, the requested document is not supplied because:

Print or Type Name

LITA MOSQUEDA

Signature**Telephone**

DSN 756-3605 comm: (831)-656-3605

(For DTIC Use Only)

AQ Number 403-09-2241

We certify that we have read this thesis and that, in our opinion, it is satisfactory in scope and quality as a thesis for the Master of Science in Civil Engineering.

THESIS COMMITTEE



Peter G. Nicholson, Chairperson



Horst Brandes



Phillip Ooi

AQU03-09-2241

ABSTRACT

Researchers have studied cementation of calcareous sands for decades. While cementation increases static and cyclic strengths, it also reduces skin friction on piles. Cementation of sands in their own environment varies widely with many different factors. Obtaining undisturbed samples can be difficult and costly, and laboratory reproduction of samples has become an accepted method for testing calcareous materials.

The focus of this research is on understanding the processes and effects of early cementation in calcareous sand. Understanding of these processes will allow researchers the ability to better estimate light cementation effects for various types of calcareous sands. The project compared results of cyclic and static triaxial tests, cone penetrometer tests, and Scanning Electron Microscope (SEM) photographs to show the differences between two distinctly varied calcareous sands at similar densities and aged for relatively short periods of time.

“Natural aging” was the baseline used for this project. All samples were saturated with distilled water and aged under a confining pressure of one atmosphere. Although not truly representative of the “natural” environment, it provides a relative baseline of how calcareous sands react in the absence of any additional cementing agent.

The results of the project bring about many conclusions, as well as raising additional questions. The SEM pictures provide critical information to the project. The photographs provide a visual sense of the bonds caused from the cementation and give a visual picture of the mechanisms causing increases in static and cyclic strength. The

SEM photos show two distinctly different types of bonding between the two types of sands investigated, and generally show an increase in bonding as aging time is increased. Data from all laboratory tests also show related strength increases, which can be attributed to the increase in cementation shown in the SEM photographs.

TABLE OF CONTENTS

| | |
|--|------|
| ABSTRACT..... | iii |
| LIST OF TABLES | vii |
| LIST OF FIGURES..... | viii |
| LIST OF ABBREVIATIONS..... | xii |
| CHAPTER 1 – INTRODUCTION..... | 1 |
| CHAPTER 2 – SCOPE AND OBJECTIVE..... | 4 |
| CHAPTER 3 – ENGINEERING PROPERTIES OF CALCAREOUS SOILS..... | 7 |
| 3.1 Geology of Hawaii..... | 7 |
| 3.2 Properties of Calcareous Soils..... | 8 |
| 3.2.1 Origin and Geology of Calcareous Soils..... | 8 |
| 3.2.2 Mechanical Properties of Calcareous Soils..... | 10 |
| 3.2.2.1 Cementation..... | 10 |
| 3.2.2.2 Grain Crushing..... | 12 |
| 3.2.2.3 Grain Angularity and Porosity..... | 12 |
| 3.3 Soils Tested..... | 13 |
| 3.4 Index Properties..... | 14 |
| CHAPTER 4 – TRIAXIAL TESTING..... | 18 |
| 4.1 Setup of Specimens..... | 18 |
| 4.2 Static Triaxial Behavior..... | 19 |
| 4.2.1 Waikiki Static Results..... | 20 |
| 4.2.2 Ewa Static Results..... | 21 |
| 4.3 Liquefaction Theory..... | 22 |
| 4.4 Cyclic Triaxial Behavior..... | 25 |
| CHAPTER 5 – CONE PENETROMETER TESTING..... | 57 |
| 5.1 Laboratory CPT Testing Behavior..... | 57 |
| 5.2 Specimen Preparation..... | 59 |
| 5.3 CPT Results for Waikiki Sand..... | 60 |
| 5.4 CPT Results for Ewa Sand..... | 62 |

| | |
|---|----|
| CHAPTER 6 – SCANNING ELECTRON MICROSCOPE IMAGING..... | 72 |
| 6.1 Specimen Preparation..... | 72 |
| 6.2 Waikiki Sand Imaging..... | 74 |
| 6.3 Ewa Sand Imaging..... | 76 |
| CHAPTER 7 – SUMMARY AND CONCLUSIONS..... | 92 |
| 7.1 Conclusions..... | 92 |
| 7.2 Future Research..... | 95 |
| 7.3 Summary..... | 97 |
| REFERENCES..... | 99 |

LIST OF TABLES

| <u>Table</u> | <u>Page</u> |
|--|--------------------|
| 1. Index Properties of Various Calcareous Soils..... | 15 |
| 2. Index Properties for Ewa and Waikiki Sands..... | 15 |
| 3. Ewa Max Density Results..... | 16 |
| 4. Waikiki Max Density Results..... | 16 |
| 5. Summary of Test Results..... | 92 |
| 6. Summary of Static Test Results..... | 93 |

LIST OF FIGURES

| <u>Figure</u> | <u>Page</u> |
|---|--------------------|
| 3.1 – Waikiki and Ewa Gradations Chart..... | 17 |
| 4.1 – Aging Station..... | 28 |
| 4.2 – Triaxial Setup..... | 29 |
| 4.3 – Comparison of Unaged Results of Waikiki Sand..... | 30 |
| 4.4 – Mohr’s Circles for Waikiki Sand..... | 31 |
| 4.5 – Comparison of Results for Cemented Waikiki Sand..... | 32 |
| 4.6 – 30-Day Waikiki Sand Stress Path Diagram..... | 33 |
| 4.7 – 60-Day Waikiki Sand Stress Path Diagram | 34 |
| 4.8 – Comparison of Unaged Results of Ewa Sand..... | 35 |
| 4.9 – Mohr’s Circles for Unaged Ewa Sand..... | 36 |
| 4.10 – 30-Day Ewa Sand Stress Path Diagram..... | 37 |
| 4.11 – 60-Day Ewa Sand Stress Path Diagram..... | 38 |
| 4.12 – Comparison of Results for Cemented Ewa Sand..... | 39 |
| 4.13 – CSR Graph for Waikiki Sand at 50% Relative Density..... | 40 |
| 4.14 – Waikiki Unaged Cyclic Test with CSR of 0.3..... | 41 |
| 4.15 – Waikiki Unaged Cyclic Test with CSR of 0.295..... | 42 |
| 4.16 – Waikiki 30-Day Cyclic Test with CSR of 0.32..... | 43 |
| 4.17 – Waikiki 60-Day Cyclic Test with CSR of 0.325..... | 44 |
| 4.18 – Waikiki 60-Day Cyclic Test with CSR of 0.3375..... | 45 |
| 4.19 – Waikikj increase in cycles to failure with increased aging | 46 |

| | |
|--|----|
| 4.20 – CSR Graph for Waikiki Sand at 50% Relative Density | 47 |
| 4.21 – Ewa Unaged Cyclic Test with CSR of 0.35..... | 48 |
| 4.22 – Ewa Unaged Cyclic Test with CSR of 0.33..... | 49 |
| 4.23 – Ewa Unaged Cyclic Test with CSR of 0.34..... | 50 |
| 4.24 – Ewa 30-Day Cyclic Test with CSR of 0.395..... | 51 |
| 4.25 – Ewa 30-Day Cyclic Test with CSR of 0.42..... | 52 |
| 4.26 – Ewa 60-Day Cyclic Test with CSR of 0.40..... | 53 |
| 4.27 – Ewa 60-Day Cyclic Test with CSR of 0.43..... | 54 |
| 4.28 – Ewa 60-Day Cyclic Test with CSR of 0.43..... | 55 |
| 4.29 – Ewa increase in cycles to failure with increased aging..... | 56 |
| 5.1 – Schematic of 6 Millimeter Mini-Cone Used in Testing..... | 63 |
| 5.2 – Mini-CPT Results in Unaged Waikiki Sand..... | 64 |
| 5.3 – Mini-CPT Results in 30-Day Cemented Waikiki Sand..... | 65 |
| 5.4 – Mini-CPT Results in 60-Day Cemented Waikiki Sand..... | 66 |
| 5.5 – Comparison of Mini-CPT Results in Waikiki Sand..... | 67 |
| 5.6 – Mini-CPT Results in Unaged Ewa Sand..... | 68 |
| 5.7 – Mini-CPT Results in 30-Day Cemented Ewa Sand..... | 69 |
| 5.8 – Mini-CPT Results in 60-Day Cemented Ewa Sand..... | 70 |
| 5.9 – Comparison of Mini-CPT Results in Ewa Sand..... | 71 |
| 6.1 – Waikiki sand image at 200x magnification..... | 79 |
| 6.2 – Waikiki unaged sand at 100x magnification..... | 79 |
| 6.3 – Waikiki unaged sand at 200x magnification..... | 80 |

| | |
|--|----|
| 6.4 – Waikiki sand with cement filled pores at 500x magnification..... | 80 |
| 6.5 – Waikiki 30-Day cemented sand at 200x magnification..... | 81 |
| 6.6 – Waikiki 30-Day cemented sand at 500x magnification..... | 81 |
| 6.7 – Waikiki 30-Day cemented sand at 1000x magnification..... | 82 |
| 6.8 – Waikiki 30-Day cemented sand at 500x magnification..... | 82 |
| 6.9 – Waikiki 60-Day cemented sand at 500x magnification..... | 83 |
| 6.10 – Waikiki 60-Day cemented sand at 1000x magnification..... | 83 |
| 6.11 – Waikiki 60-Day cemented sand at 1000x magnification..... | 84 |
| 6.12 – Ewa unaged sand at 500x magnification..... | 84 |
| 6.13 – Ewa unaged sand at 500x magnification..... | 85 |
| 6.14 – Ewa unaged sand at 1000x magnification..... | 85 |
| 6.15 – Ewa 30-Day cemented sand at 200x magnification..... | 86 |
| 6-16 – Ewa 30-Day cemented sand at 500x magnification..... | 86 |
| 6-17 – Ewa 30 Day cemented sand at 1000x magnification..... | 87 |
| 6-18 – Ewa 30-Day cemented sand at 2000x magnification..... | 87 |
| 6-19 – Ewa 30 Day cemented sand at 2000x magnification..... | 88 |
| 6-20 – Ewa 30-Day cemented sand at 200x magnification..... | 88 |
| 6-21 – Ewa 30-Day cemented sand at 500x magnification..... | 89 |
| 6-22 – Ewa 30-Day cemented sand at 1000x magnification..... | 89 |
| 6-23 – Ewa 30-Day cemented sand at 2000x magnification..... | 90 |

| | |
|---|----|
| 6-24 – Ewa 60-Day cemented sand at 1000x magnification..... | 90 |
| 6-25 – Ewa 60-Day cemented sand at 2000x magnification..... | 91 |

LIST OF ABBREVIATIONS

| | |
|------|--------------------------------------|
| CSR | Cyclic Stress Ratio |
| CPT | Cone Penetrometer Test |
| SEM | Scanning Electron Microscope |
| CIPS | Calcite In Situ Precipitation System |

CHAPTER 1 - INTRODUCTION

In recent decades, research has become a necessity to help engineers better understand the differences between calcareous and terrigenous soils. Calcareous soils come in a wide range of shapes and sizes and are predominantly found underwater, which is where they are formed. Very fine particles of calcareous material, often referred to as oozes, and calcareous sands cover a large area of the ocean sea floor. As expanding geological searches for oil, communication needs and defense applications call for geotechnical knowledge of the sea floor, a better understanding of these materials has become necessary. Calcareous materials are also found on land in regions where tropical or subtropical marine conditions have existed in some point in time.

Calcareous soils are not ideal materials for foundations. They are often unsuitable because of a high susceptibility towards grain crushing and because in situ and laboratory tests are often unconservative when estimating the soil's strength characteristics. Noticeable differences in soil characteristics and mechanical properties are the cause for the lower strengths. Most past research in calcareous materials has involved the study of pile capacity, because piles are most often used in offshore and near shore platforms for the oil and gas industry (McClelland, 1988).

As oil and gas deposits were found throughout tropical regions, platforms were designed for drilling and recovery of this valuable natural resource. Problems with pile capacities arose in 1968 when a pile embedded itself 50 feet under its own weight in Iranian waters. It came to rest on very well cemented rock, which provided suitable end bearing capacity for the pile. Because the pile capacity was acceptable, the lack of

strength in the upper layers was essentially ignored. Later construction attempts in calcareous material would not be so lucky (McClelland, 1988).

Tests performed on calcareous material in the Bass Strait off the coast of Australia produced capacities that were only 20% of the design value computed for silica and quartz sands. At the Northwest Shelf of Australia, the largest platform ever designed to be founded in calcareous soils was constructed. Despite numerous in situ and laboratory tests, pile capacities failed to meet minimum safety values for the platform. Extensive and costly remediation was attempted on the platform foundation, which spawned extensive research into determining a new set of design parameters for calcareous materials (McClelland, 1988).

Calcareous sands are individually unique. Sands in Australia are different from those in the Middle East and are again different from those found in Hawaii. New classification systems have been proposed to distinguish calcareous sediments from terrigenous soils (Beringen, 1982). Comparative testing has been conducted for a variety of different engineering properties including static and cyclic strength, in situ testing methods, and pile performance. Variations in cementation have been noted in many reports, and attempts to collect undisturbed samples were taken from numerous locations in order to test the performance of cemented versus uncemented strength (Clough, 1989; Huang, 1991; Morioka, 1999). Due to the significant expense of collecting undisturbed samples, research has also been conducted to develop new ways to replicate the cementitious effects of calcareous sands in the laboratory (Joer, 1997).

Portland Cement is one of the most widely used artificial additives used to cement sands together in a short period of time. Experiments using several different percentages

of cement have been used to try to replicate the cementitious bonds formed between grains. Although some studies have shown comparative results between in situ cementation and artificially cemented samples, other test results show the need to further examine the cementation process and mechanisms in order to best replicate the properties of in situ conditions (Clough, 1989; Huang, 1991; Joer, 1997, Morioka, 1999).

CHAPTER 2 - OBJECTIVE AND SCOPE

Extensive research has been conducted on calcareous soils to eliminate some of the many unknowns associated with them. Grain characteristics such as angularity, chemical composition, crushability, void ratio, cementation and others have been analyzed as variables to test static strength, liquefaction resistance, soil moduli, and pile capacity and have been the focus of many research reports. These test results have been compared to in situ tests to see how well they actually model conditions outside the laboratory. Testing has been performed on various types of calcareous soils all over the world, and these results have been compared to the tests of other terrigenous and calcareous material. This study looks specifically at cementation and its effects on engineering properties of calcareous sands.

Several methods have been used in artificially constructing variably cemented specimens in the lab (Rad, 1982; Rad, 1986; Currie, 1988; Clough, 1989; Poulos, 1989; Huang, 1991; Joer, 1997; Ismail, 1998; Morioka, 1999). Methods of artificial cementation include the use of gypsum, Portland cement, epoxies and the newly developed proprietary Calcite In Situ Precipitation System (CIPS) to cement calcareous soil together. Various triaxial, mini-cone and other laboratory tests have shown similarities and differences between artificial and undisturbed cemented samples. The similarities include increases to static strength, cone tip resistance, and liquefaction resistance, while at the same time, problems have been found with artificially cemented sands increasing the fines and not exemplifying the behavior of calcareous sands after cement bonds are broken. This project focuses on the cementation process and studies the relationships of naturally aged, lightly cemented carbonate sand. This work will

provide a baseline for future work in understanding the properties and mechanisms of naturally cemented samples, and may aid in construction of more representative artificially cemented specimens.

Research has shown that aged calcareous sands have higher values of strength, cone tip resistance, and resistance to liquefaction than non-aged sands (Beringen, 1982; Flynn, 1997; Morioka, 1999; Joer, 1997). Morioka questioned the cementation effects of the carbonate sand when naturally aged specimens did not experience a similar increase in static strength that an artificially cemented specimen experienced. Lee (1982) and Morioka (1999) concluded that it was difficult to determine whether cementation was the sole reason behind the strength increase in their tested specimens, or if mechanical factors such as grain crushing and resulting densification controlled the strength increase.

Naturally aging calcareous sands involved saturating laboratory prepared specimens with distilled water and leaving them under pressure for a predetermined time. The elimination of calcite, cement, or any other cementing agent allows us to see how the carbonate grains react to each other in an environment where no cementing agent is available. Semple (1988) suggests that particle sharing may occur between carbonate grains that are in contact with one another, but lack a cementing agent. These bonds and the strength curves they produce will be analyzed and can be compared with future research using various other methods of artificial and natural aging.

The objective of this report was to analyze the effects of cementation on naturally aged specimens of two different native Hawaiian carbonate sands. Although full cementation into rock formations takes thousands of years to accomplish, light cementation on and between particles is evident after several days. The Scanning

Electron Microscope (SEM) was also used in this project to study the cementation processes in the sands chosen for this research. This portion of the project was considered vital to the report because it verifies cementation is occurring and it shows how the bonds are formed. Details on the SEM, specimen preparation, and photographs are discussed in Chapter 6.

The scope of the project included index property testing, static and cyclic triaxial testing, lab cone penetrometer testing, and finally SEM photography to show differences in the aging process and effects on engineering strengths. Index property tests were performed on the soils to characterize each of the soils and to provide a baseline for specimen preparation. A total of eleven triaxial tests, consolidated undrained (CU) static and cyclic, and three cone penetrometer tests were performed on each specimen. Tests were performed on each specimen for aging at one, 30 and 60 days to show differences in cementation effects over time. CU tests were performed at different confining pressures to determine strength parameters of each material. These results were then correlated to grain characteristics of both sands. Finally, conclusions and an outline for future research are provided.

CHAPTER 3 ENGINEERING PROPERTIES OF CALCAREOUS SOILS

3.1 GEOLOGY OF HAWAII/OAHU

The Hawaiian Islands consist of eight islands formed from a series of underwater volcanoes whose lava flows crested above the ocean surface. They stretch out approximately 1600 miles from northwest to southeast from $18^{\circ} 54'$ to $28^{\circ} 15'$ North latitude to $171^{\circ} 75'$ to $154^{\circ} 40'$ West longitude. Oahu, the third largest of the islands, was formed from the merging of two of these flows forming the Waianae and the Koolau Ranges. The Waianae Range was formed first, became extinct, and was followed by the Koolau Range. Lava flows from the Koolau Range overlapped those of the Waianae Range, creating what is known as the Schofield Plateau. The coastal plains are located to the north and south of this plateau and on the coastline. These lower level areas are rich in calcareous material due to periods of fluctuating sea levels (Stearns, 1966).

Geology has shown evidence of sea level fluctuations throughout time. During the Pleistocene period, approximately one million years ago, water levels had a fluctuation of about 3000 feet, from roughly -1800 to 1200 feet above present mean sea level. During this time, marine sediments were deposited in the coastal plains which were underwater during periods of higher sea level. Coral reef structures, limestone and carbonate sands have been found throughout the island of Oahu on and between various layers of volcanic rock (Stearns, 1966).

An extensive coral reef system was formed around the island of Oahu. Coral reefs are formed in tropical, clear waters in depths generally less than 200 feet. Hawaii is considered to be at the northern end of the tropical region, and therefore reefs are formed slower than in places such as Midway which are closer to the equator. Coral is

formed from the deposition of skeletal deposits of microscopic plants and animals. These particles are bonded together through cementation by the secretion of lime from coralline algae and nullipores. This cementation process takes hundreds to thousands of years to produce coral from 6 to 20 feet high.

3.2 PROPERTIES OF CALCAREOUS SOILS

Past experiences and research has shown many differences between calcareous and terrigenous sands. Origin and location of the different types of soils is one of the largest differences. Terrigenous soils originate from land and are formed by mechanical processes, while calcareous soils are formed in the ocean by biological, chemical, and mechanical processes. Factors such as cementation, high susceptibility to grain crushing, more angular particles and high void ratios are among the many differences between the two types of soils (Semple, 1988; Poulos, 1989).

3.2.1 ORIGIN AND GEOLOGY OF CALCAREOUS SOILS

Most calcareous sediments are formed from the deposition of dead marine organisms on the sea floor. When they die, smaller particles dissolve into the sea water. They start to precipitate when in higher concentrations and in warmer water temperatures. Calcareous material is found mainly in tropical waters in areas such as Hawaii, the Persian Gulf, the Gulf of Mexico, and Northern Australia. Although deposited in the ocean, calcareous soil may also be found on land due to sea level fluctuations. The key element of all calcareous material is calcium carbonate (CaCO_3). Calcareous sediments can be formed biologically, mechanically and chemically and consist of four major types: skeletal, detrital, pellets and coated grains (McClelland, 1988).

Skeletal material consists of shells from marine animals deposited on the sea floor. These shells are mainly hollow, increasing the porosity, void ratio, and the susceptibility to crushing. Skeletal deposition is a biological process from sources such as mollusks, foraminifers, coccoliths, and several other various types of small marine animals (McClelland, 1988).

Detrital material is formed from a mechanical process. Fragments of pre-existing limestone or other carbonate rock break off into smaller pieces, which become weathered into smaller, more angular particles. Pellets are very small, structurally weak grains of micrite or lime mud mainly considered to be fecal in origin. They are formed from gastropods and worms ingesting carbonate mud on the sea floor. After digestion, they secrete small pellets of carbonate material making the new grain of calcareous sand. Calcareous sands are formed chemically when the water is over saturated with CaCO_3 . The CaCO_3 precipitates and attaches itself to other CaCO_3 precipitants forming oval grains (McClelland, 1988; Fookes, 1988; Price, 1988).

Carbonate content is one of the largest factors in classification of calcareous soils. Carbonate content relates to the materials hardness, cementation, and grain crushing. Carbonate content has even been found to control the behavior of the soil. If a fine soil has greater than 40 percent carbonate content, it will have granular behavior. If it is less than 40 percent, it will exhibit cohesive behavior (Poulos, 1989).

The principle mineral in calcareous material is CaCO_3 . This could either be referred to as calcite or aragonite, based on the chemical structure of the crystal. The difference between the two is that calcite has an orthorhombic structure, while aragonite has a rhombohedral structure (McClelland, 1988). Dolomites ($\text{CaMg}(\text{CO}_3)_2$) are another

form of carbonate material. Over time and in the presence of magnesium, a diagenesis can occur turning CaCO_3 into dolomite.

3.2.2 MECHANICAL PROPERTIES OF CALCAREOUS SOILS

There are many mechanical properties that make calcareous soils unique. Research became more intense on calcareous soils because it displayed less bearing capacity and skin friction than terrigenous sands and from tests done in the laboratory. Some of the differences between calcareous sands and other sands include cementation, grain crushing, angularity of particles, porosity, and stiffness. Many of these properties can be correlated to one another. An example of this is the high void ratio and higher porosity of calcareous sands which makes them more susceptible to grain crushing than silica sands.

3.2.2.1 CEMENTATION

Cementation is the focus of this report. Carbonate sands vary in levels of cementation from no cementation to a fully cemented rock like structure with virtually all voids filled. Cementation occurs in confined saturated calcareous material. Cementation can occur between or within intraparticle voids of calcareous soils. When cementation occurs, the intraparticle voids begin to be filled with cement, reducing the compressibility of the soil and also reducing the permeability. Variation in cementation makes it difficult to predict soil properties of a site due to a large number of variables controlling the rate of cementation (Semple, 1988).

Light cementation can occur along a soil/water interface where calcite and aragonite can precipitate on the sediments. Several factors play a large part in the degree of cementation. The amount and deposition of the cementing agent, and whether it is calcite, aragonite, or dolomite, are large factors (Coop, 1993). Without the cementing

agent, particles bond together with particles they are in contact with through a material exchange. In the material exchange, particle sharing between grains occurs at contact points (Semple, 1988). Pictures of this can be seen in Chapter 6. Environmental conditions are also a factor in the cementation process. Water temperature is important because it affects the rate of precipitation or cementing agent and most of the organisms that make up carbonate soils live in warmer waters. Low turbidity is important because the precipitants must have a chance to bond with the sediments on the sea floor. Because of all these factors, it is quite common to get varying degrees of cementation below and beside a tested area (Semple, 1988).

Although cementation generally adds to the peak strength of the soil, once the cementitious bonds are broken, the residual strength is similar to that of the uncemented soil. Cementation provides a cohesive strength to the sand by bonding particles together. Cohesion can be defined as an attachment or bonding of two or more soil particles increasing the shear strength of a soil, and although it normally applies to fine grained soils, it also applies to cemented calcareous sands. Laboratory tests on calcareous soils tend to be under conservative because cementation causes soil arching after shear induced volume reduction, reducing the lateral effective pressures (McClelland, 1988; Semple, 1988; Poulos 1989).

Cementation can also decrease the liquefaction potential of a site. Liquefaction occurs in loose, saturated, granular material. Cementation increases the density of the soil and also provides a bonding agent between the grains to give it some cohesive strength, therefore making it more difficult to reduce the effective stress to zero without breaking the bonds.

3.2.2.2 GRAIN CRUSHING

Calcareous soils display tendencies of grain crushing when subjected to heavy loads. The grains are more susceptible to crushing than quartz sands because of their lower hardness and skeletal structure. Carbonate is much softer than quartz and has a Moh's hardness of two to three compared to quartz sands' seven (Fahey, 1993). Grains are also more susceptible to crushing because some grains have large intraparticle void ratios. This is usually due to hollow skeletal particles. Partially cemented sands are also susceptible to grain crushing because they become more brittle when they become cemented.

Grain crushing is a function of many different variables. Grain crushing increases with an increase in mean effective stress and with shear stress application. Particle shape, size, hardness and intra particle void ratio all play key roles in the amount of grain crushing. As the shape, size and angularity of the particles increase, grain crushing increases. As expected, the softer the particle, the easier it is to crush.

3.2.2.3 GRAIN ANGULARITY AND POROSITY

Calcareous sediments tend to be more angular than terrigenous sands. Angularity of the particles also increases the void ratio and therefore the porosity. Friction angles of calcareous soils are directly affected by the angularity of the particles. Semple (1988) found that the mineral calcium carbonate had a friction angle ranging from 31°-34°, where quartz's friction angle was only 23°. Cementation effects for angular particles were also found to be stronger than those of with more rounded grains (Clough, 1988). One of the main reasons for the angularity is the origin of the particles. Skeletal remains and detrital material can both lead to very angular particles.

Calcareous sediments tend to be more porous than terrigenous sands. Particles not only have high porosity because of their angularity, but they also have intraparticle voids where water can pass through. As cementation increases, porosity decreases, both between grains and in intraparticle voids.

3.3 SOILS TESTED

The soils tested for this project are both native to Hawaii. ASTM D2488-90 and the Munsell Soil Color Chart were used as guidelines to describe characteristics of the sand. The first soil, referred to as the Waikiki sand for the remainder of the report, is a fine grained, poorly graded sand containing detrital pieces of coral and some flat white shells. It is classified as grey to light grey with some light brownish grey. It was dredged off the coast of Waikiki and neighboring an area designated a high potential for liquefaction by a study conducted by Harding Lawson Associates (Flynn, 1997). The grains vary from very angular to rounded with the coral pieces ranging from very angular to subangular.

The sand has strong reactivity with hydrochloric acid (HCl) and carbonate content was found to be 96%. The sand is very brittle and crushes easily with very light hammer taps. The gradation of the sand is shown in Figure 3.1. The index properties for the soil are contained in the next section.

The second soil, referred to as the Ewa sand for the remainder of the report, was a medium size, poorly graded sand from the Ewa plains area on the southern portion of Oahu and is also shown in Figure 3.1. It is quarry sand obtained from the Barber's Point Quarry and represents typical sands from the coastal plains of Oahu. Particles vary in shape from angular to subrounded and spherical to elongated. The majority of the particles are spherical and subangular. It is classified as predominantly very pale brown

with some rare white and grey pieces. This sand exhibits brittle behavior as well, crushing with light hammer taps. It is also strongly reactive to HCL, but not as reactive as the Waikiki sand, and test results show a carbonate content of 94%

3.4 INDEX PROPERTIES

Calcareous soils have shown dissimilar characteristics to terrigenous soils in mechanical and index properties. In general, calcareous soils have higher void ratios and specific gravities (G_s) than their terrigenous counterparts. Higher void ratios also account for the higher porosity found in calcareous sediments. The void ratios are higher because of grain shape, angularity and intraparticle void ratios.

Morioka (1999) created a table, reproduced here as Table 1, displaying some index properties of calcareous soils from various regions. As can be seen from the Table, specific gravities are higher for calcareous sands given that the G_s for calcite, dolomite and aragonite are 2.72, 2.85, and 2.95, respectively while terrigenous G_s are in the range of 2.5-2.7. Index properties conducted on the two soils tested for this project are listed in Table 2.

Minimum densities were conducted by wet and dry pluviation and graduated cylinder tipping. In both cases, graduated cylinder tipping gave the lowest density. Maximum densities were performed using a variation of the modified Japanese method using a six inch California Bearing Ratio mold and a ten pound weight. Sand was placed into the mold at five equivalent lifts. At each lift, the weight was put on top of the sand and the side of the mold was hit with a rubber mallet. The mallet blows occurred on all

| Soil | CaCO ₃ (%) | G _s | e _{min} | e _{max} | LL (%) | PL (%) |
|--------------------|--------------------------|----------------|------------------|------------------|-----------|-----------|
| North Africa Coast | 40-70 | 2.75 | 2.06 | 2.72 | 55-80 | 30-40 |
| Venezuelan Basin | 56-75 | 2.65 to 2.69 | --- | --- | 66-70 | 42-57 |
| Halibut | 66-79 | 2.72 | 0.79 | 1.09 | --- | --- |
| Kingfish B | 84 | 2.75 | 1.12 | 1.48 | --- | --- |
| Bass Strait | --- | 2.73 | --- | --- | --- | --- |
| Guam | 90 | 2.8 | 1.12 | 1.36 | --- | --- |
| Florida | 92 | 2.84 | 1.06 | 1.44 | --- | --- |
| Panama Basin | --- | 2.58 to 2.71 | 2.38 | 3.27 | | |
| West Coast, India | >85 | 2.79 to 2.81 | 0.77 | 1.39 | --- | --- |
| Lakshdweep Island | >85 | 2.78 | 0.8 | 1.2 | --- | --- |
| Dog's Bay | 85-90 | 2.75 | 0.98 | 1.83 | --- | --- |
| Ballyconeely | 90-95 | 2.72 | 1.67 | 1.98 | --- | --- |
| Bombay Mixture | 70-80 | 2.8 | 0.75 | 1.07 | --- | --- |
| Barry's Beach | 89 | 2.73 | --- | --- | --- | --- |
| North Rankine | 91 | 2.73 | --- | --- | --- | --- |

Data compiled by Morioka (1999).

Table 1 - Index Properties of Various Calcareous Soils

| Soil | G _s | ρ _{max} (g/cm ³) | ρ _{min} (g/cm ³) | ρ _{50%} (g/cm ³) | e _{max} | e _{min} |
|----------------|----------------|--|---------------------------------------|--|------------------|------------------|
| Ewa | 2.70 | 1.74 | 1.28 | 1.51 | 1.11 | 0.55 |
| Waikiki | 2.80 | 1.28 | 1.00 | 1.14 | 1.8 | 1.19 |

Table 2 – Index Properties for Ewa and Waikiki Sands

| Blows | Density |
|-------|---------|
| 0 | 1.685 |
| 50 | 1.722 |
| 100 | 1.715 |
| 150 | 1.743 |
| 200 | 1.742 |
| 250 | 1.739 |

| Blows | Density |
|-------|---------|
| 0 | 1.247 |
| 50 | 1.251 |
| 100 | 1.267 |
| 150 | 1.280 |
| 200 | 1.280 |
| 250 | 1.279 |

Table 3 - Ewa Max.Density Test

Table 4 – Waikiki Max. Density Test 100,

sides of the mold and were roughly equivalent in magnitude. Five tests were done on each soil, each with a different number of blows. Blow counts used for testing were 50, 150, 200, and 250. Tables 3 and 4 show the maximum density leveled off after 150 blows.

Initial void ratio may be one of the most important aspects controlling the behavior of calcareous sands. Semple (1988) found that calcareous sands have similar behavior to terrigenous sands when they are both tested at similar initial void ratios. Fahey (1993) points out that Semple's work was contradicted by Le Tirant, who said that not all calcareous soils display similar behavior at constant void ratios. Detrital material displays behavior more similar to silica sands at similar initial void ratios but biogenic material does not.

Void ratios vary from 0.8 -1.4 for calcareous sediments while terrigenous material generally has a void ratio range of only 0.4 -0.9 (Morioka, 1999). In the weathering process, sands become less angular. The angularity is important because it makes it more difficult to fit the particles closer together when grains are more angular. The intraparticle voids created from the skeletal remains increase the already large voids created from the highly angular particles. The larger void ratio of calcareous sands

causes many difficulties. Intraparticle voids add to the softness and susceptibility to grain crushing because the particles lack the structure to support themselves under higher stresses. The high void ratio also restricts an increases in lateral earth pressures during higher stresses because volume reduction takes place instead of dilation.

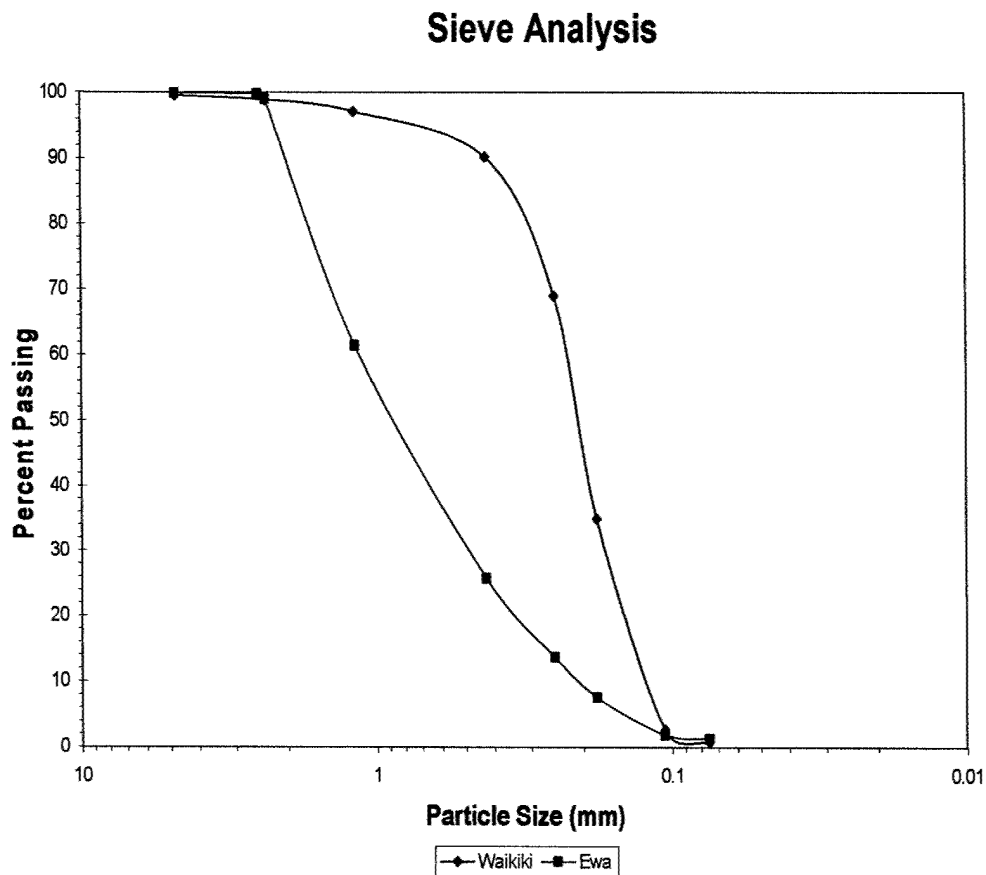


Figure 3.1 – Waikiki and Ewa Gradation Chart

CHAPTER 4 TRIAXIAL TESTING

4.1 SETUP OF SPECIMENS

In setting up triaxial specimens, it was important to maintain a constant density throughout each specimen. Initial maximum and minimum void ratios were obtained through testing and used to determine relative densities for each specimen. The specimens were air dried before they were built. Molds with a diameter of 70 mm and cell membranes with a thickness of 0.305 mm were used in the construction of each specimen. To prevent losing a specimen due to leakage of a membrane, two membranes were used for all triaxial tests.

The specimens were constructed in a series of seven lifts. A replica specimen was used with plastic spacers representing the soil to give the proper compaction height of each lift (layer) of the sand. The weight of each lift was varied by one percent to account for the repeated compaction throughout the construction of the specimen so that the bottom three lifts were -3%, -2%, and -1% and the top three lifts were 1%, 2%, and 3% of the required density to achieve the desired relative density. The middle lift contained the optimal density for the specimen. Approximately 5 mm of distilled water was added to the sand after dry weight measurements were taken to “fluff” or bulk up the sand and ease compaction.

Once a specimen was constructed, vacuum was used to pull deaired distilled water through the specimen. With a vacuum on the specimen, the mold was removed; the second membrane was placed on the specimen and secured with a second set of O-rings. Measurements were taken to obtain volume, enabling calculation of a density for each specimen. Pi-tape was used to measure the diameter at the top, middle and bottom

of the specimen. An average of the three diameters minus the thickness of both sides of the two membranes was used when entering specimen data in the triaxial program. After securing the top cap and rod and filling the cell with water, a constant effective pressure of 100 kPa was placed on the specimen. Specimens were aged for one, thirty, and sixty days at the aging station under 100 kPa of pressure. Figures 4.1 and 4.2 show the aging station and the triaxial set up, respectively, used for this research program.

After aging of the specimen was complete, back pressure saturation was used to obtain a B-value of greater than 0.93. 0.93 was chosen as the acceptable minimum from prior research done on the Waikiki sand by Flynn and Nicholson (1997). Three days was typically taken to back pressure saturate each specimen to avoid using high back pressures for saturation. This time was considered part of the aging process. One day specimens actually varied from two to four days depending on how long it took to obtain an acceptable B-value.

4.2 STATIC TRIAXIAL BEHAVIOR

Both consolidated drained (CD) and consolidated undrained (CU) static triaxial tests have previously been performed on both artificial and naturally cemented specimens. CD tests have shown that friction angles of cemented calcareous sands are about the same as those for uncemented sand and depend on the density of the material and the angularity of the particles. Cementation does add cohesive strength to the soil which increases the overall strength. The strength increases as cement increases its bonding between grains and fills up the pores inside grains (Rad, 1982). Research has shown that laboratory tests are unconservative because of the effects of grain crushing and cementation (Semple 1988; Poulos, 1989; McClelland, 1988).

The effects of cementation should increase the strength of the soil. Although the soil gets stronger, the sand also becomes more brittle until the cementitious bonds are broken, and the soils exhibit a ductile behavior similar to that of uncemented grains (Clough, 1989). Failures can be gradual by one bond breaking followed by others, or very rapid failure of all the bonds. Very rapid failure is more common. Cemented bonds generally break between 1-5 MPa (Poulos, 1989).

4.2.1 WAIKIKI STATIC TESTING RESULTS

Strain controlled, undrained triaxial (CU) tests were run on the Waikiki soil to determine strength characteristics of the sand. Unaged specimens were tested at confining stresses of 50, 100, and 150 kPa. Test results from the unaged specimens are shown in Figure 4.3. Mohr circles were drawn to determine a friction angle for the unaged specimens and are shown in Figure 4.4. The tangent line of the Mohr circles produces a friction angle of approximately 39.4° with a cohesive value of 15 kPa. This small cohesive value shows the specimen starting to cement in the few days used to back pressure the specimens.

Rad (1982) determined that cemented specimens possess the same friction angles as uncemented ones, but added strength is due to a cohesive bond formed by cementation between the grains of sand. Therefore, only limited numbers of tests were necessary on aged specimens to provide an accurate depiction of the result of increased strength due to cementation. Stress paths were analyzed to validate the continuity of frictional values and determine the increase in cohesion.

The results of aged Waikiki sands were tested and can be seen in Figure 4.5. An increase in strength is apparent as the aging time increases. The strength can be attributed to the increase in cementation, which increased the cohesion from 15 kPa to

97.4 kPa in the 30-day specimens and to 125.5 kPa in the 60-day specimens as shown in Figures 4.6 and 4.7. The friction angle for the 30-day specimen was shown to be almost exactly the same as the unaged specimen, while the friction angle of the 60-day specimen was slightly less, but still relatively close.

4.2.2 EWA STATIC TESTING RESULTS

CU tests were also used for the Ewa sand. Unaged specimens were tested at confining pressures of 50, 100, and 150 kPa and the results can be seen in Figure 4.8. Figure 4.9 shows the Mohr's circles drawn from data for each test. The unaged Ewa sand has a friction angle of 36.9° and cohesion of 15 kPa.

Naturally aged Ewa specimens showed evidence of very light cementation as seen in Figure 4.10. Mohr's circles for the aged sands are found in Figures 4.11 and 4.12. Part of the increase in strength on the 60-day specimen can be attributed to a somewhat higher density. The 1-day and 30-day specimens were exactly the same density, resulting in an increase in cohesion of 27.5 kPa to 31.3 kPa. The 60-day aged specimen cohesion increased slightly to just 37.5 kPa, although part of the increase could be due to the higher density as previously mentioned. The friction angles for all Ewa samples were 36.9° , despite the density of the 60-day specimen being measured about 5% higher than the other two specimens. It is unclear how much of the increase can be attributed to cementation. Cementation appears to cause only slight increase in strength. The lower cementation effects may be the result of the type of cementation formed between the grains. This type of bond will be discussed in Chapter 6.

Pore pressures for the cemented sands can be seen in Figure 4.3 and 4.5. The increase in aging resulted in generation of lower pore pressures. Lower pore pressures

result in higher effective stresses. The lower pore pressures also resemble an increase in confining pressure or density. The increase in strength and the lower pore pressures support Rad's (1982) theory that cementation has the same results as increasing the density.

Although the Ewa sand was coarser than the Waikiki sand, strength values were lower. Friction angles and cohesive values were both lower for unaged and aged specimens of Ewa sand. The higher strength in the specimens of the Waikiki sand can be attributed to the greater angularity of that sand. As angularity increases, both friction angles and strength increase. The angularity of the Waikiki sand can be seen in pictures in Chapter 6.

4.3 LIQUEFACTION THEORY

The study of liquefaction is essential in seismic areas. Liquefaction is defined as the reduction of effective shear strength to zero or close to zero, caused by the increase in pore water pressure in a cyclically loaded soil. Liquefaction is the result of vibrating or shaking loose, saturated, granular material. The shaking causes a tendency for loose samples to densify, causing the pore water pressures in undrained specimens to increase. The effective stress will then decrease, until the pore water pressure equals or closely equals the effective stress of the soil. The effective stress of the sand then becomes zero using Equation 4.1. The result is that the liquefied sand has no shear strength, resulting in often catastrophic loss of bearing capacity, large settlements and lateral deformation causing damage to structures above and around the site. One good thing that results from liquefaction is that the liquefied area generally becomes denser, and therefore less susceptible to future occurrences of liquefaction (Seed, 1982).

$$\sigma' = \sigma - u \quad (4.1)$$

Liquefaction can be reduced several ways. Looking again at Equation 4.1, if you remove the pore water pressure, 'u', then the effective stress will be equal to the drained strength of the sand. Another way to eliminate the possibility of liquefaction is to increase the density of the sample. When the cyclic loads are applied, a dense sample will tend to dilate, and the pore pressures will decrease. Equation 4.2 demonstrates that a soil's shear strength comes from both its frictional and cohesive components. A material may still have some shear strength remaining after cyclic loading because it will only lose the frictional strength component from Equation 4.2. Although cohesive bonds add strength to soil, some cohesive soils have been shown to liquefy in cases where the clay fraction is less than twenty percent and the plasticity index is less than or equal to 13 (Perlea, 2000).

$$\tau = c + \sigma \tan(\phi) \quad (4.2)$$

Laboratory analysis of liquefaction was performed in this study by use of the cyclic triaxial test. Analysis of liquefaction can be done by determining a Cyclic Stress Ratio, or CSR, for each sand tested. CSR is defined as the maximum shear stress of the soil divided by the effective confining stress or one half the deviator stress over the effective confining stress. These relationships are shown in Equation 4.3

$$CSR = \frac{\sigma_d}{2\sigma'} = \frac{\tau}{\sigma'} \quad (4.3)$$

The analysis can be used to obtain CSR graphs like that shown in Figure 4.13. Seed and Idriss (1982) also developed Table 3 to relate earthquake magnitudes to a number of

| <u>EQ Magnitude</u> | <u>Cycles</u> |
|----------------------------|----------------------|
| 5.25 | 2-3 |
| 6 | 5 |
| 6.75 | 10 |
| 7.5 | 15 |
| 8.5 | 26 |

Table 3: Table relating cyclic cycles at failure to earthquake magnitude (after Seed and Idriss (1982))

cycles to failure for the cyclic triaxial compression test. From the results of cyclic triaxial tests, a CSR graph similar to Figure 4.13 can be made for a sample at different densities. Table 3 can be used to pick out the CSR for the design earthquake. Equation 4.4 calculates the average shear stress of a site. 65 percent of the maximum shear stress is a good estimate for the average uniform shear stress τ_{av} . The maximum ground

$$\tau_{av} = 0.65 * \frac{\gamma h}{g} * a_{max} * r_d \quad (4.4)$$

Where: τ_{av} = Average Shear Stress

γ = Unit Weight of the soil

h = depth

g = acceleration due to gravity

a_{max} = maximum ground surface acceleration

r_d = stress reduction coefficient

surface acceleration can be obtained from accelerograph information from past seismic events. This value divided by the confining stress at each depth gives you the field CSR

value. A factor of safety against liquefaction can be developed by comparing CSR values from laboratory triaxial tests and the field CSR by Equation 4.5 where C_r is 0.57 for a K_0 value of 0.4 and 0.9 to 1 for a K_0 value of 1.

$$FS = \frac{C_r(CSR_{triax})}{CSR_{Field}} \quad (4.5)$$

4.4 CYCLIC TRIAXIAL BEHAVIOR

Cyclic tests results for the Waikiki sands and the results can be seen in Figures 4.14-4.18. Tests were terminated when axial strain of the specimen had reached 10%. Based on these results, CSR curves were constructed for 50% relative density to determine susceptibility to liquefaction. These curves can be seen in Figure 4.13. Morioka (1999) showed that cyclic resistance to liquefaction was greater in unaged calcareous sands than in terrigenous sands at the same density. That study also found that pore pressures have more relaxation between cycles than terrigenous sands.

The CSR curves of Figure 4.13 show the increase in liquefaction resistance with increase in aging. Figure 4.19 shows a distinct difference in strain rate for specimens of different ages. It takes approximately three cycles to go from one to ten percent strain for unaged Waikiki sand. For the 30-day cemented sand, it doubles to six cycles and triples to nine cycles for the 60-day naturally aged sands. The figures all represent failures at roughly the same number of cycles.

CSR curves and test results on the Ewa sand can be seen in Figures 4.20-4.28. The Ewa sand shows an increase in liquefaction resistance similar to the Waikiki sand. The Ewa sand does have a much higher resistance to liquefaction than the Waikiki sand. The Ewa sand showed no sign of static strength increase with aging, although the cyclic resistance is very similar to that of the Waikiki sand. It is possible the bond between these grains may be strong enough to withstand pore pressures, but not strong enough to withstand a static loading.

The trend of increased number of cycles from 1-10% strain was also apparent in the Ewa sand and can be seen in Figure 4.29. The Ewa sand responded similarly to the Waikiki sand in failure from 1-10% strain, with approximately twice the number of cycles to failure from unaged to 30-day aging and triple from unaged to 60-day aging.

Pore pressures in both sands show large reductions between cycles. Even at failure, the pore pressure ratios reduce to at least 40% in Figure 4.26 and sometimes below 20% seen in Figures 4.25, 4.27 and 4.28. Figures 4.21-4.24 show pore pressures start to have a double peak per cycle at ratios of about 75%. This corresponds to an axial strain of about one percent in all tests, and shows signs of the onset of failure of the specimen. This shows that the pore pressures may only need to equal approximately 75% of the normal stress in order to show effects of liquefaction.

The effects of cementation are evident in both sands. Both sands show a large increase in liquefaction resistance from 1-day to 30-day specimens. What is very noticeable is the difference in liquefaction resistance between the 1-day and 30-day and the 30-day and 60-day Ewa CSR curves in Figure 4.20. After the large increase in resistance from 1 to 30 days, there is only a minimal additional increase between 30 and

60-day curves. This could mean that most of the bonding occurs early in the aging period. The Waikiki sand shows an increase from the 30-day to 60-day specimens that is similar to that from the 1-day to 30-day, but it should be noted that the increase from the 1-day to the 60-day is lower than the increase from just the 1-day to the 30-day for the Ewa sand from Figure 4.13.

The angularity of the finer Waikiki sand probably caused the lower liquefaction resistance between the two sands. The bonding for both types of soils showed an increase in cyclic strength. For a depth of 20 feet and a maximum acceleration of 0.1g, the factor of safety for liquefaction increases approximately 17% from unaged to 60-day aged Ewa sand. With the same criteria, the Waikiki sand increased its factor of safety approximately 9%, although factors of safety are well below 1.0 all specimens of the Waikiki sand.

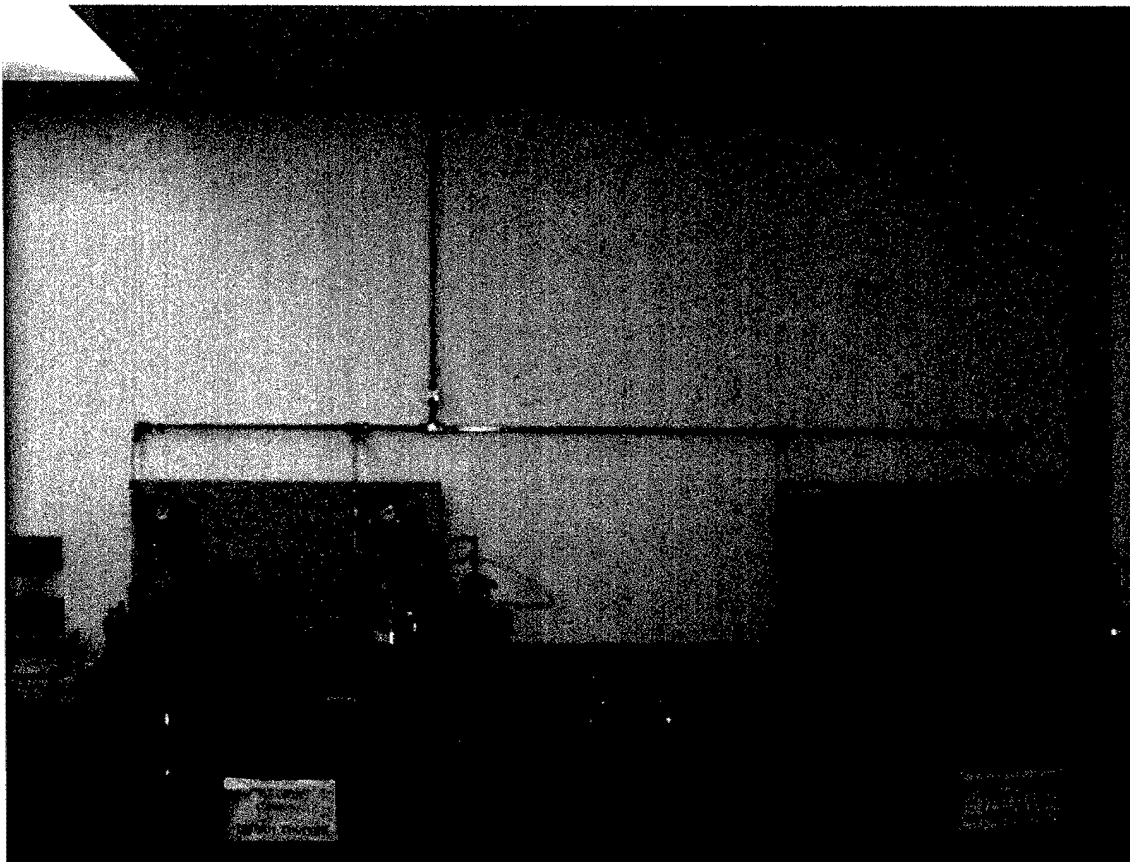


Figure 4.1 – Picture of Aging Station. Note: Silver topped cells are the modified triaxial cell used for the mini-cone tests.

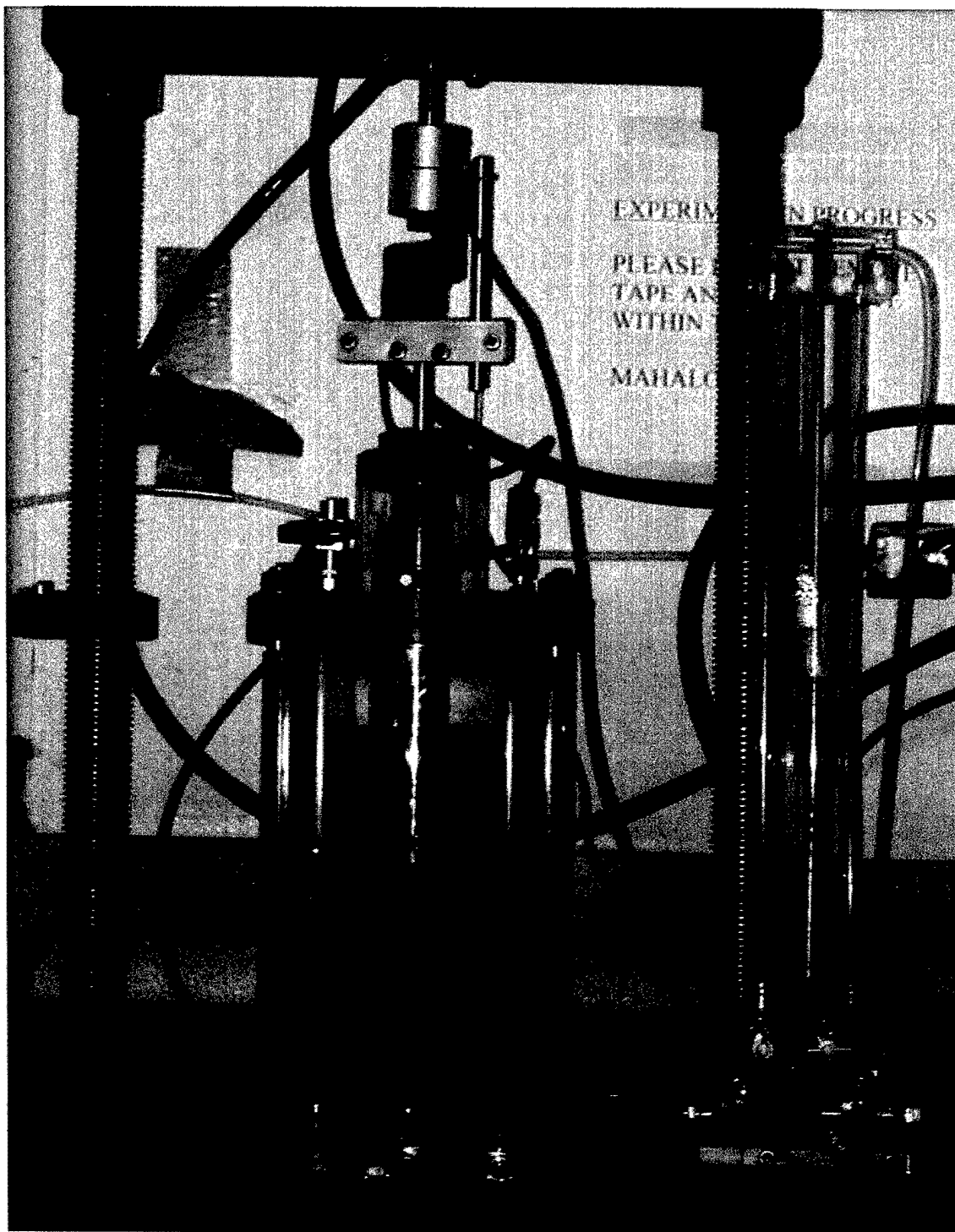
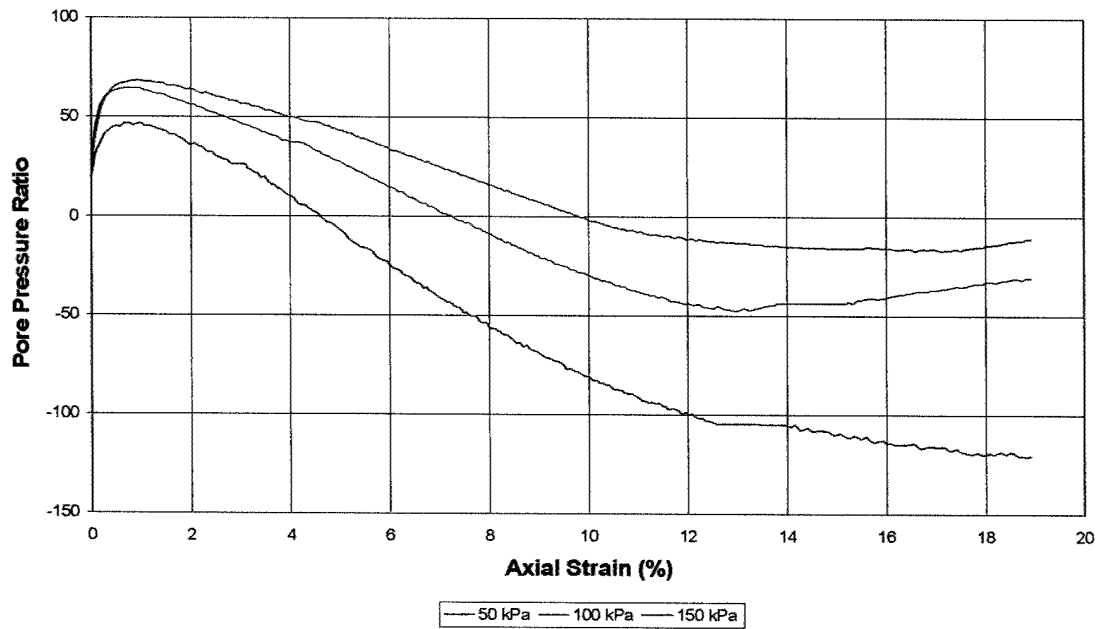


Figure 4.2 – Triaxial Set up

Waikiki Unaged Sand



Waikiki Unaged Sand

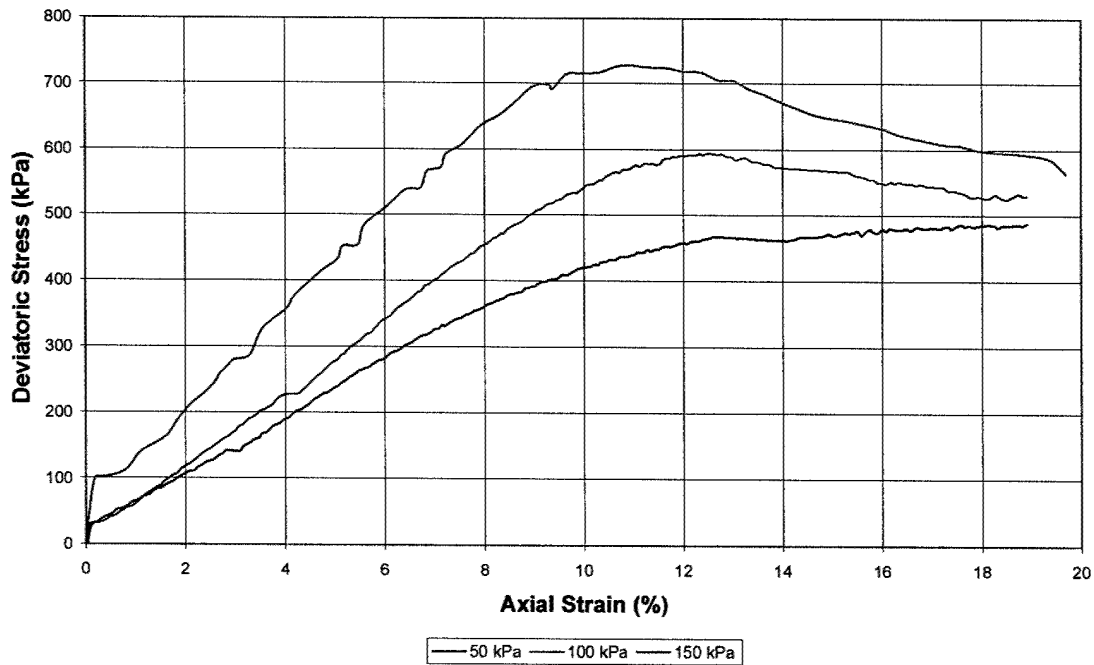


Figure 4.3 – Comparison of Unaged Results of Waikiki Sand

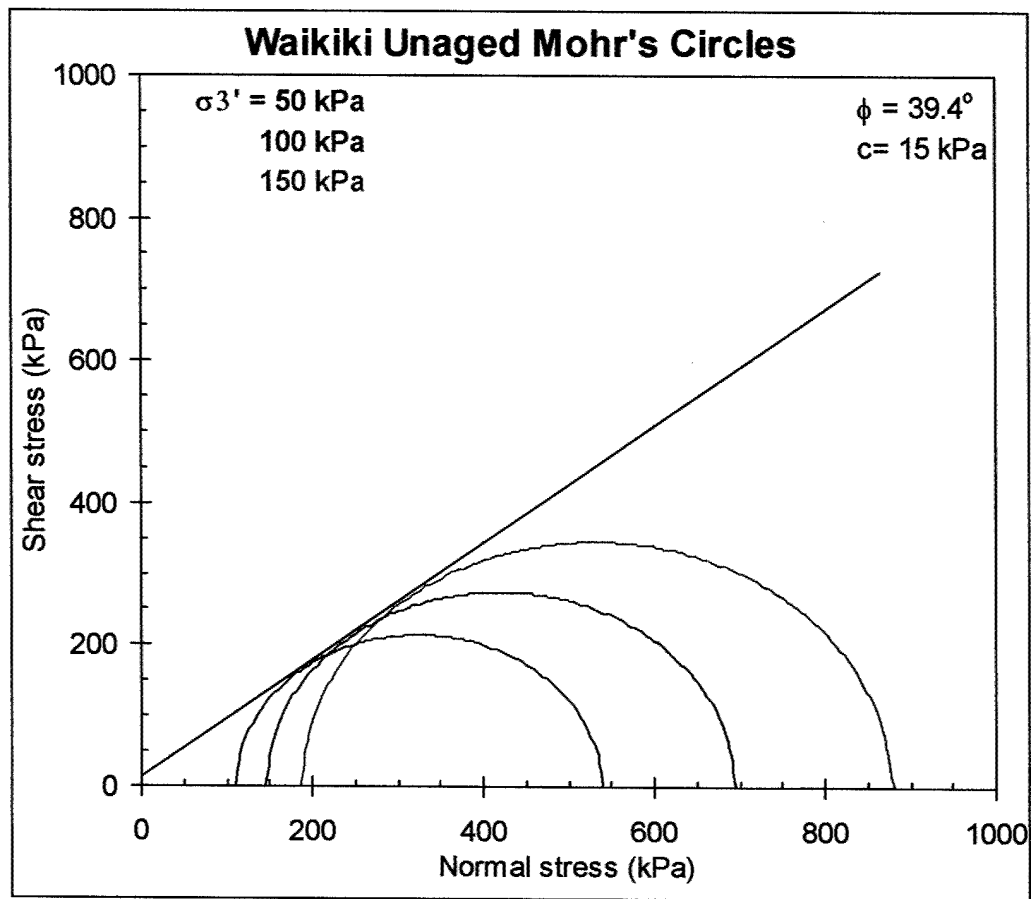
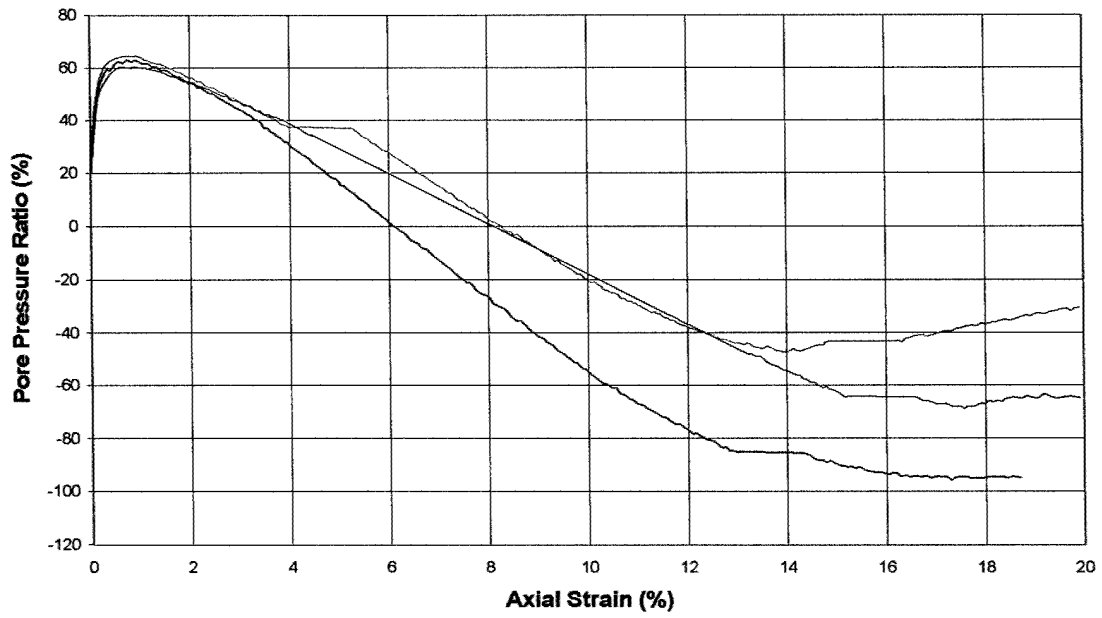


Figure 4.4 – Mohr's Circles for Unaged Waikiki Sand

Pore Pressure



Cementation Effects

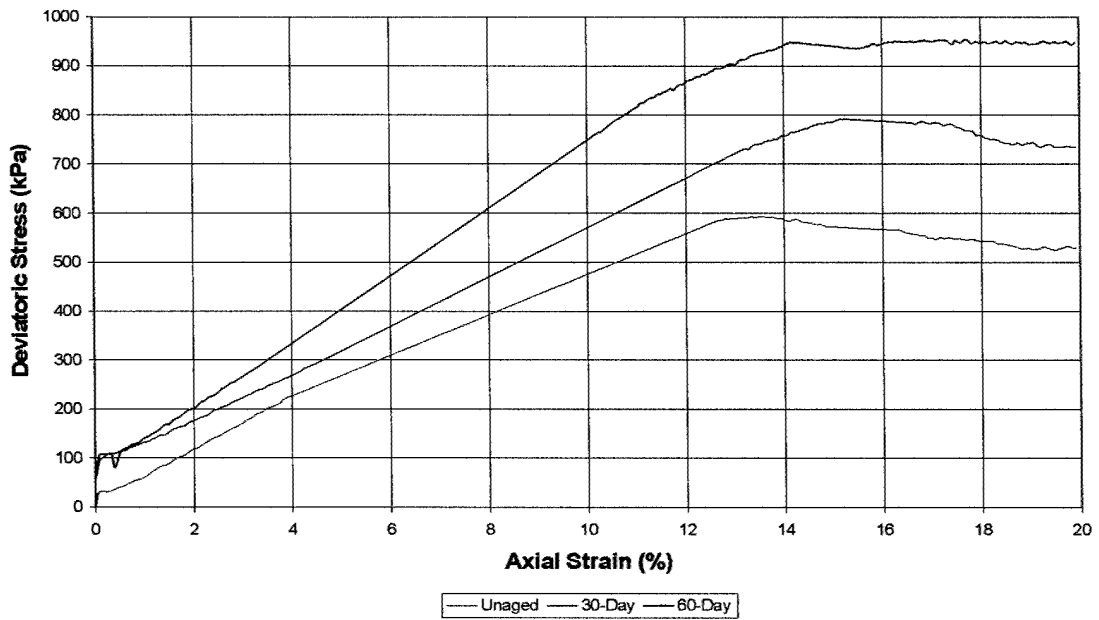


Figure 4.5 – Comparison of Results for Waikiki Cemented Sands

Waikiki 30-Day Stress Path

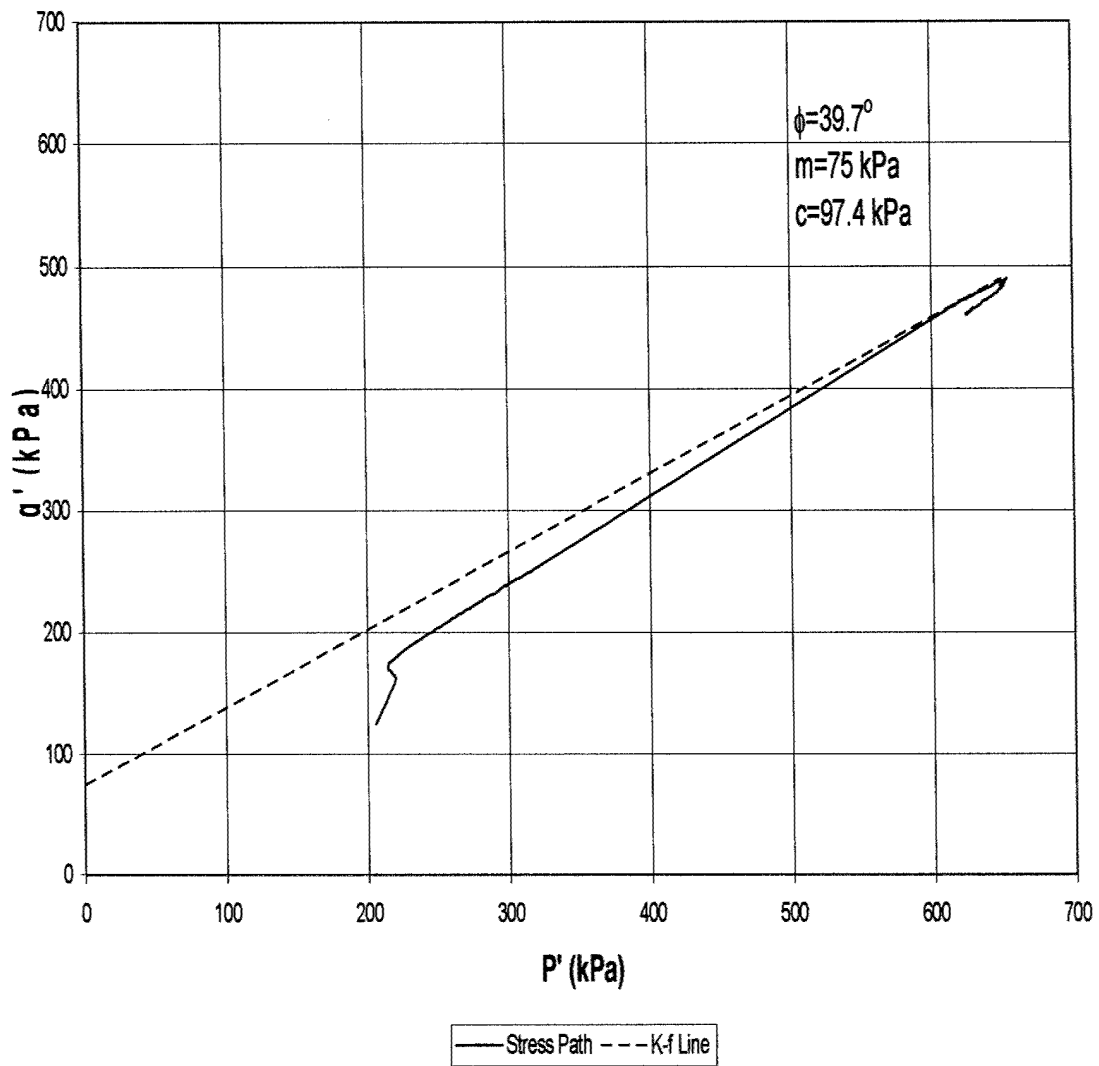


Figure 4.6 –30-Day Waikiki Cemented Sand Stress Path Diagram

Waikiki 60-Day Stress Path

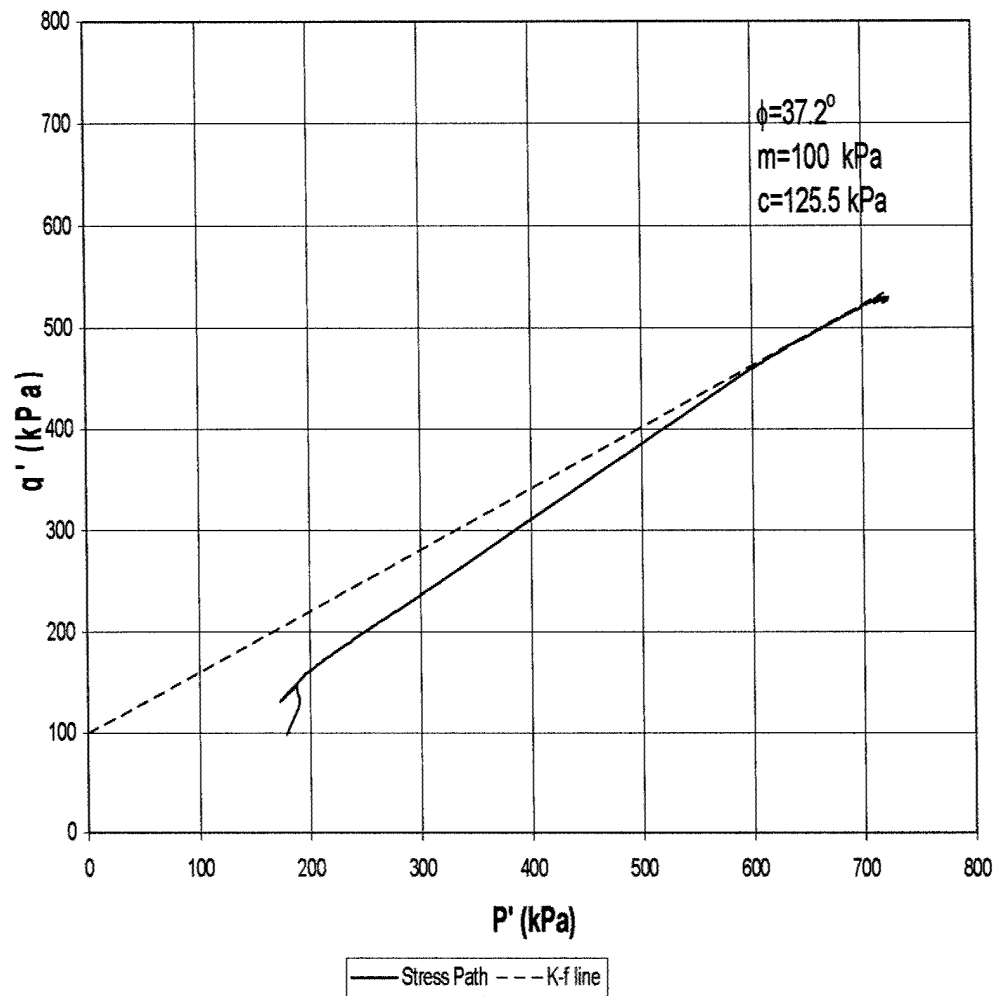
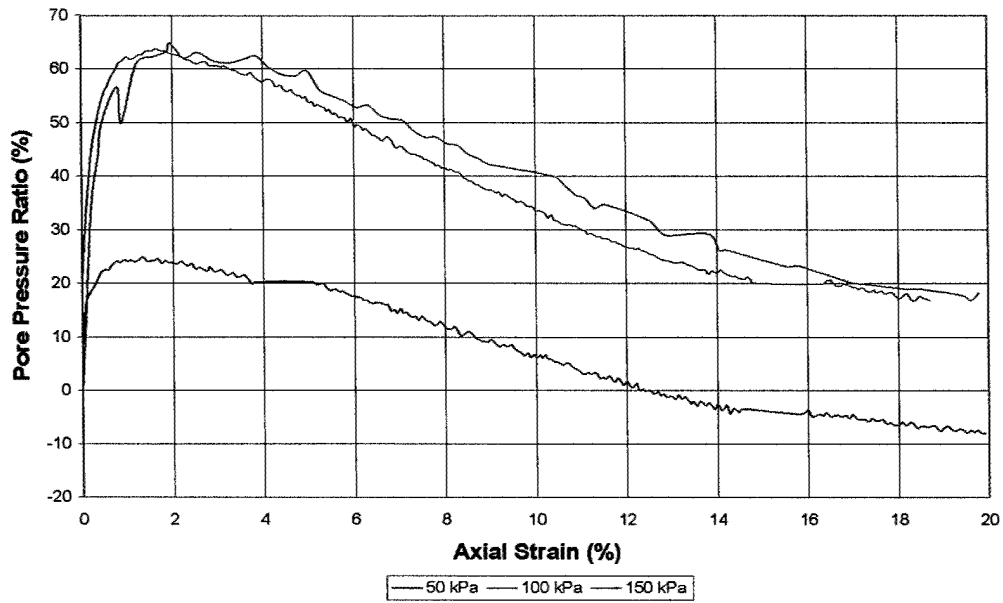


Figure 4.7 – 60-Day Waikiki Cemented Sand Stress Path Diagram

Unaged Ewa Sand



Unaged Ewa Sand

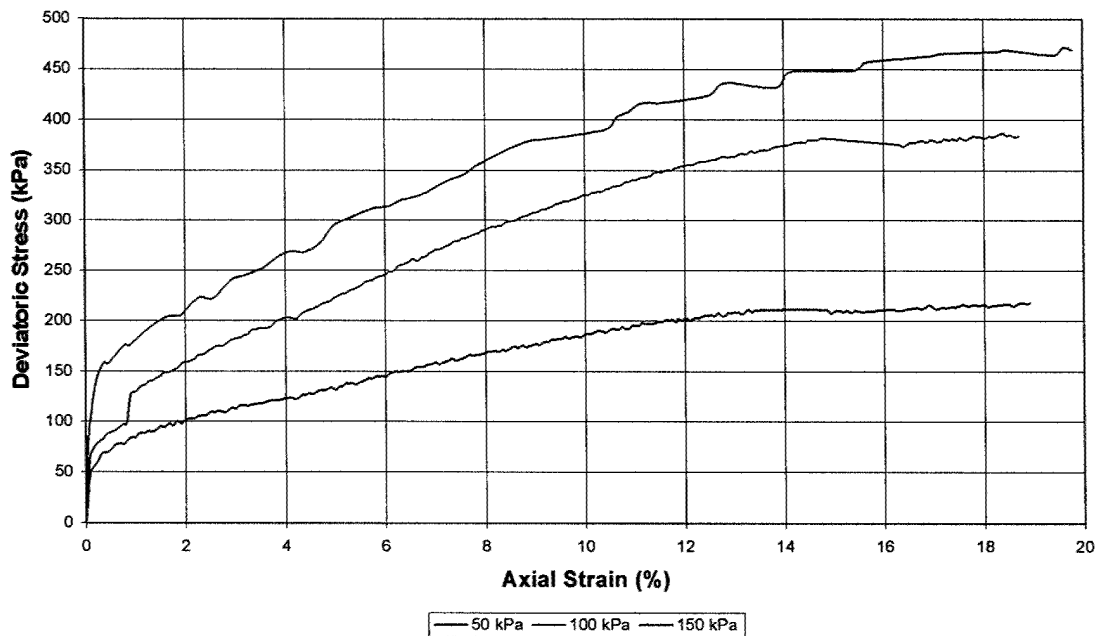


Figure 4.8 – Comparison of Unaged Results of Ewa Sand

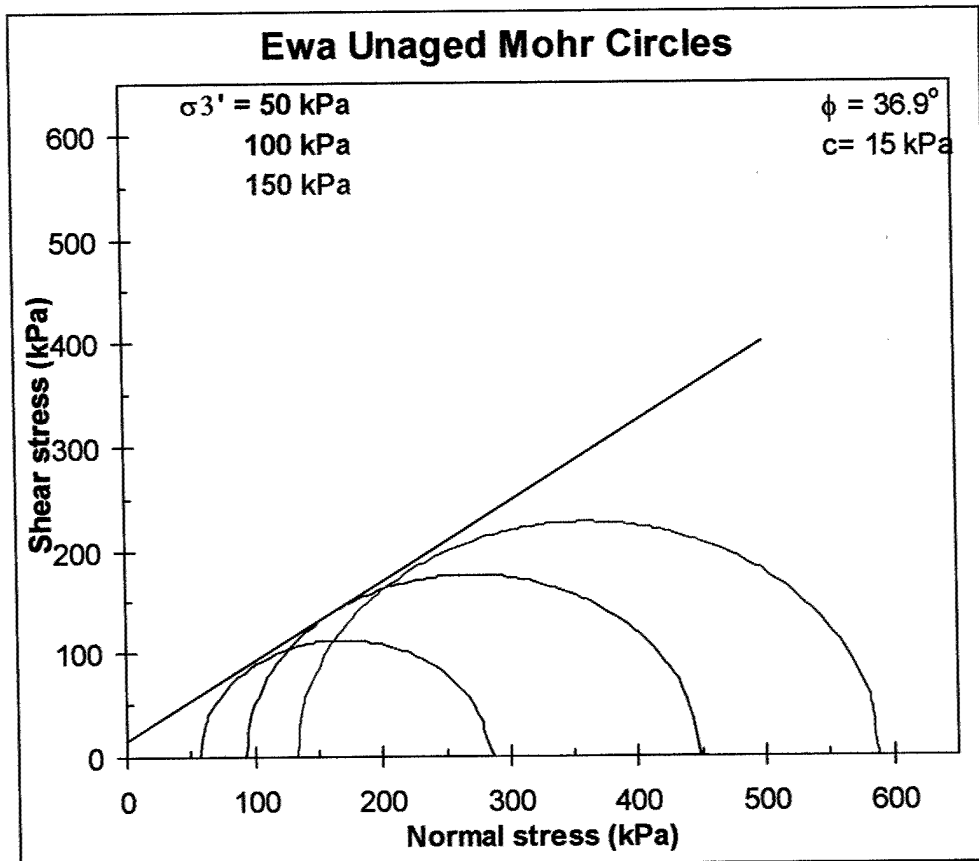


Figure 4.9 – Mohr's Circles for Unaged Ewa Sands

Ewa 30-Day Stress Path

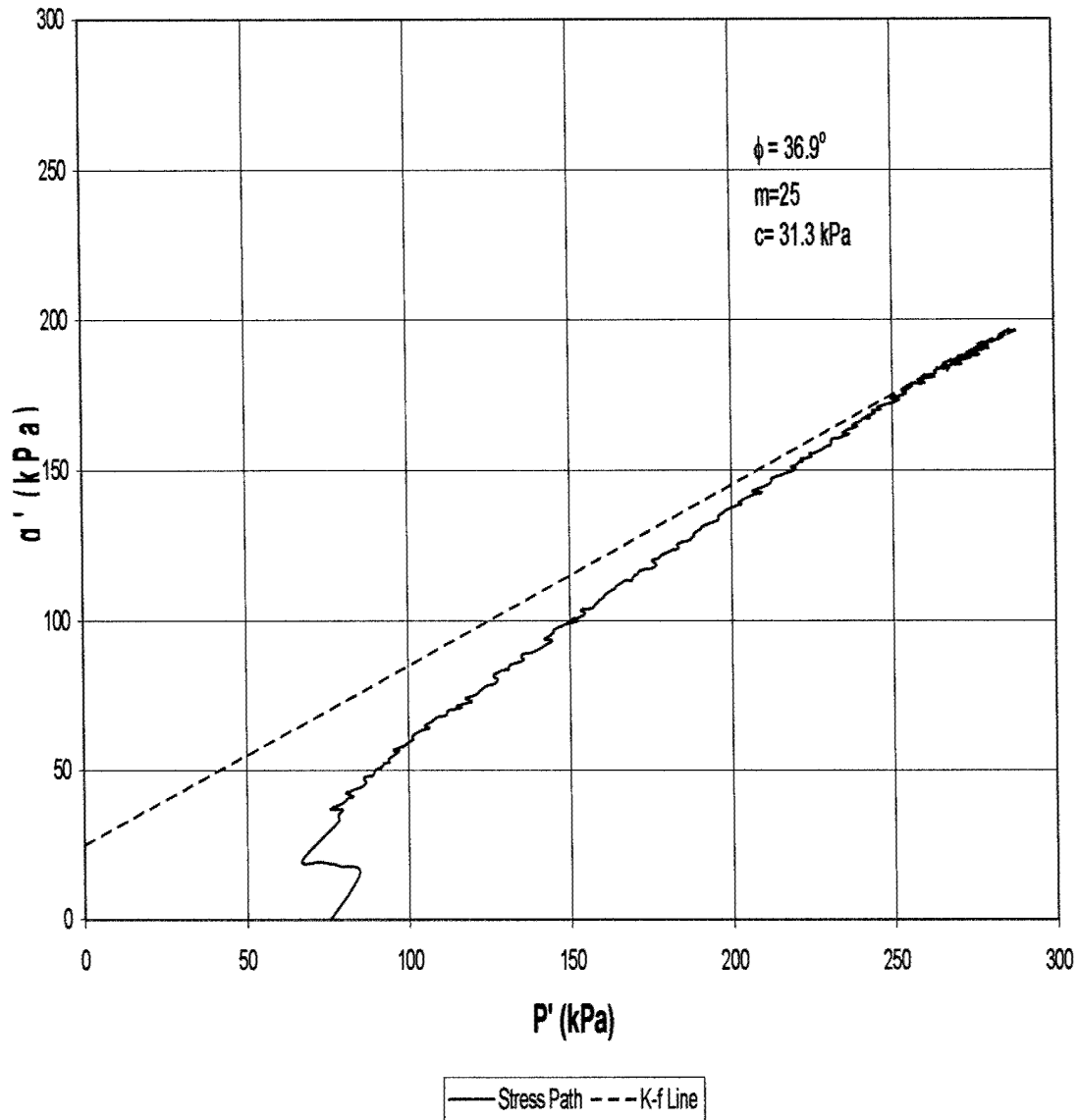


Figure 4.10 – 30-Day Ewa Sand Stress Path Diagram

Ewa 60-Day Stress Path

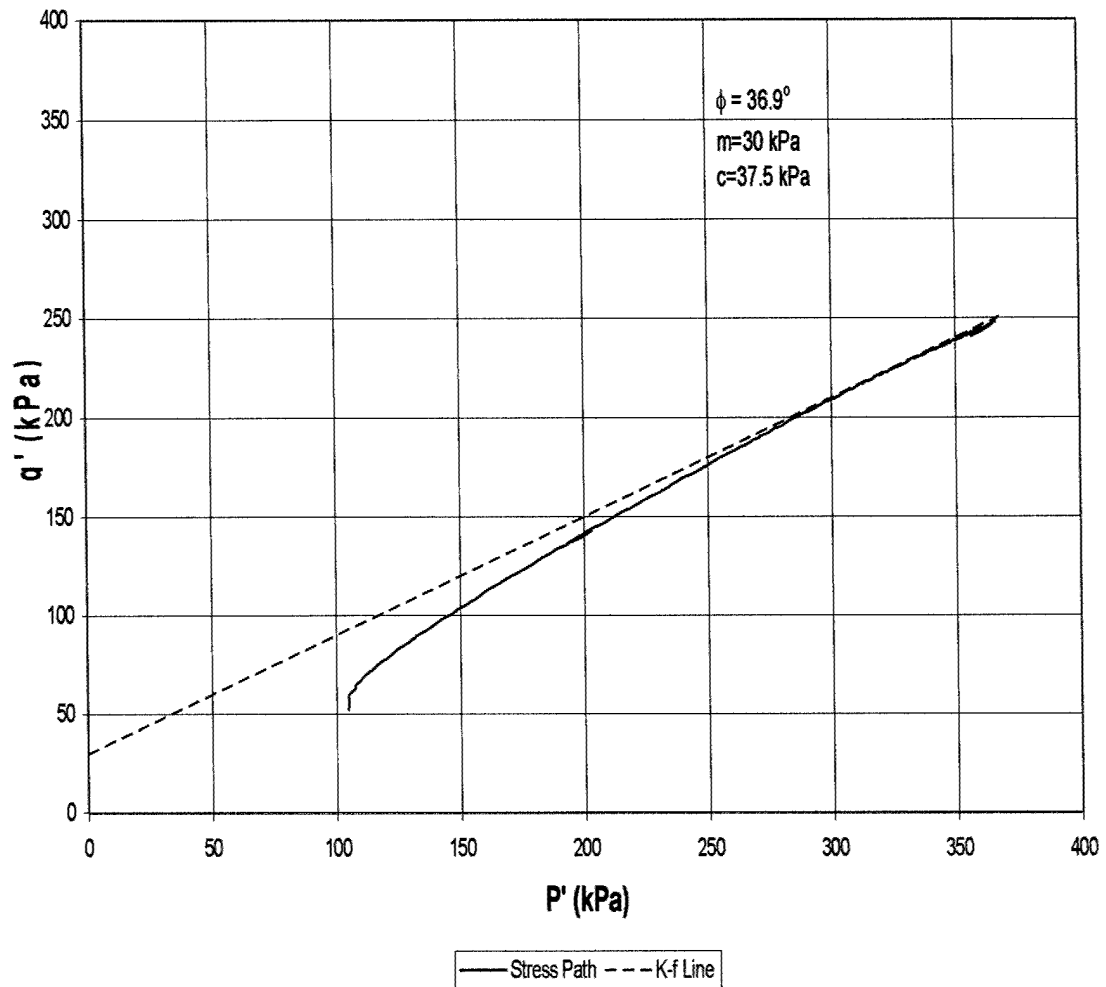
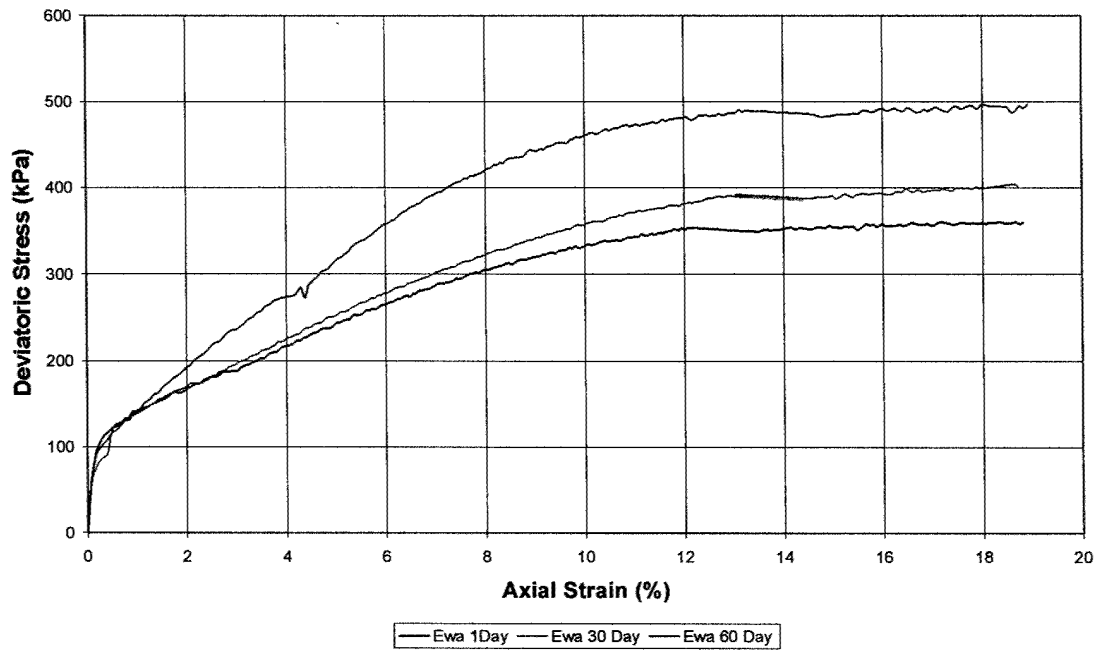


Figure 4.11 – 60-Day Ewa Sand Stress Path Diagram

Cementation Effects



Pore Pressure

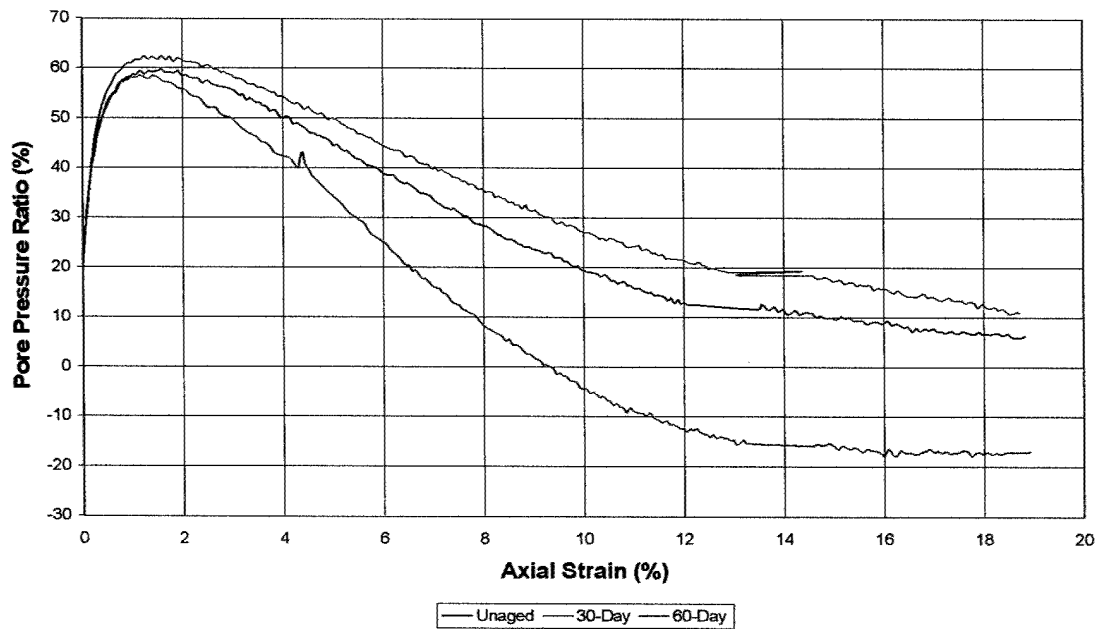


Figure 4.12 – Comparison of Results for Cemented Ewa Sands

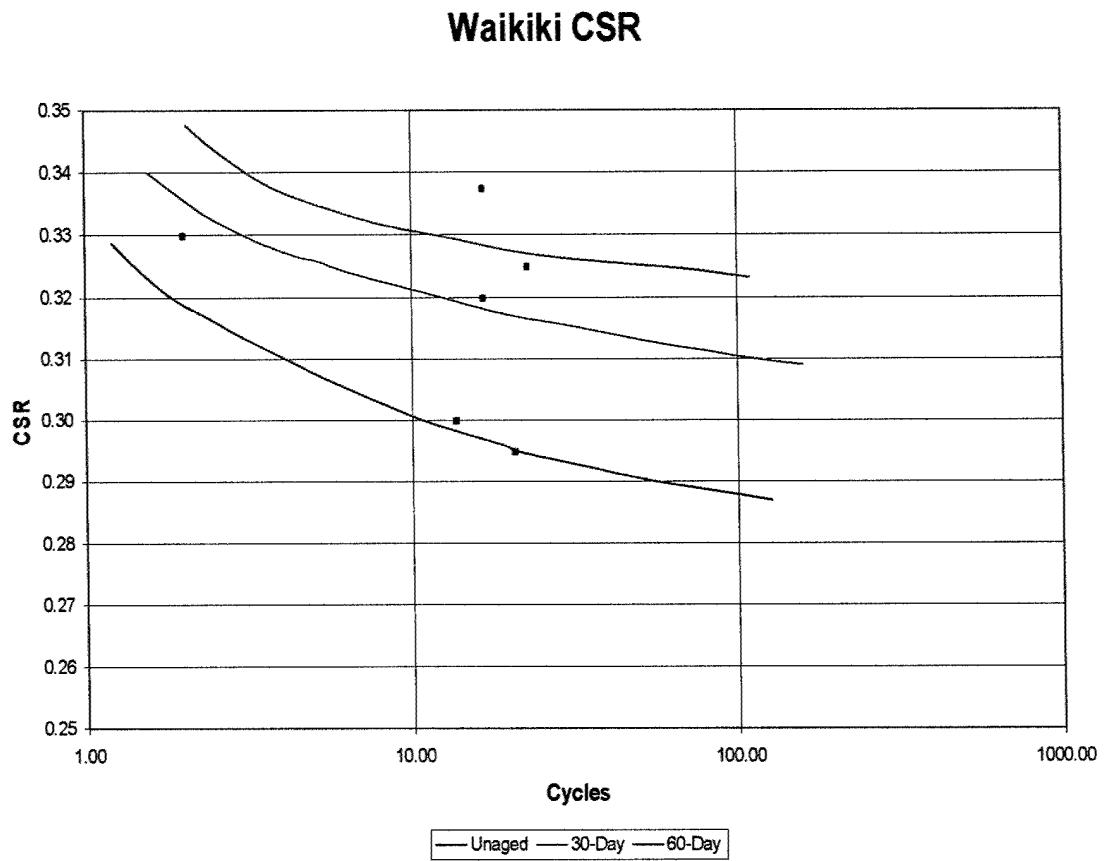
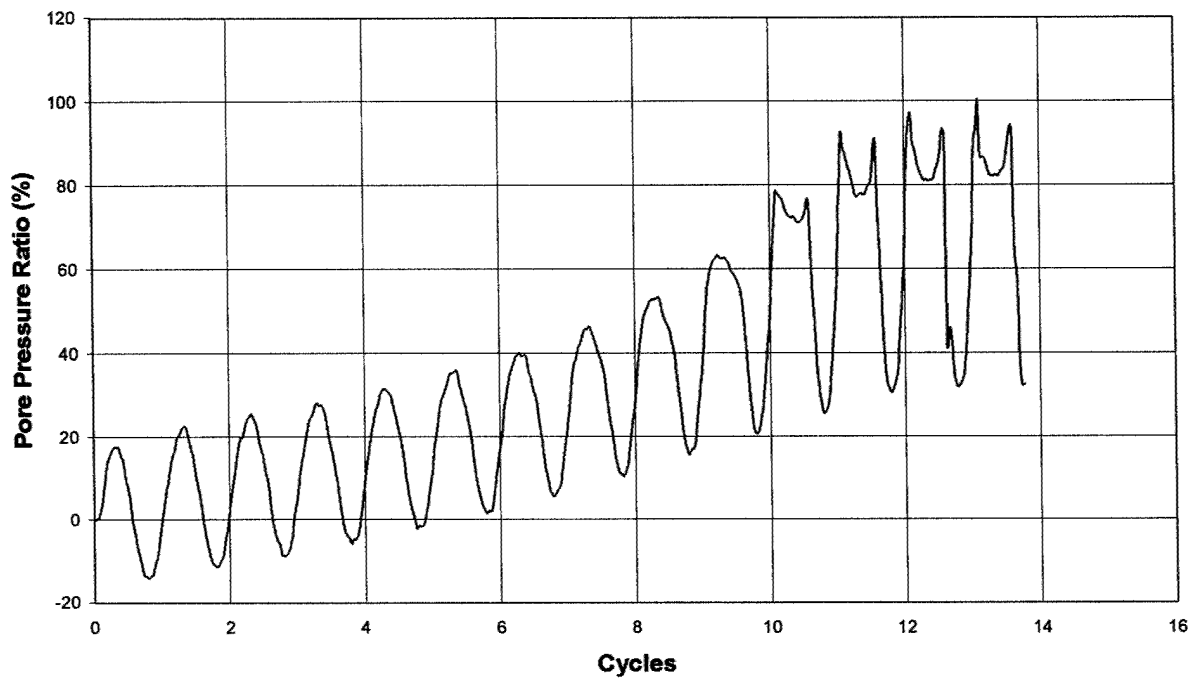


Figure 4.13 – CSR Graph for Waikiki Sand at 50% Relative Density

Pore Pressure



Axial Strain

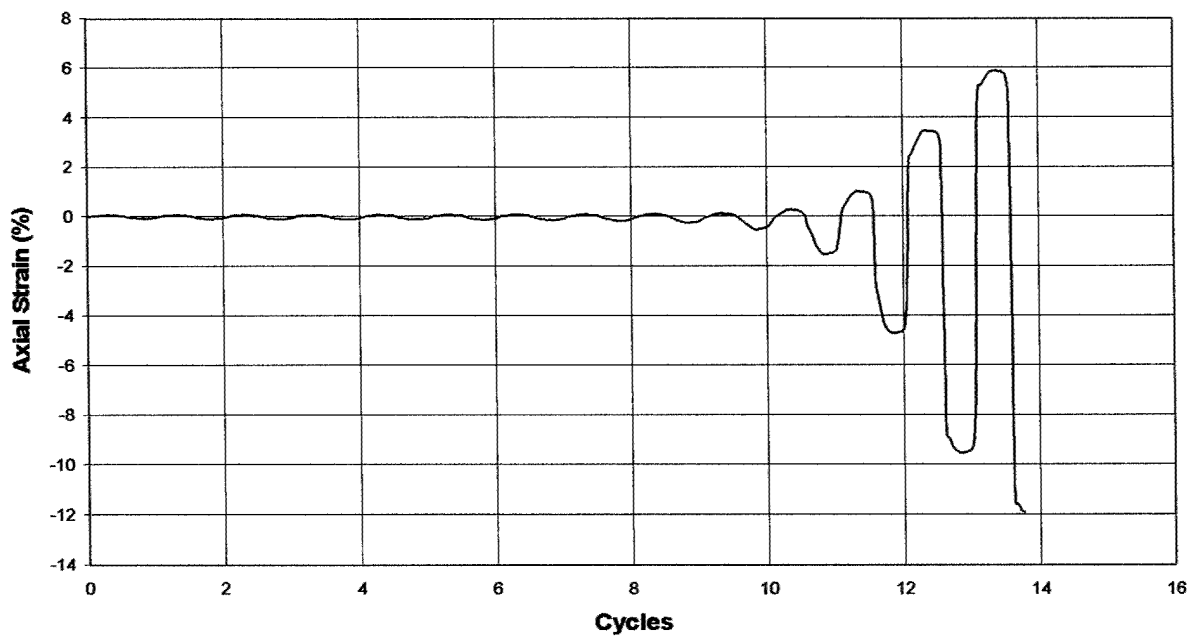
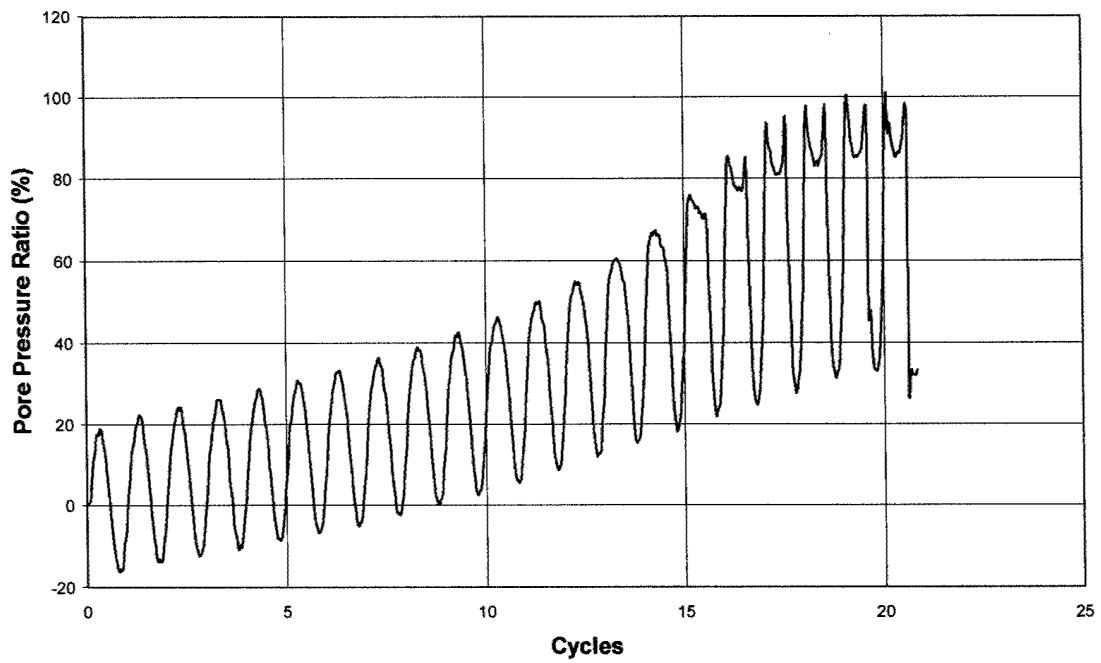


Figure 4.14 - Waikiki Unaged Cyclic Test with CSR of 0.3

Pore Pressure



Axial Strain

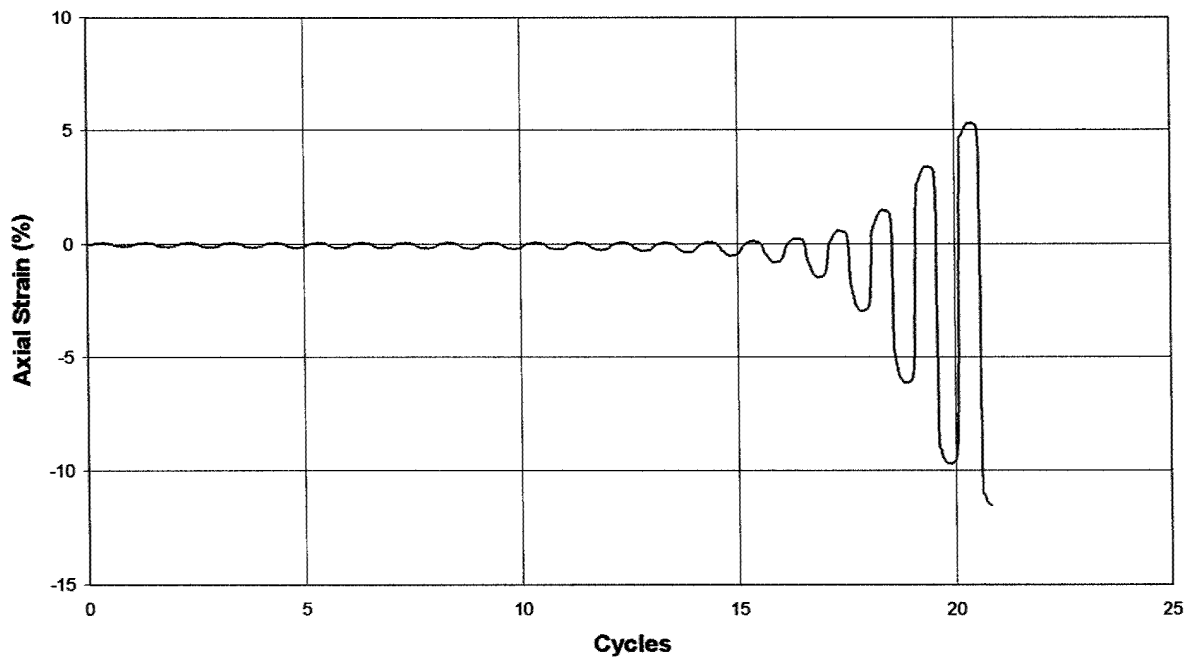
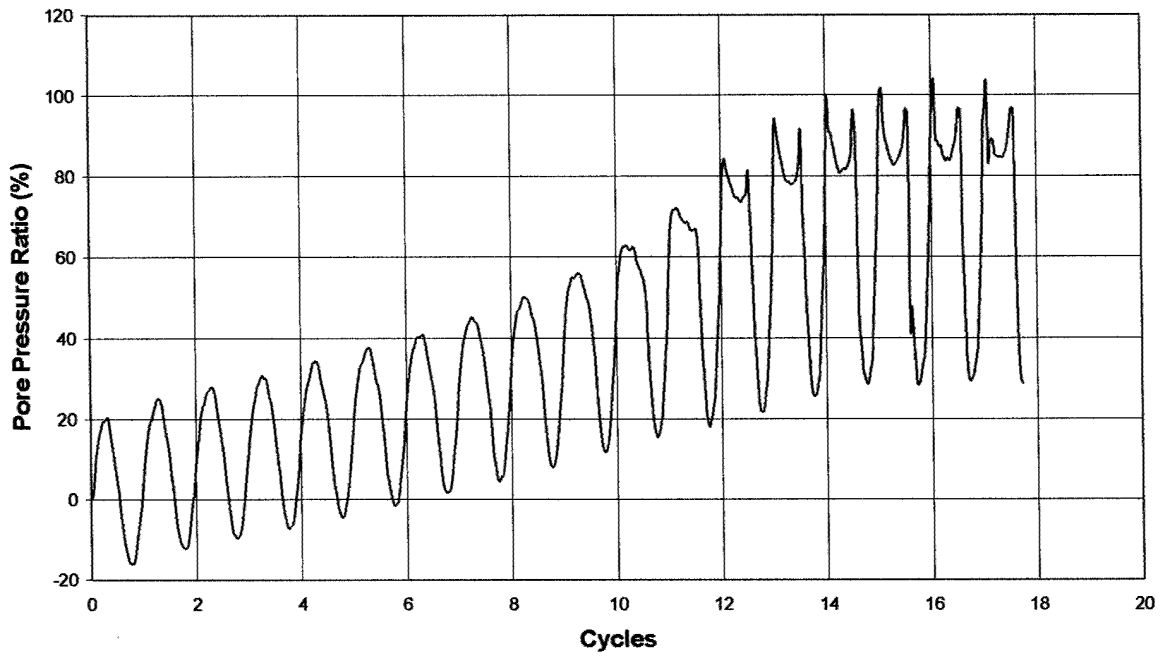


Figure 4.15 - Waikiki Unaged Cyclic Test with CSR of 0.295

Pore Pressure Ratio



Axial Strain

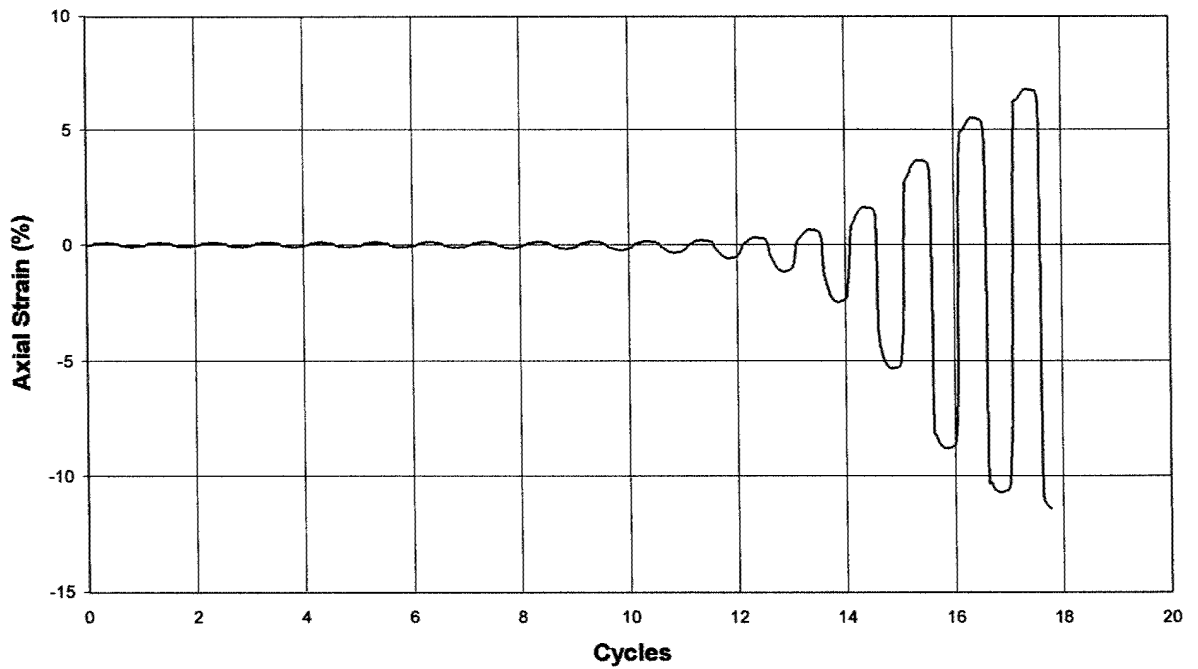


Figure 4.16 - Waikiki 30-Day Cyclic Test with CSR of 0.32

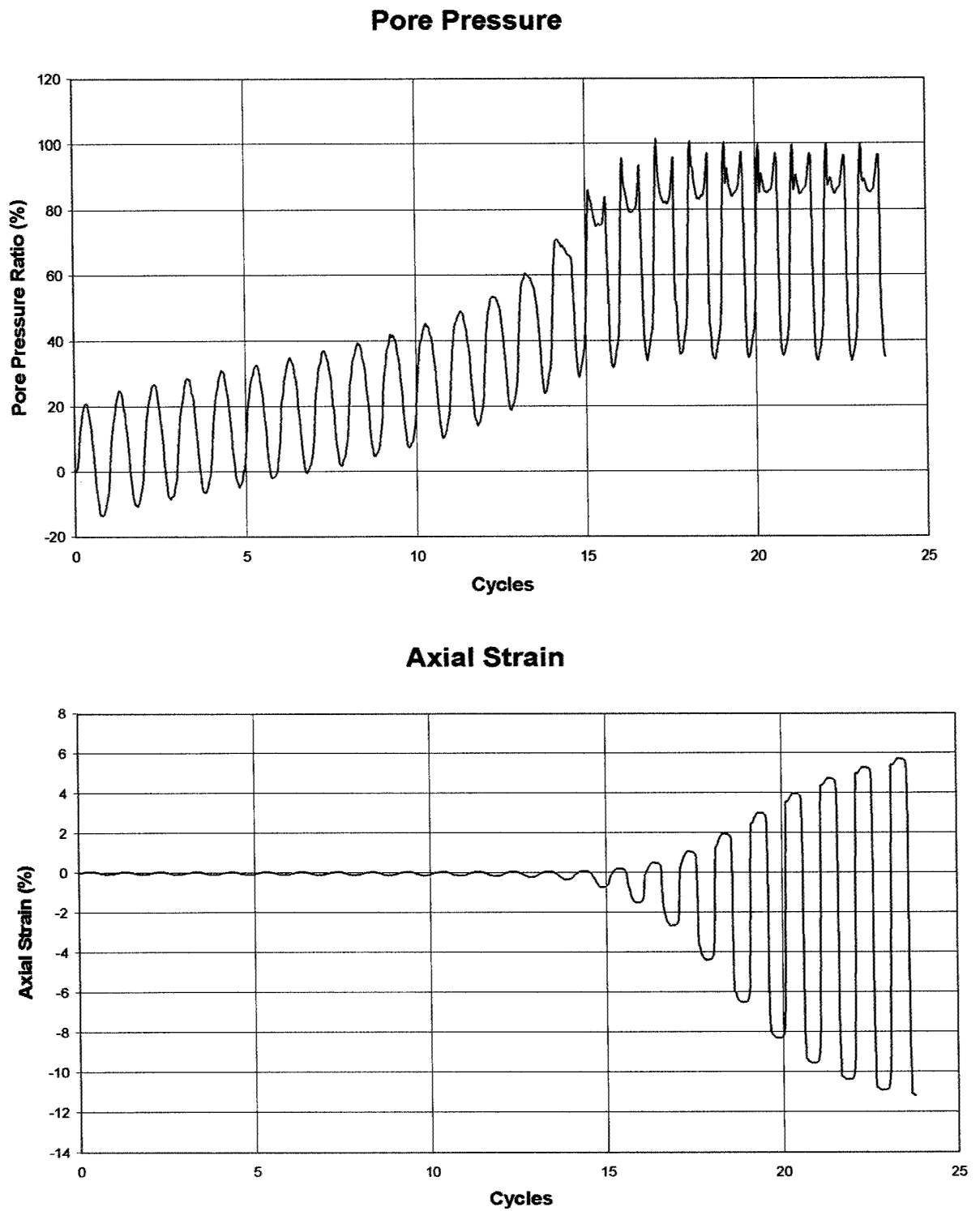


Figure 4.17 - Waikiki 60-Day Cyclic Test with CSR of 0.325

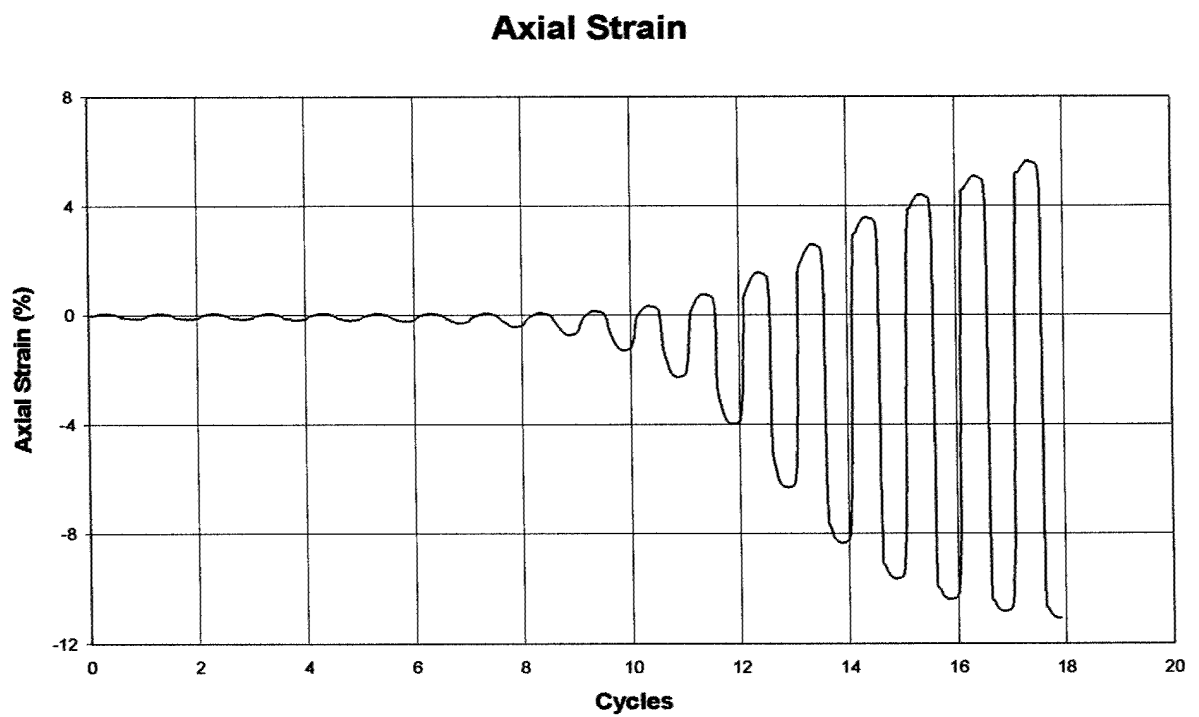
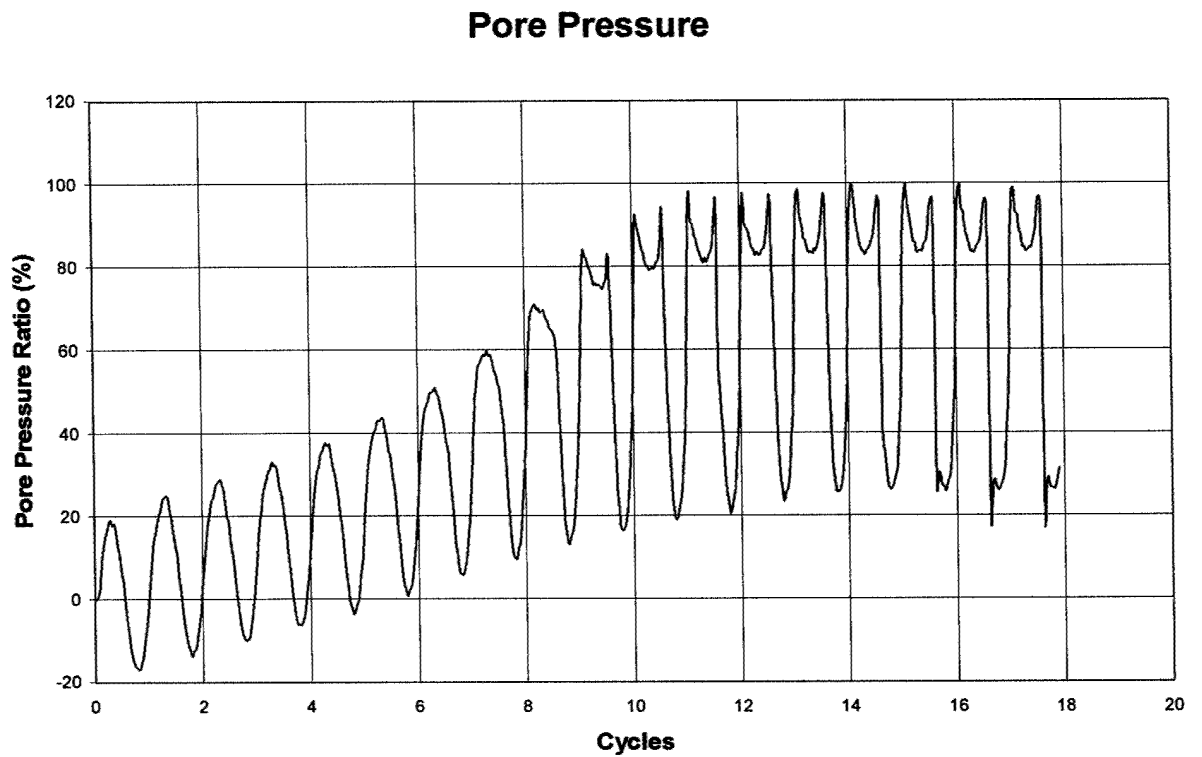


Figure 4.18 - Waikiki 60-Day Cyclic Test with CSR of 0.3375

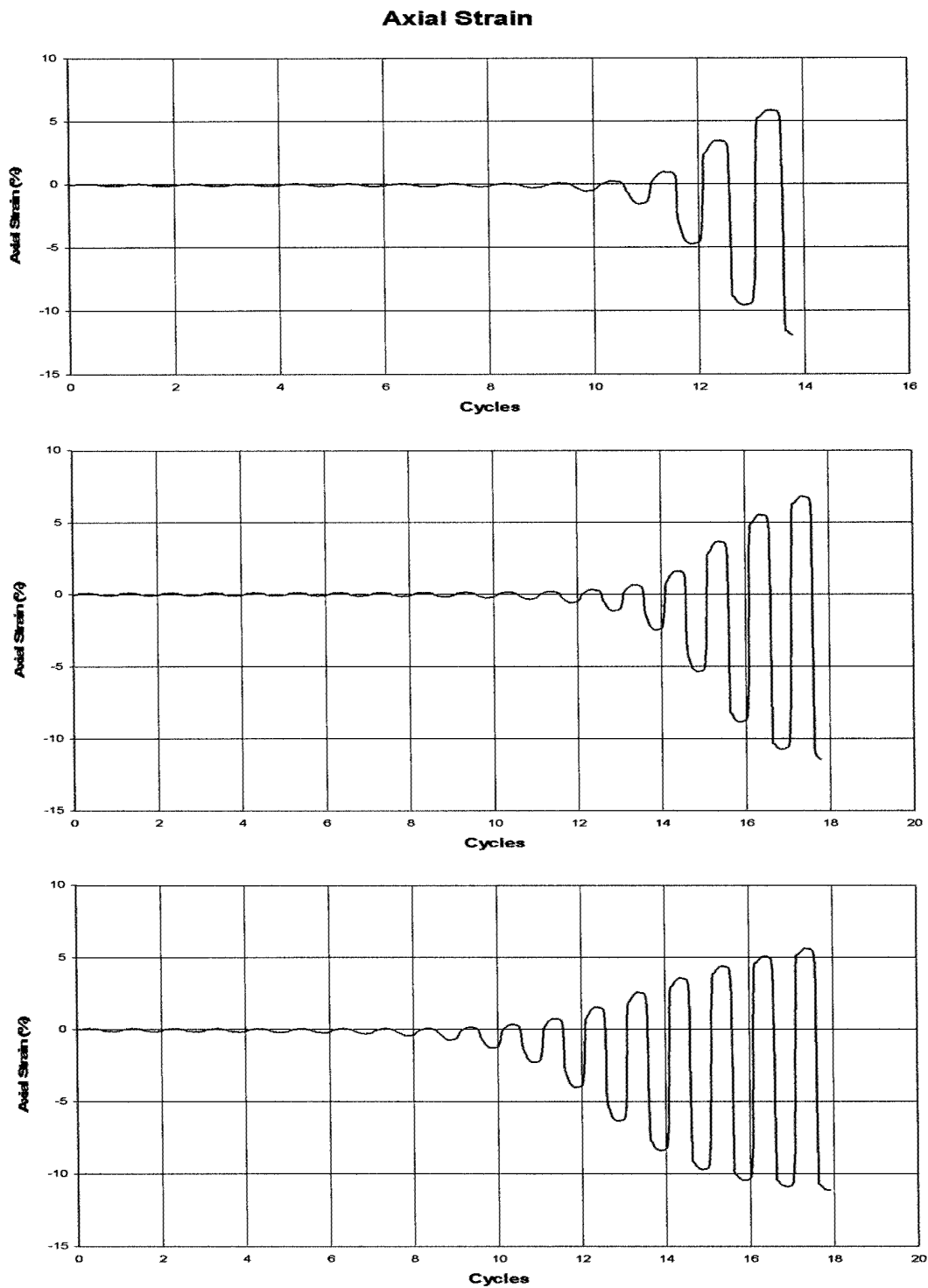


Figure 4.19 – Waikiki unaged, 30-day, and 60-day cyclic test results from top to bottom, respectively, showing increase in cycles to failure with increased aging.

Ewa CSR Curves

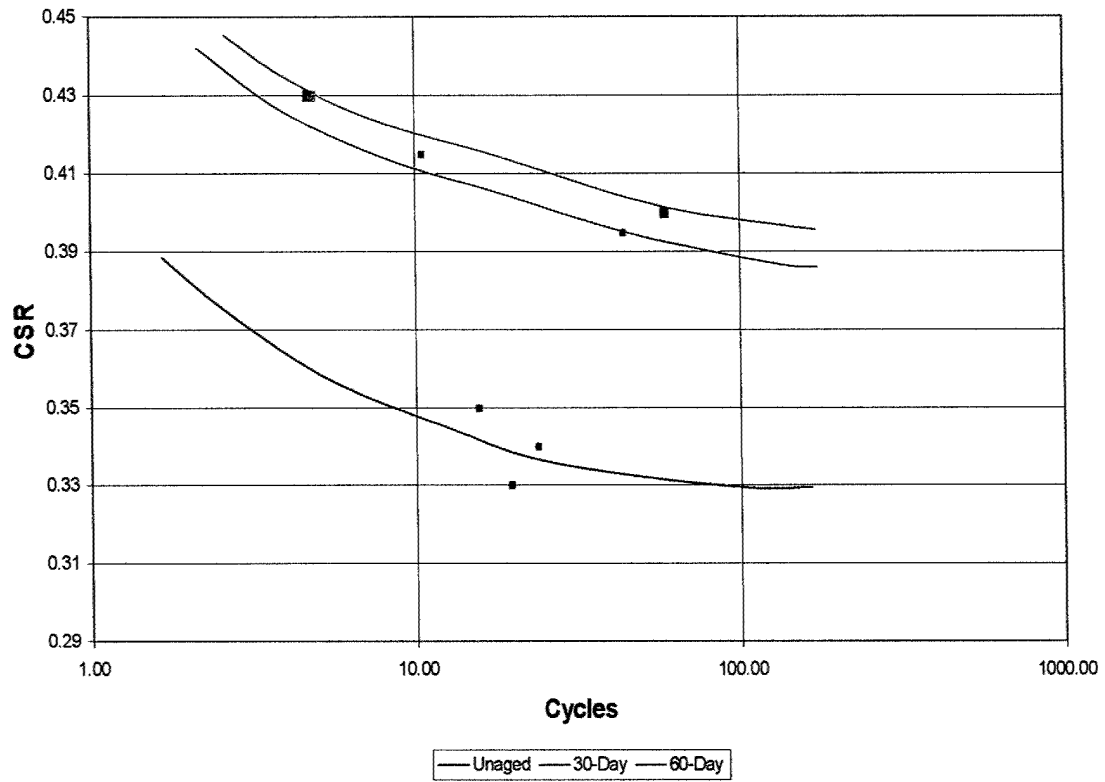
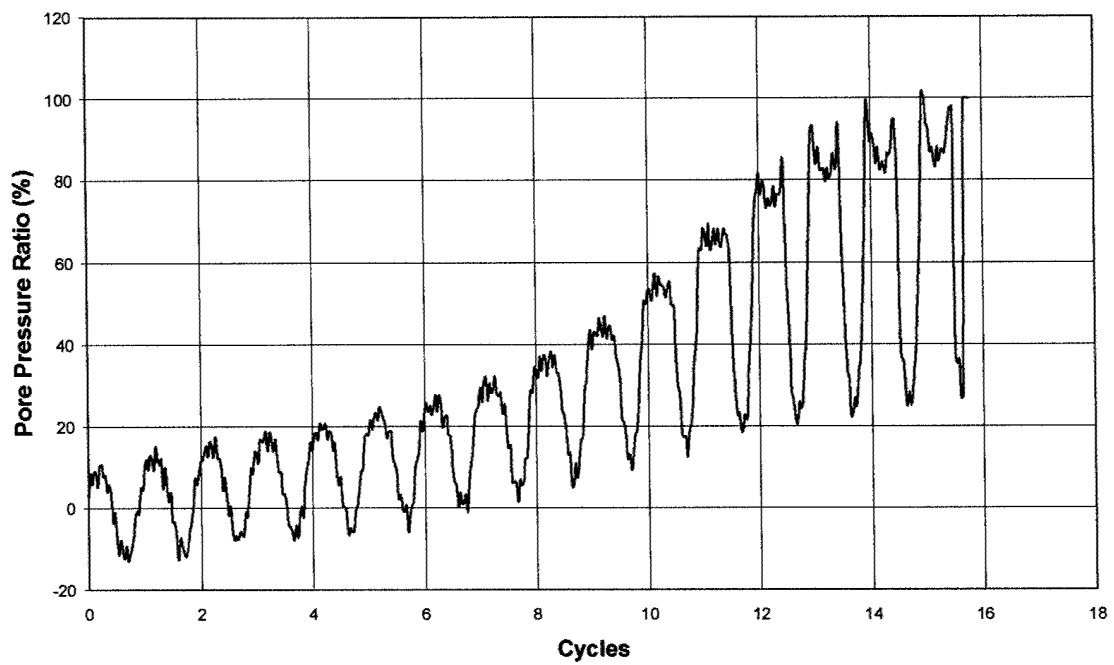


Figure 4.20 – CSR Graph of Ewa Sand at 50% Relative Density

Pore Pressure



Axial Strain

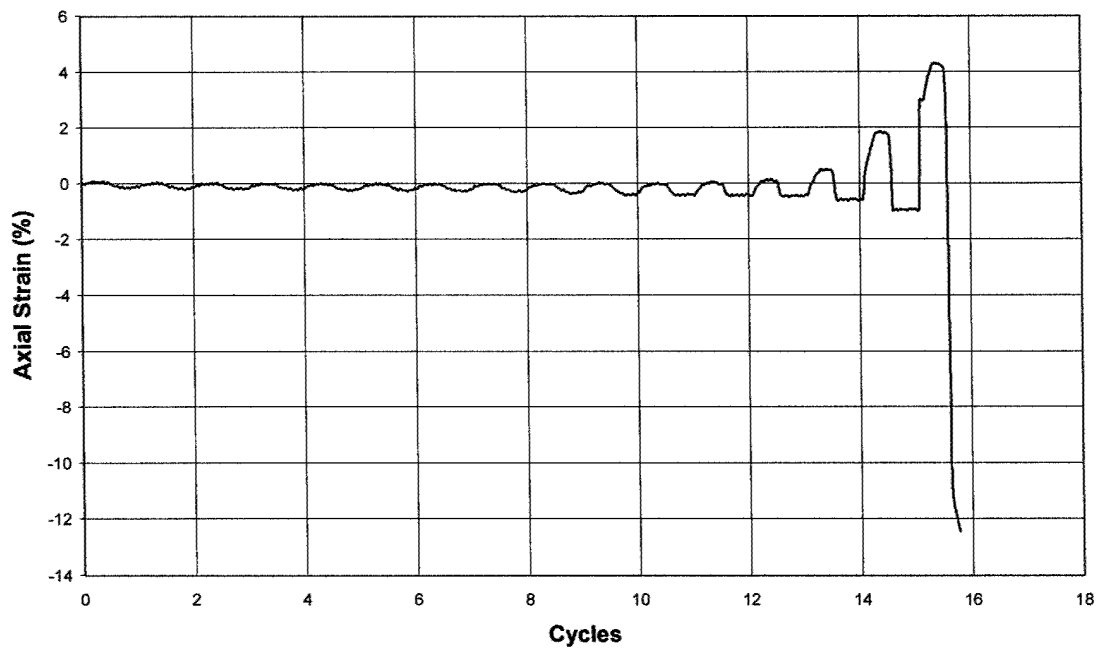
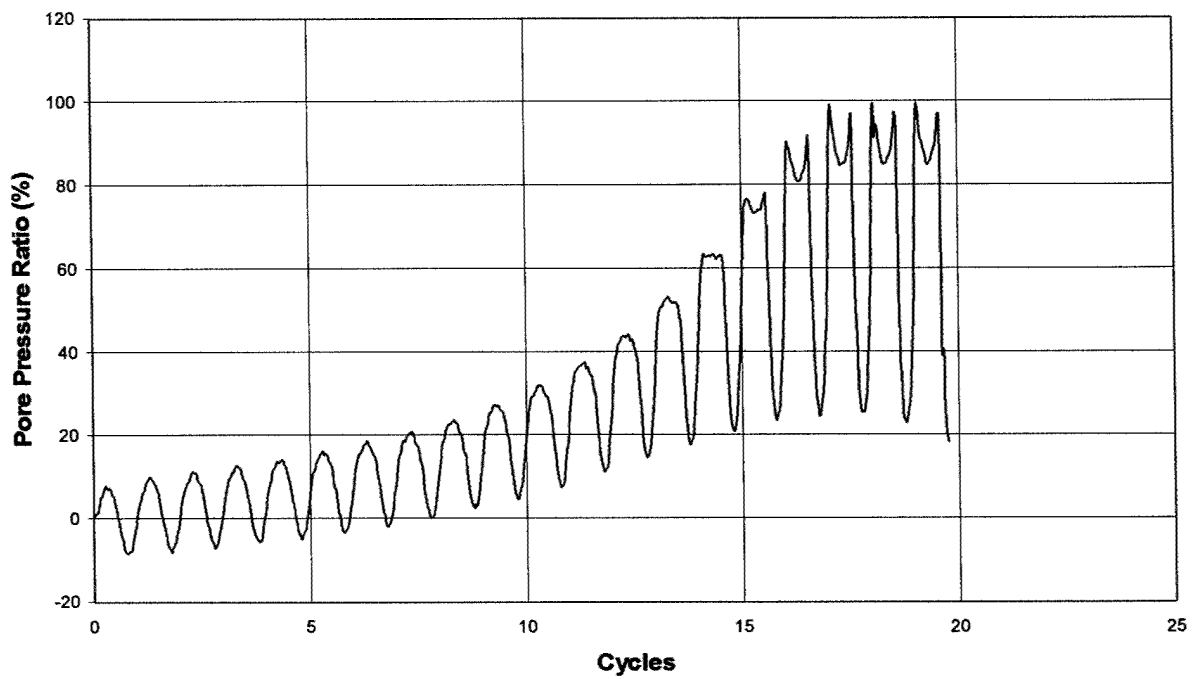


Figure 4.21 - Ewa Unaged Cyclic Test with CSR of 0.35

Pore Pressure



Axial Strain

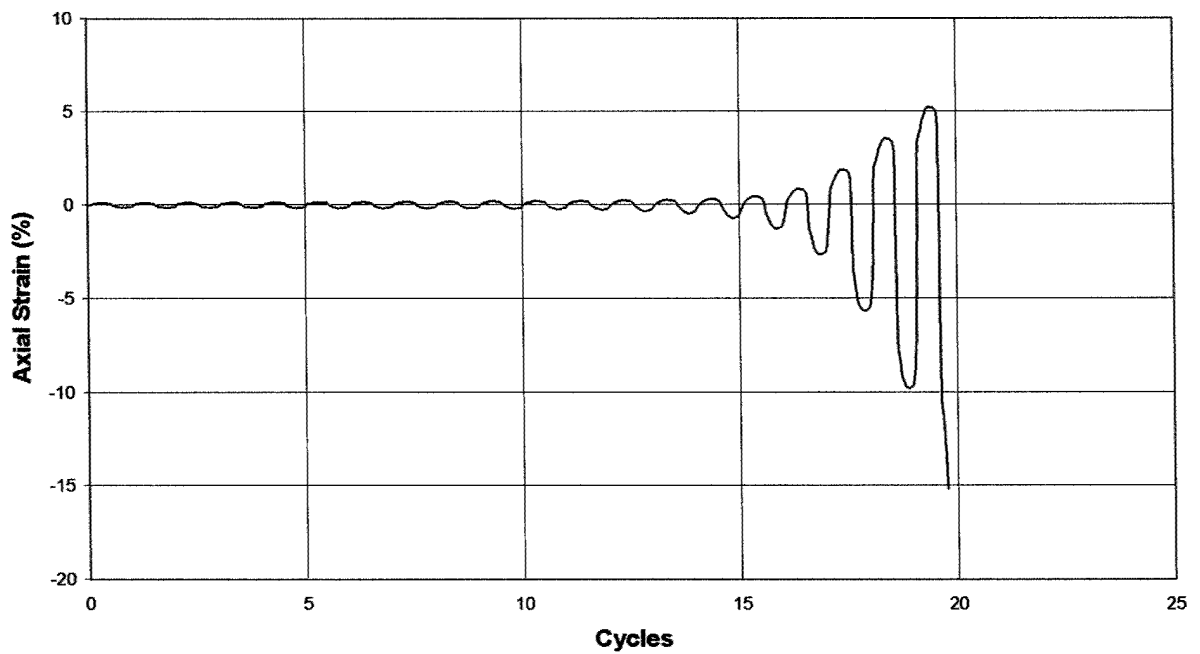
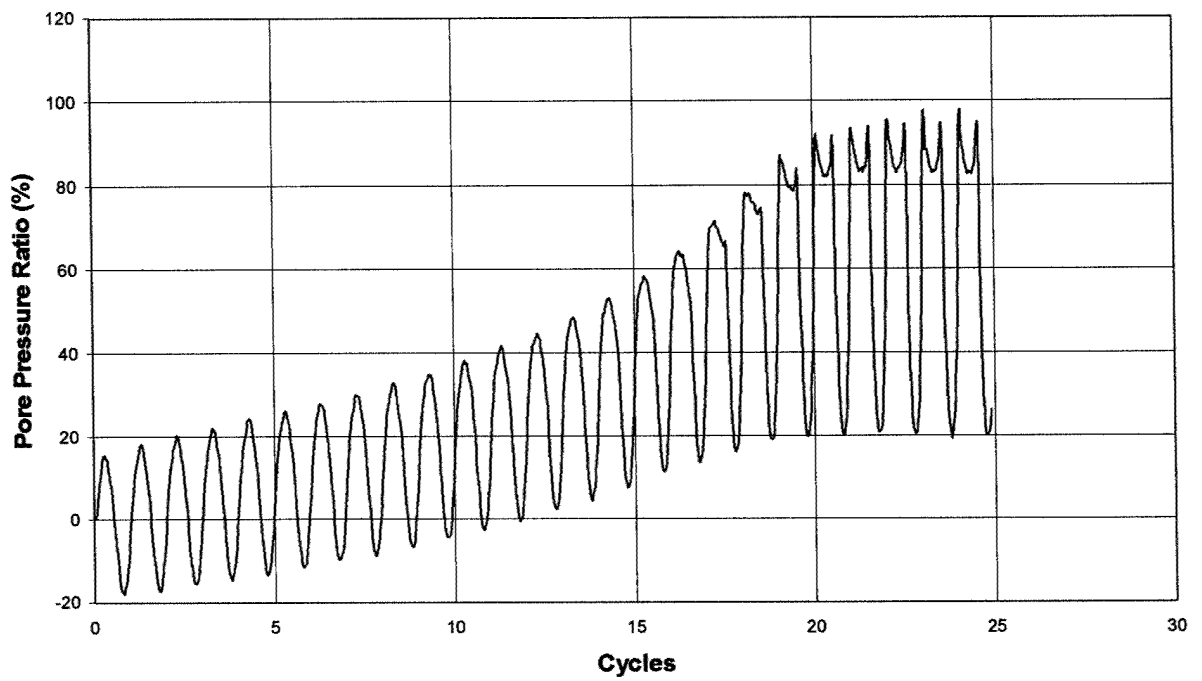


Figure 4.22 - Ewa Unaged Cyclic Test with CSR of 0.33

Pore Pressure



Axial Strain

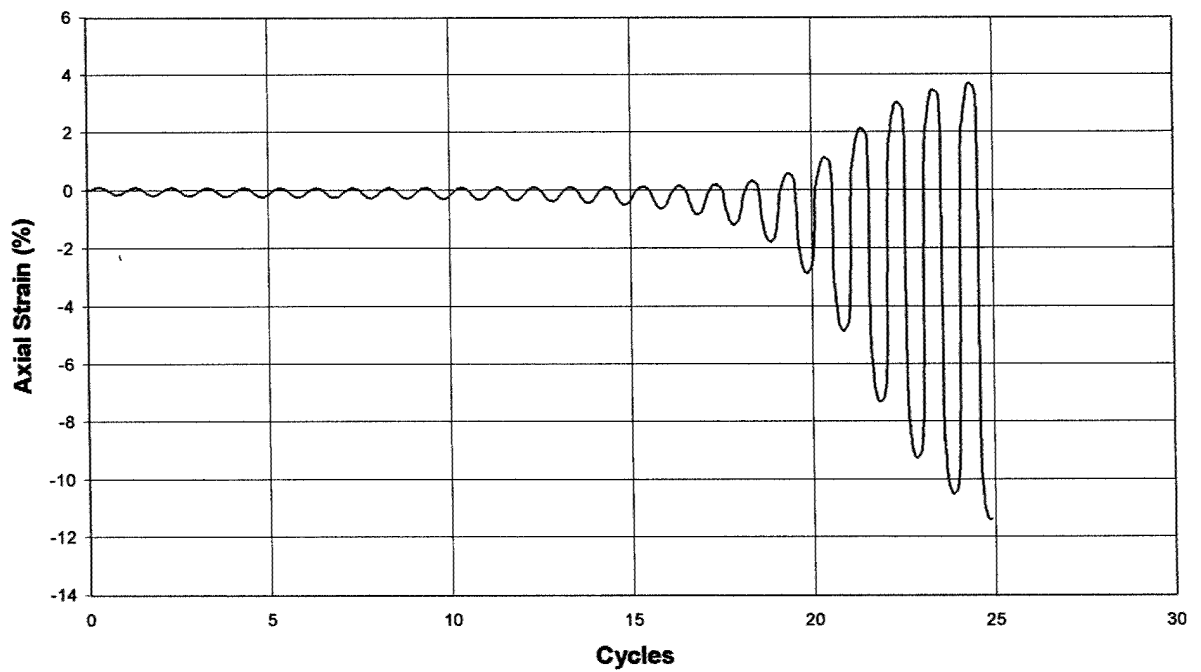
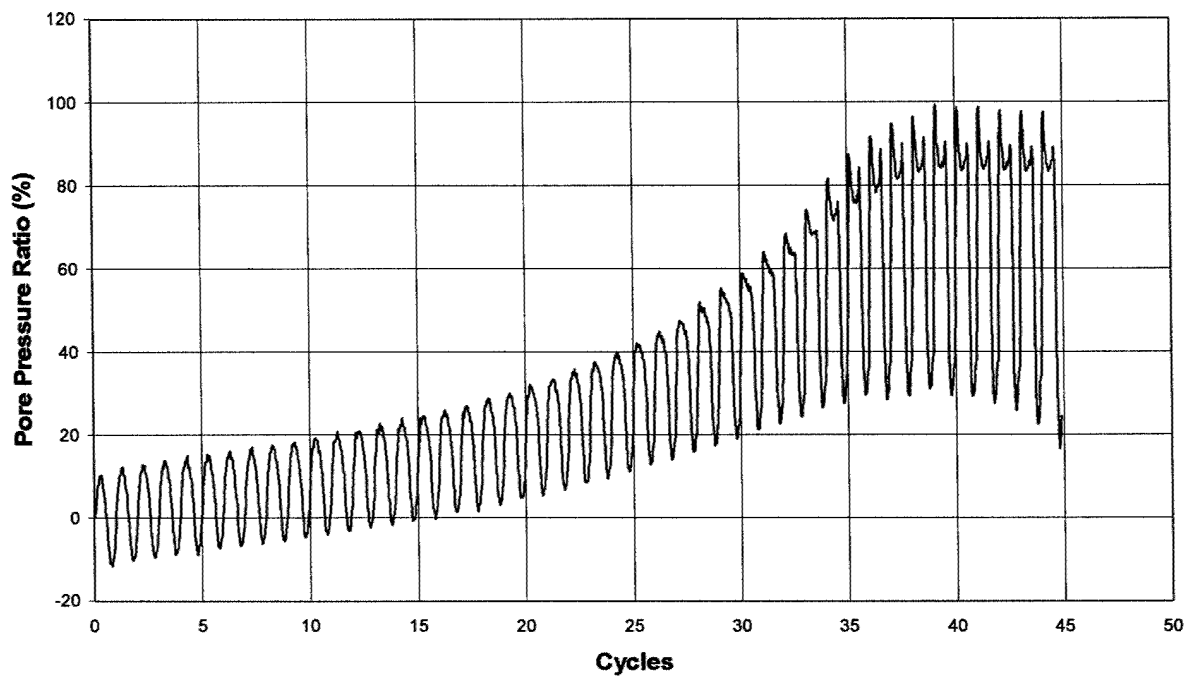


Figure 4.23 - Ewa Unaged Cyclic Test with CSR of 0.34

Pore Pressure



Axial Strain

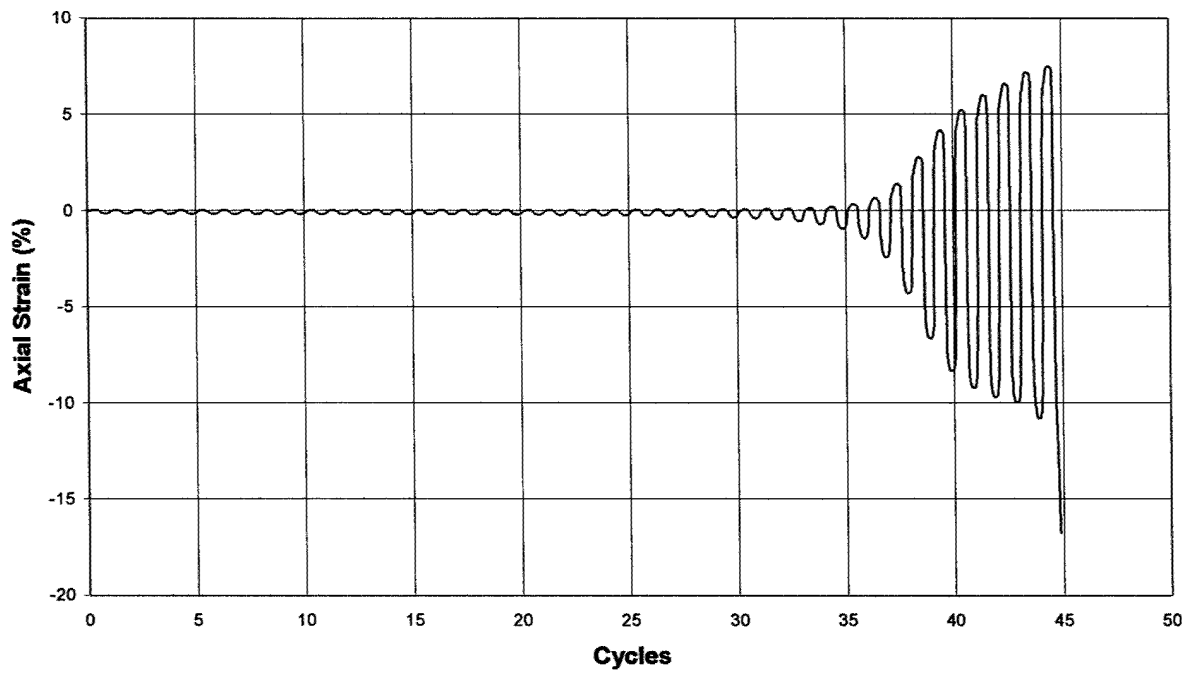
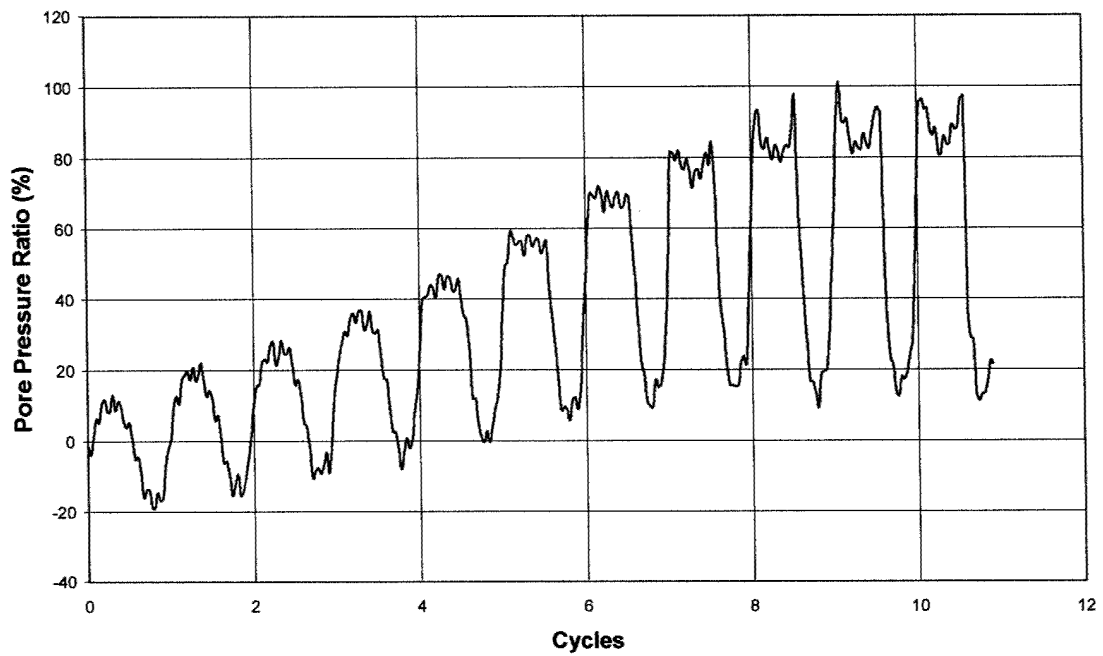


Figure 4.24 - Ewa 30-Day Cyclic Test with CSR of 0.395

Pore Pressure



Axial Strain

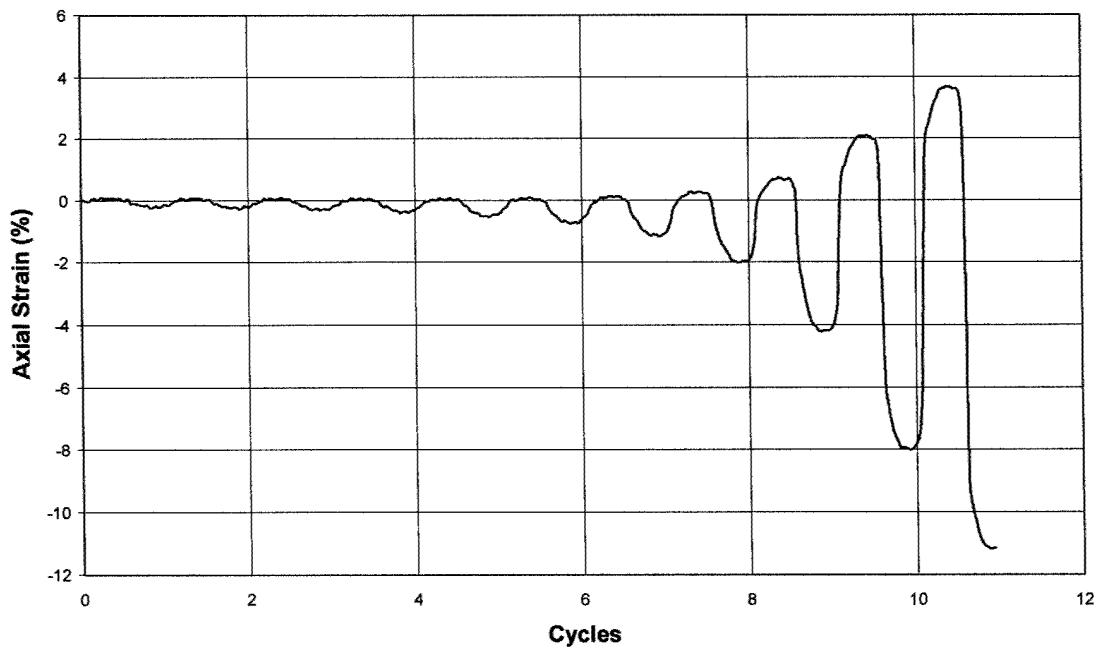
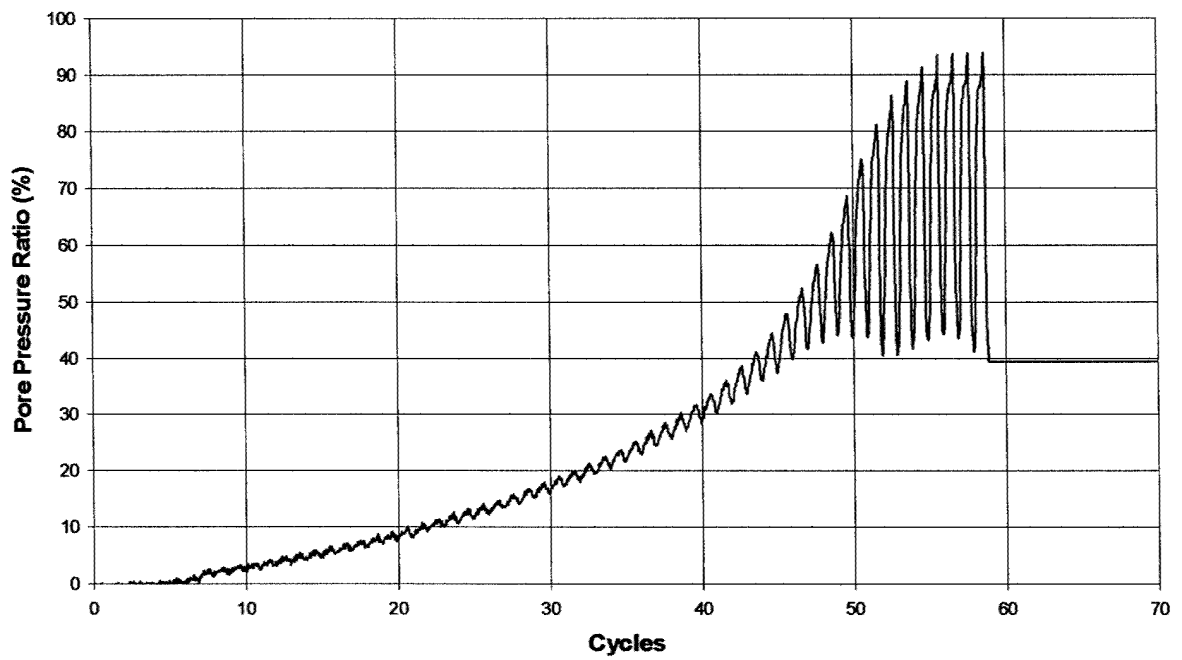


Figure 4.25 – Ewa 30-Day Cyclic Test with CSR of 0.425

Pore Pressure



Axial Strain

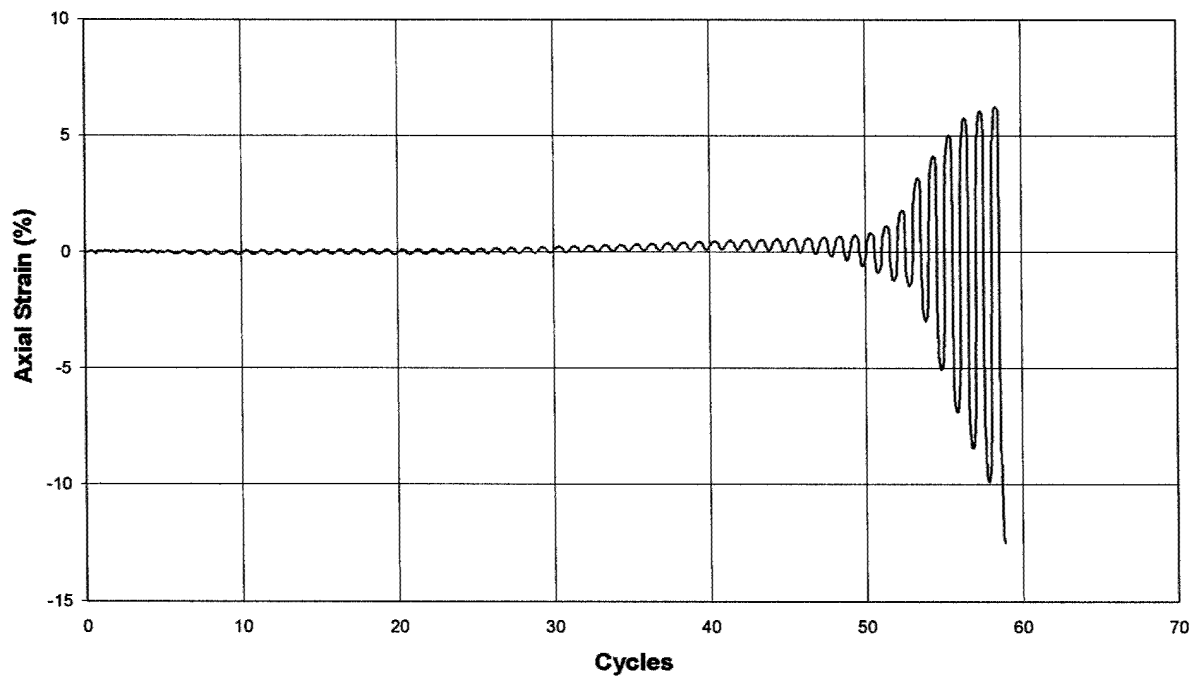


Figure 4.26 - Ewa 60-Day Cyclic Test with CSR of 0.40

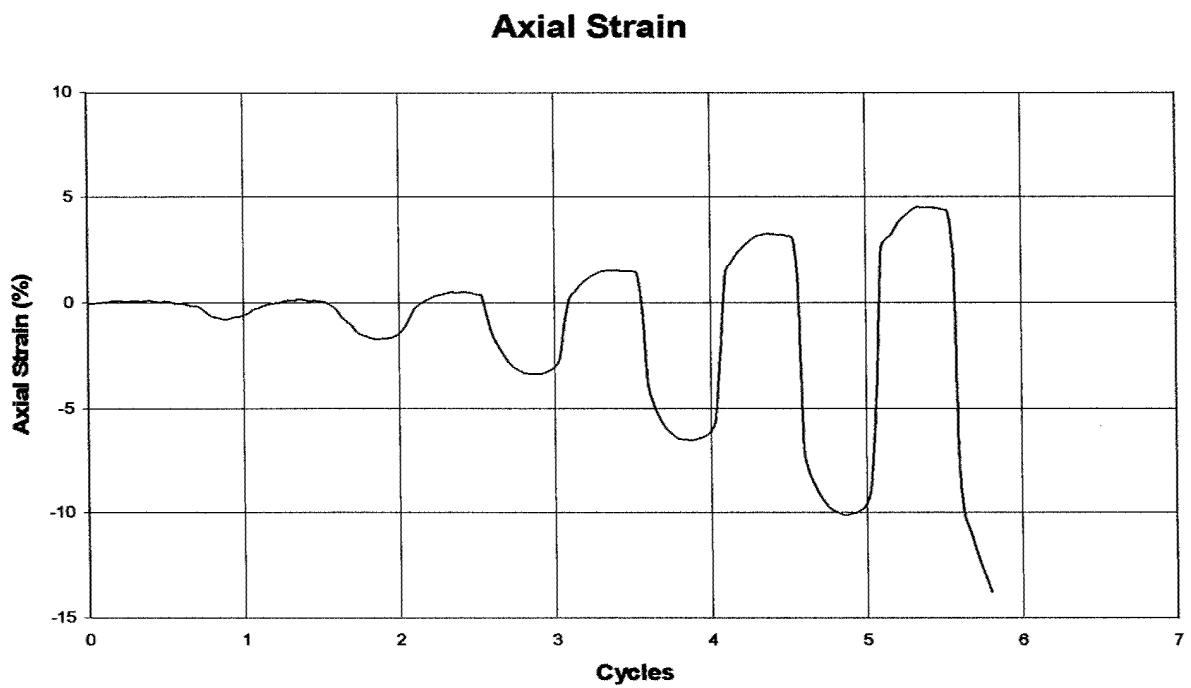
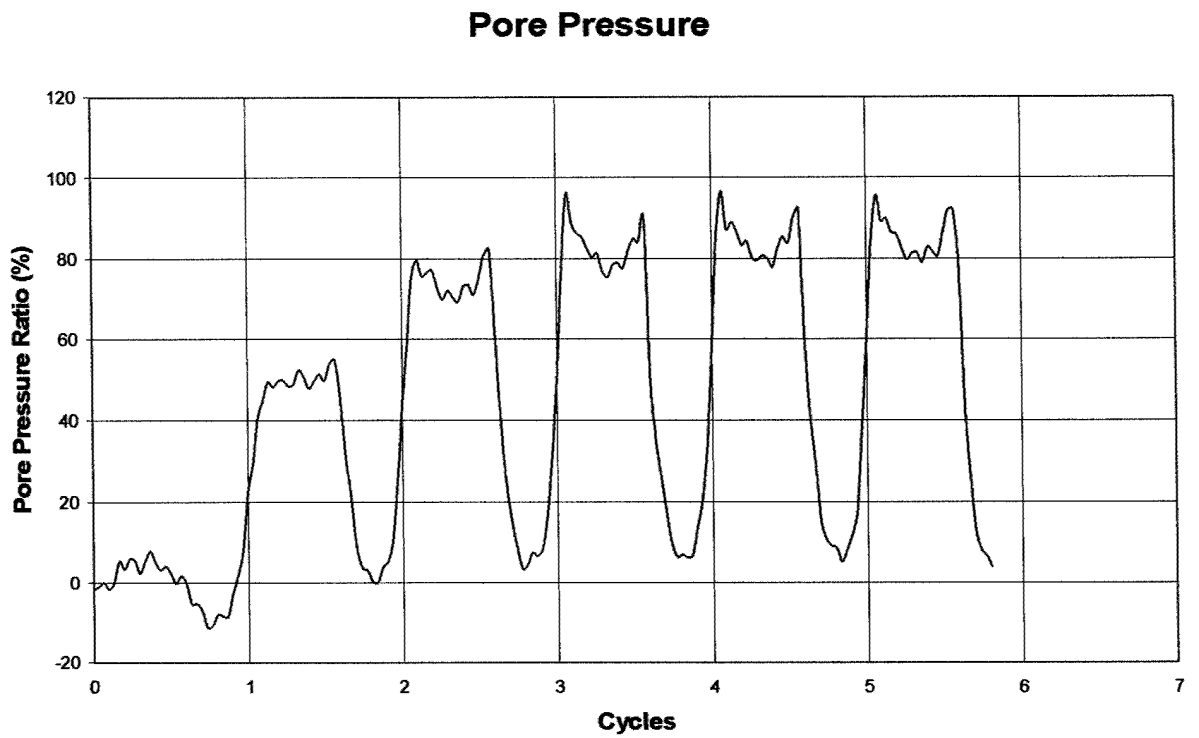


Figure 4.27 – Ewa 60-Day Cyclic Test with CSR of 0.43

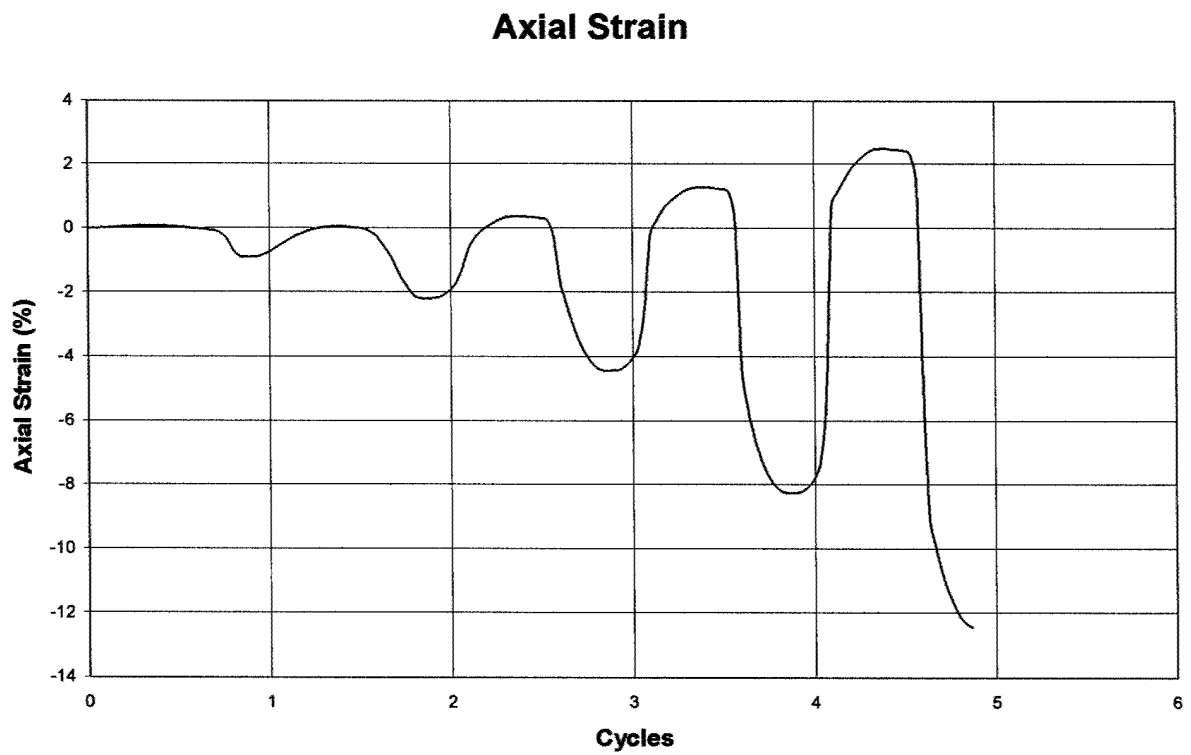
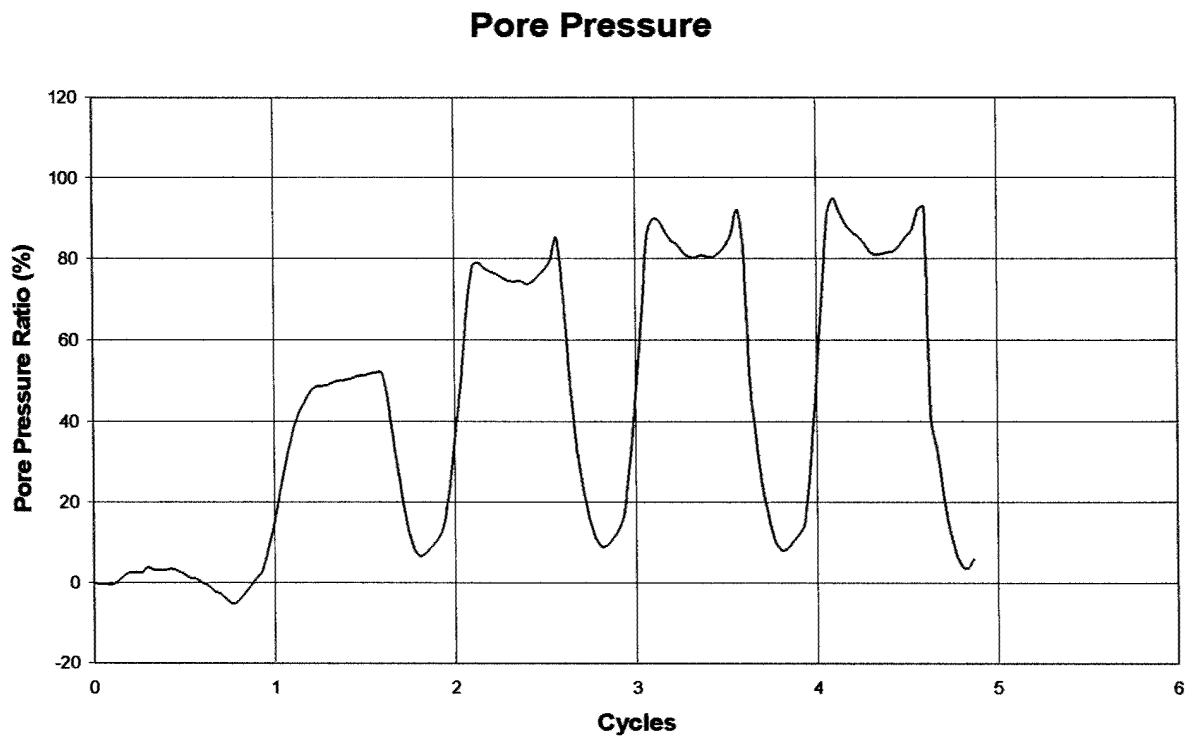


Figure 4.28 - Ewa 60-Day Cyclic Test with CSR of 0.43

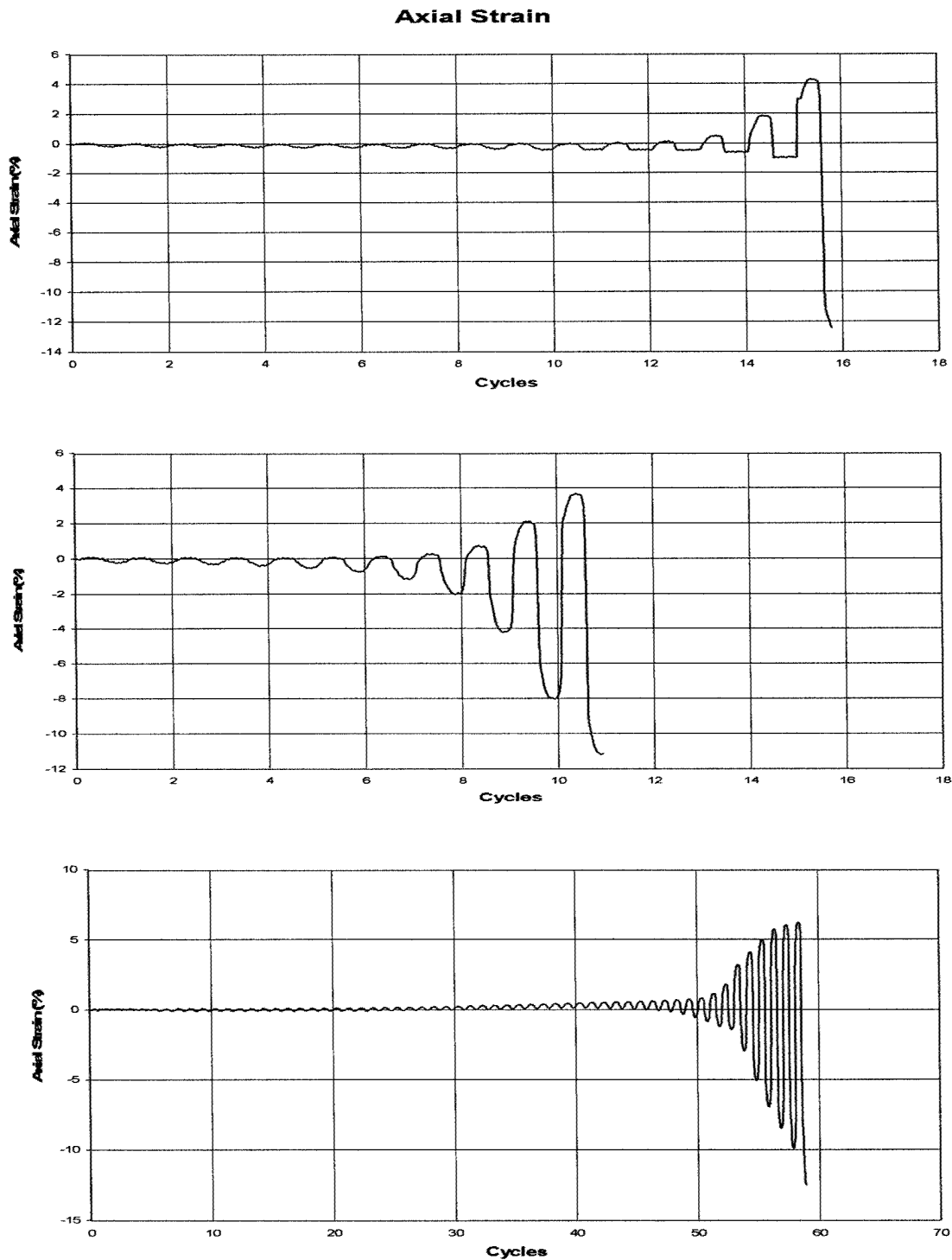


Figure 4.29 – Ewa unaged, 30, and 60-day cyclic test results from top to bottom, respectively, showing increase in cycles to failure with increased aging.

CHAPTER 5 CONE PENETROMETER TESTING

The cone penetrometer test (CPT) is becoming a more popular in situ testing method by geotechnical engineers due to its simplicity, continuous logging and cost effectiveness. The CPT works by measuring the tip resistance of a cone pushed into the ground. Sleeve friction can also be taken into account with sensors just above the cone. This measures the frictional resistance of the sand around the rod pushing the cone and can be correlated with skin friction for piles. Correlations have been made to help geotechnical engineers determine soil types and densities (Campanella et al., 1986). The CPT also provides a constant profile of soil layers, unlike the standard penetration test (SPT). One disadvantage of the CPT is that it does not provide samples. Modifications to the CPT have also allowed it to measure pore pressures and shear wave velocities.

The use of lab mini-cone penetrometers helps relate laboratory results to in situ tests. Several researchers have started using lab penetrometers to relate laboratory tests to in situ tests, to compare strength values from triaxial tests to the cone tests, and to test cone reactions to samples of varying cementation. The latter is the reason for the cone's use in this project. It is assumed that cemented specimens should have higher tip resistances resulting from increased strength and lower sleeve friction values than noncemented specimens due to sand surrounding the cone not collapsing back towards the rod because it is held in place by other cement bonds.

5.1 LABORATORY TESTING CPT BEHAVIOR

Beringen (1988) found that using CPT was not only a good means of getting in situ soil data, but is also helpful in classification of calcareous sediment. He found that the cone tip resistance could help identify the degree of cementation, which was already used as a

type of classification but qualitative forms of measurement were not very accurate. He made direct correlations between cementation and cone tip resistance.

Beringen also noted trends in the friction ratio, or the ratio between the sleeve friction and the tip resistance. It was observed that as cementation increases, the friction ratio decreases. He also noted that the friction ratio is lower for carbonate sands than terrigenous soils. The friction ratio was reported as 2% and 8% for clays, about 3% for quartz, and between 0.5% and 2% for carbonate sands. Renfrey et al. (1988) found similar results while doing in situ cone testing at the North Rankin 'A' platform. They found friction ratios of 2% to 3% for uncemented sands and between 0.5% and 2% for cemented sands.

The lower skin friction is attributed to the cementation of the sand. Uncemented sands will collapse back towards the sleeve after the cone tip has passed through that area, causing frictional resistance on the sleeve. Cemented sands do not collapse back toward the rod because they are held back by cemented bonds (Rad, 1986). The cementation is also believed to be the cause for the reduced pile capacity for many offshore platforms (McClelland, 1988).

Joer et al. (1997) conducted research on cone penetrometer testing using artificially cemented samples. They performed tests on various size specimens and with various penetration rates and found similar results between the differing size specimens and with different penetration rates. He also found that as cement content was increased, the tip resistance of the cone increased.

5.2 SPECIMEN PREPARATION

Specimen preparation for testing with the laboratory mini-cone penetrometer was conducted very similar to that of the triaxial specimen preparation. Modified top caps for the specimen and a modified top to the triaxial cell were made to allow the mini-cone to pass through a hollowed shaft connecting the top cap of the specimen to the outside of the triaxial cell. The challenge was in saturating and pressurizing the specimen without sending specimen material up through the passageway intended for the cone. It was also important to get the second membrane on the specimen because of the potential of a membrane leaking due to the angularity of the sand.

Before saturation, the top cap of the specimen was put on without the hollowed shaft for the cone. A rolled membrane and two o-rings were rested on top of the cap and the shaft was then placed on top. This was critical because the extra membrane could not stretch over the long shaft for the cone. Once the shaft was in place, a stopper with a thin layer of vacuum grease was placed over the hole in the top of the shaft for the mini-cone. This allowed vacuum saturation to take place. With the specimen under vacuum, the mold was taken off the specimen and the second membrane put on the specimen. Density measurements were taken similar to those in Chapter 4. The top cap for the cell was placed on along with compression ring to hold the pressure inside the cell. The top cap and the compression ring were slid over top of the shaft while holding the stopper on to ensure the vacuum was maintained. Once on, the compression ring was tightened as well as the bolts to hold the top cap on. As general saturation was the main goal rather than necessarily obtaining a high B-value, back pressure saturation was not used. This was

also necessary since the modified triaxial setup did not allow for positive back pressure. Specimens were aged naturally under 100 kPa similar to those in Chapter 4.

A six millimeter mini-cone was used for laboratory testing. A schematic of the cone is shown in Figure 5.1. Tests were performed using a motorized strain-controlled load frame. The rate of penetration was only 0.08 inches per minute or about 2 millimeters per minute,. This was deemed acceptable as Joer (1997) has found that mini-cone penetration test results were independent of the rate of penetration. It should also be kept in mind that only relative test results were of primary interest for this study. 100 kPa pressure was continued as the confining stress throughout the test period. The machine was only capable of measuring slightly greater than two inches of penetration, which was adequate for the purpose of the testing. The cone was also hooked up to a 500 pound load cell. As the friction from the guide sleeve was previously determined by measurement to be negligible, the frictional resistance of the specimen was obtained by subtracting the tip resistance from the total load applied. An LVDT was used to measure penetration distance. All measurement instruments were connected to a data acquisition system.

5.3 CPT RESULTS FOR WAIKIKI SAND

Figures 5.2-5.4 show mini-cone test results for the Waikiki sand. The Waikiki sand showed an increase in the tip resistance for both the 30 and 60-day tests. A comparison of the tests is provided in Figure 5.5. The strength increase could be attributed to cementation, but Lee (1982) and Morioka (1999) suggest not to jump too quickly to the assumption that cementation is fully responsible for the effect of strength increase without taking into account other effects.

Figure 5.4 shows an increase in the resistance from about 0.4 inches to 1.4 inches. This bulge is most likely due to a non-uniform layer with a higher density than the layers above and below it. The tip resistance increases and decreases symmetrically around the maximum tip resistance point. This behavior is not believed to be associated with behavior of cementation.

Figures 5.3 and 5.4 both show rapid increases and decreases in tip resistance in cemented sands. This relationship is shown as sharp horizontal lines or spikes on the graph and is believed to be caused by the cone breaking through cemented bonds. It takes more force to break through the bond, causing an increase in cone tip resistance. Once it breaks through, the tip resistance drops dramatically, causing the spikes on the chart. The increase in size of the spikes shows a momentary increase in strength of the cementitious bonds between grains. It is relatively small in the 30-day cemented specimen, but is much more apparent in the 60-day specimen.

A comparison of the frictional resistance of the three tests on Waikiki sand is shown in Figure 5.5. The decrease in frictional resistance in the 60-day specimen shows that the sand was less likely to move back toward the cone sleeve after the tip passed through. This means that a cohesive bond is holding back the sand. The cohesive bond is a result of the increase in cementation in the older specimens resulting in less frictional resistance than for the uncemented specimen.

Rad (1986) discusses this same effect in artificially cemented silica sands. Rad found that if you increase the level of cementation, the tip resistance increases as the frictional resistance decreases. He also concluded that cementation has similar effects in cone tip resistance results as increasing the density. Since the friction ratios were lower,

it is safe to conclude that the increase in strength is related directly to the increase in cementation of the specimen.

5.4 CPT RESULTS FOR EWA SAND

Figures 5.6-5.8 show mini-cone test results for the Ewa sand. The Ewa sand showed little if any increase in the tip resistance for both the 30 and 60-day tests. A comparison of the tests is provided in Figure 5.9. Differences in tip resistance between unaged and 60-day relative to 30-day in the 1 to 2 inch region of penetration are not considered to be representative of differences in strength due to aging. They are most likely due to variation in density in the bottom of the 30-day specimen.

The lack of strength increase in the tip resistance in the Ewa sand is comparable to the Static Triaxial results discussed in Chapter 4. The weak bonds formed in the Ewa sand do not provide a pronounced increase in strength like that seen in the Waikiki sand. Morioka (1999) also saw a lack of static strength increase in aged specimens of sand from the coastal plains of Oahu. Evidence of reduced friction on the cone sleeve was inconclusive.

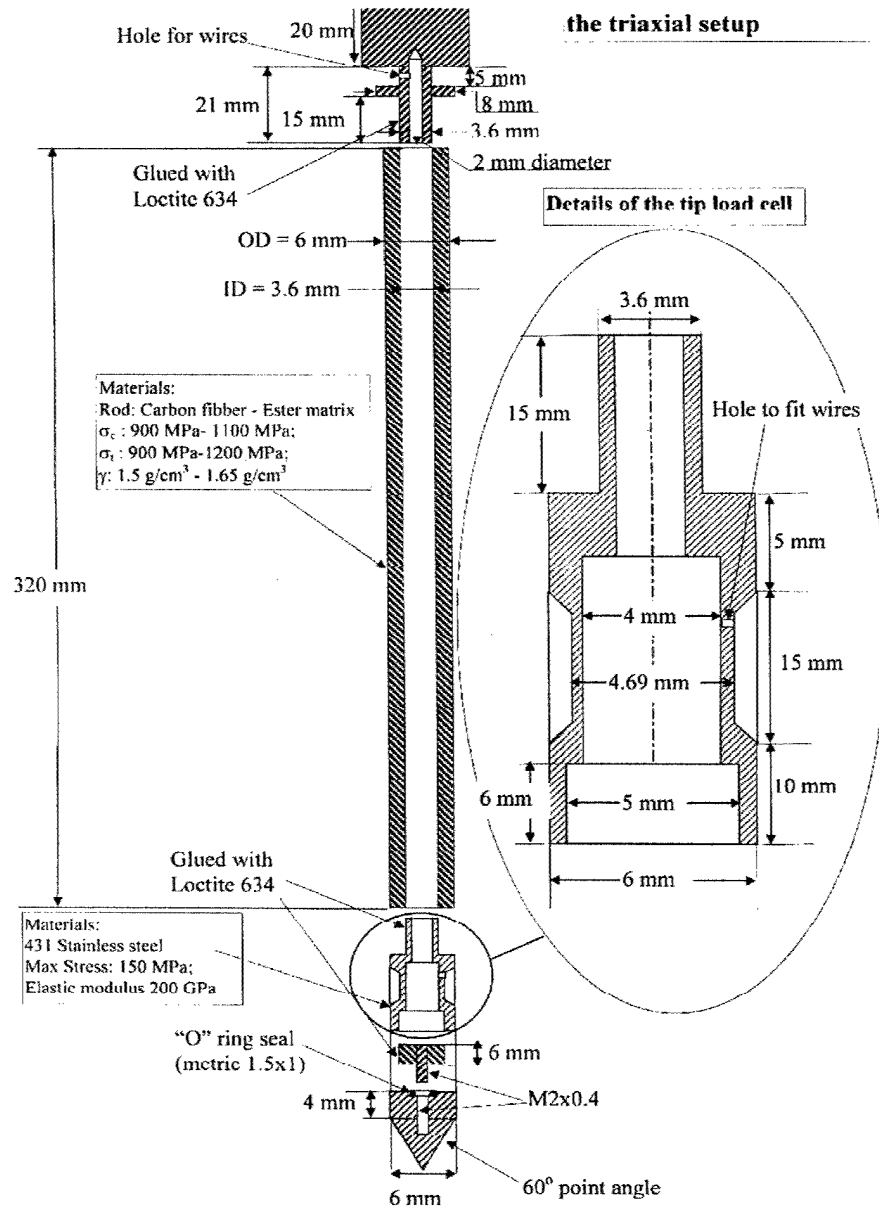


Figure 5.1- Schematic of 6mm Mini-cone Used in Testing

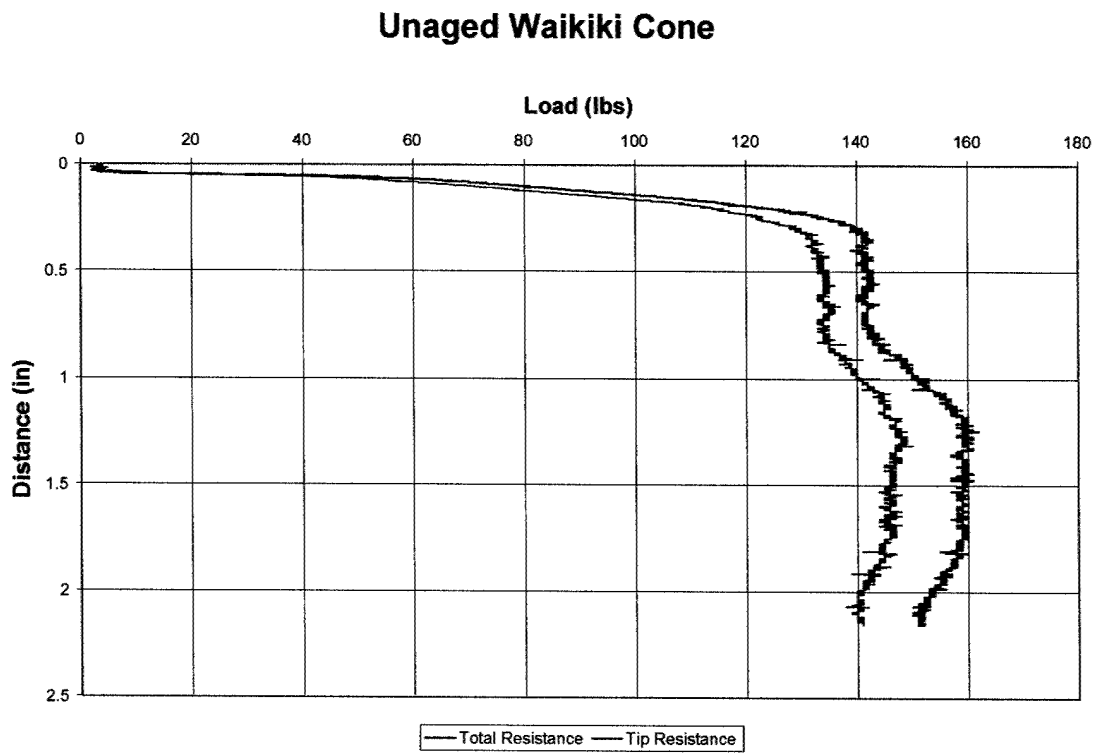


Figure 5.2 – Mini-CPT Results in Unaged Waikiki Sand

Waikiki 30-Day Cone

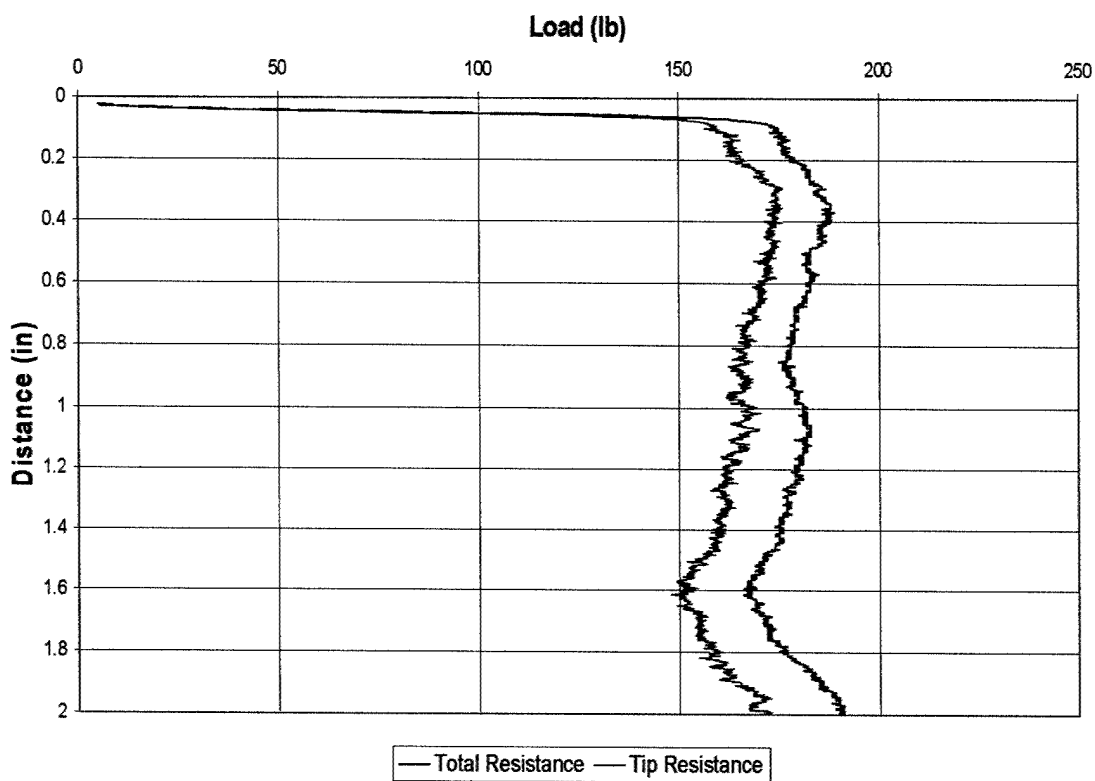


Figure 5.3 – Mini-CPT Results in 30-Day Cemented Waikiki Sand

Waikiki 60-Day Cone

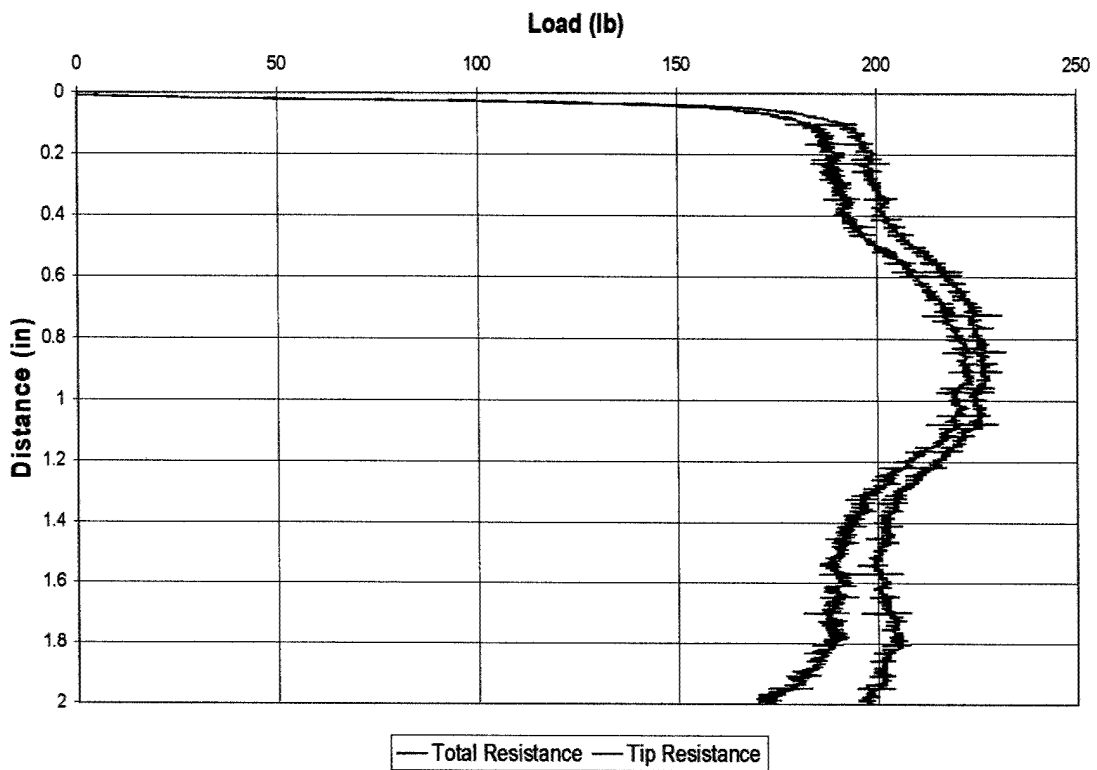


Figure 5.4 – Mini-CPT Results in 60-Day Waikiki Sand

Waikiki Cone Comparison

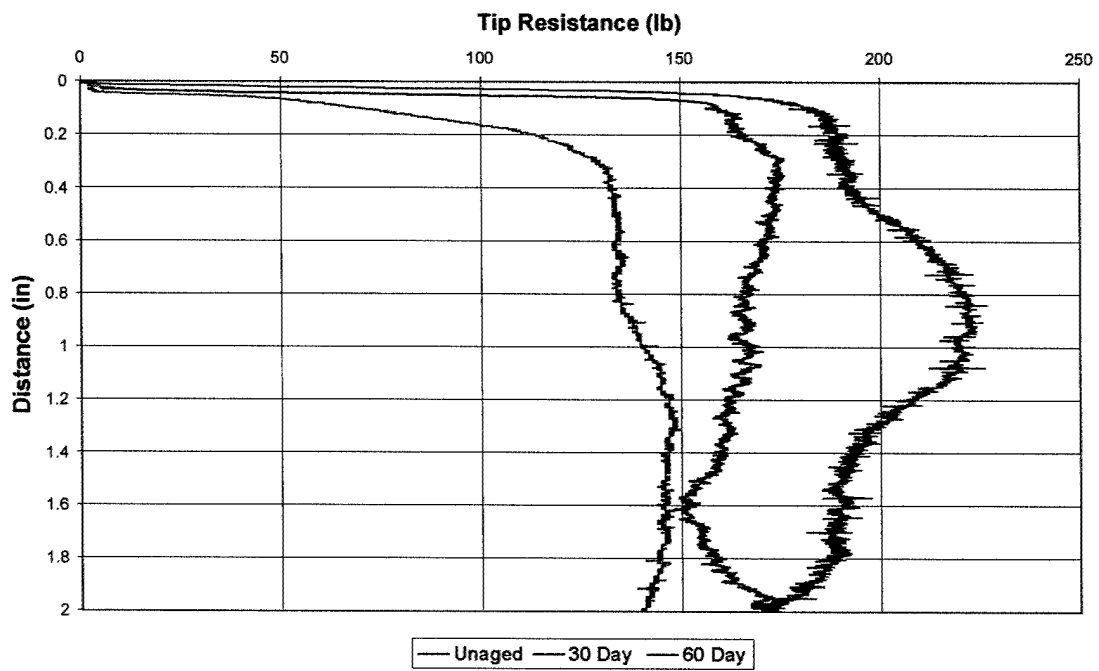


Figure 5.5 – Comparison of Mini-CPT Results in Waikiki Sand

Ewa Unaged Cone

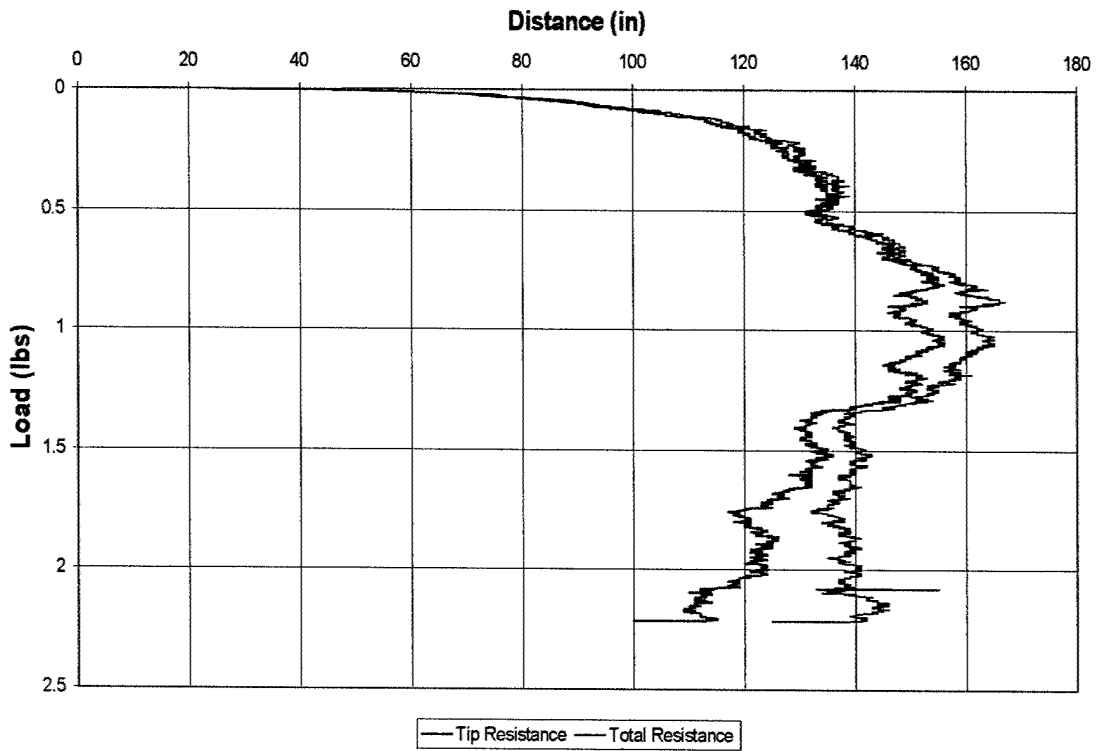


Figure 5.6 - Mini-CPT Results in Unaged Ewa Sand

Ewa 30-Day Cone

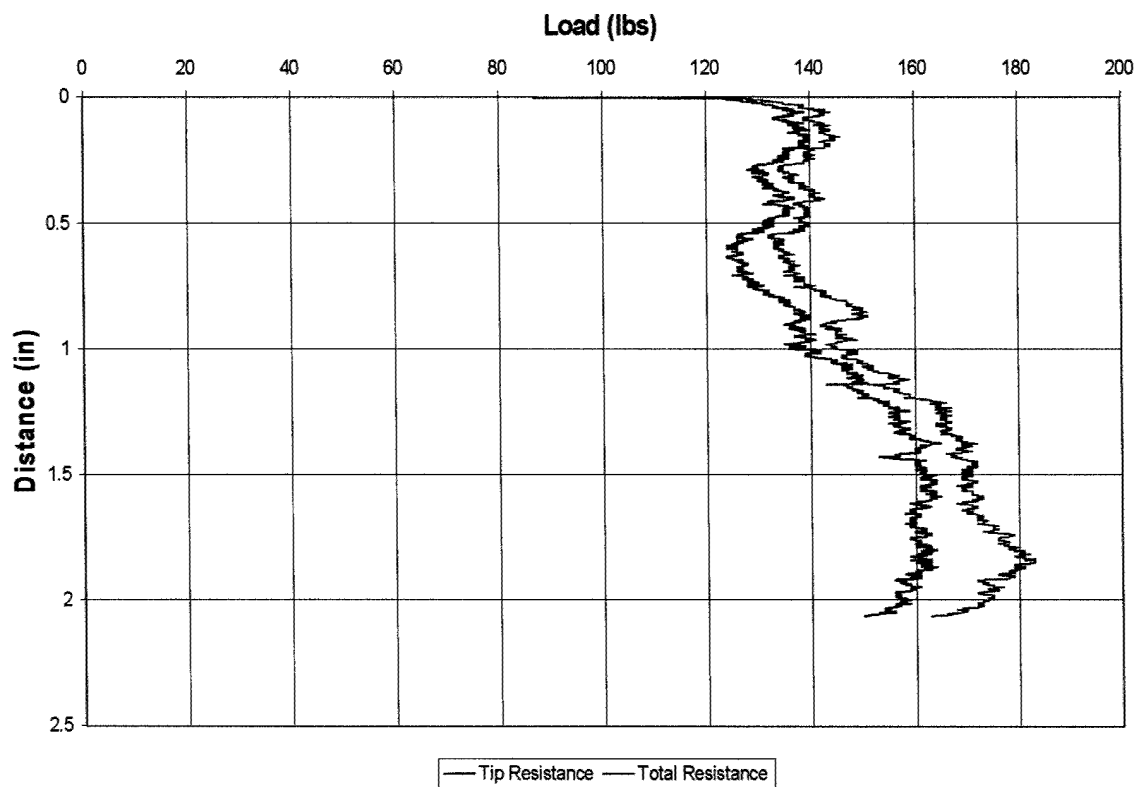


Figure 5.7 - Mini-CPT Results in 30-Day Ewa Sand

Ewa 60-Day Cone

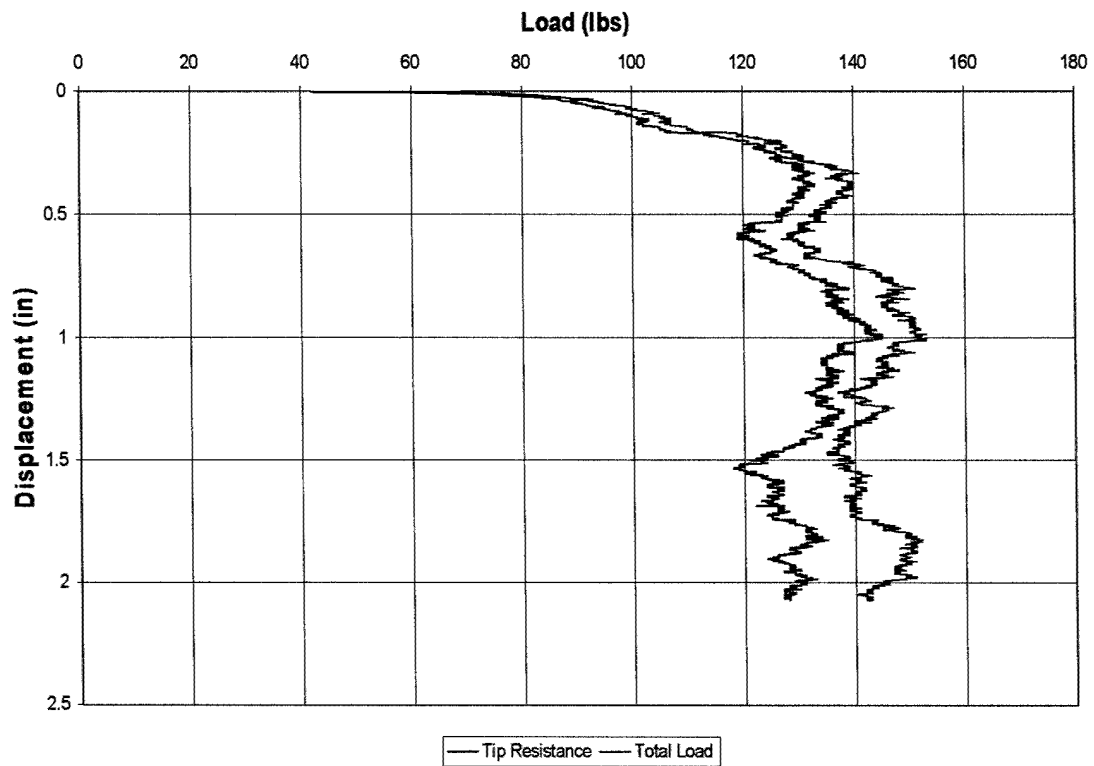


Figure 5.8 - Mini-CPT Results in 60-Day Waikiki Sand

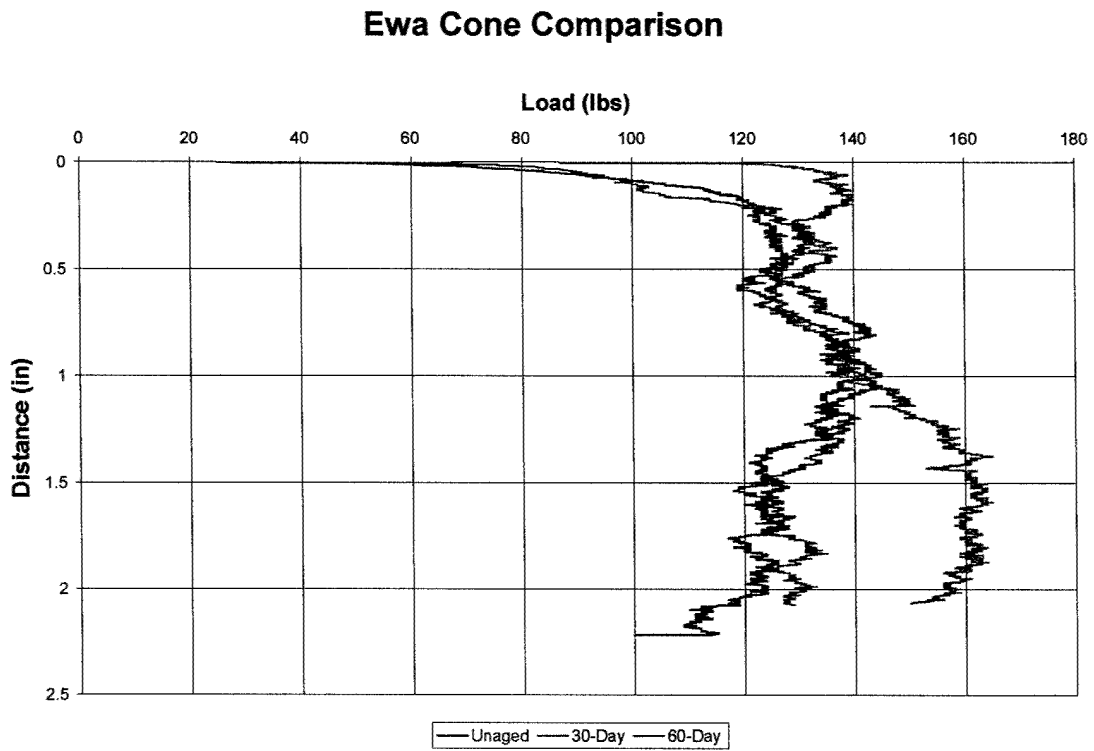


Figure 5.9 – Comparison of Mini-CPT Results for Ewa Sand

CHAPTER 6 SCANNING ELECTRON MICROSCOPE IMAGING

The Scanning Electron Microscope (SEM) was used in this research program to observe the intergranular behavior and mechanics of bonding of the calcareous sands tested. The microscope has the capability of providing image magnification of up to 300,000.

Magnifications of this level were not necessary for this study. The largest magnification used was 3000, and pictures were taken at various magnifications normally starting at 500 and moving up to 2000.

To take the pictures, a filament inside the microscope sends a beam through electromagnetic lenses onto the specimen. The specimen then emits its own electrons, which are gathered in a detector inside the chamber. This detector sends an image to a screen that can be seen by the operator of the SEM to determine the level of magnification and orientation of the beam. The beam can become finer or larger depending on the amount of magnification required and allowed by the specifications of the specific microscope. Chemical make-up of a specimen can also be determined by the SEM, but was not done because the carbonate content and basic mineralogy was already known prior to the taking of photographs.

6.1 SPECIMEN PREPARATION

Individual specimens were prepared to represent each of the variable parameters tested in the study. The specimens were prepared in small metal containers with a diameter of about one inch. These containers were thoroughly cleaned and scrubbed with acetone to clean off any human oils transferred to the specimen container. After acetone cleansing, rubber gloves or tongs were used in touching the container. Sand was placed in these containers and compacted using a small tamper so that the density of the specimens was

consistent with densities from the triaxial and cone tests. Water was then added to saturate the specimens. A rubber membrane was cut to fit over the top of the container and sealed with an o-ring. Finally, specimens were labeled and placed in a sealed triaxial cell under one atmosphere of pressure.

Six specimens were made for SEM photography. Aged specimens of thirty and sixty days were made for both sands as well as unaged ones. A thin carbon coating was then applied to the specimens to make them electrically conductive. This coating allows the specimen to emit the electrons needed to make the clear images. Once the carbon coating was on the specimen, they were placed in the microscope chamber for imaging.

Just prior to carbon coating, the prepared saturated specimens were oven dried to halt cementation processes and to remove excess conductivity not associated with the coated grains. The effects of oven drying are unclear at this time. It has been suggested that oven drying would precipitate the calcium carbonate back onto grains of sand. This could possibly distort images, although no distinct differences were seen between aged and unaged specimens. It is recommended that future research utilize other methods of preparing specimens for SEM photography.

The microscope was only capable of taking pictures on the surface of the specimen. The intergranular bonds between grains that rested on top of each other were not imaged. The only images taken were grain to grain contacts on the surface level. While scanning the pictures, it was critical to check the shadows and light reflections of the microscope to make sure the two grains were actually touching each other and not one grain touching another grain behind it. In some instances, the grains were touching each other, but the bonds between them could not be clearly seen because of angle

limitations allowed by the specimen container. These characteristics will become evident from the SEM images presented in this paper.

6.2 WAIKIKI SAND IMAGING

Images of the Waikiki unaged sand are shown in Figures 6.1-6.4. The pictures show several things not obvious to the naked eye. Grain characteristics such as porosity from intraparticle voids, angularity and structure are very evident with the magnification of the SEM. Figure 6.1 displays a mixture of angular particles and one with a plate like structure synonymous with bioclastic sands.

It is important to note that there were no additives to the specimens that were tested or photographed. These specimens were naturally cemented together, without any additional cementing agent provided. This means that in the presence of water, some precipitated calcite or aragonite went back into solution. It then precipitated on other particles and between the grains. Although this adds strength to the specimen, taking away CaCO_3 from other places may also be detrimental to the specimen, especially when it is pulled from the intraparticle voids. It should also be noted that this type of testing is not representative of the natural environment of the sands, where CaCO_3 is likely already in the water solution. Further testing should be performed to initiate the cementation of calcareous materials in an environment more closely representative of the natural setting.

Figure 6.4 shows the pores being filled from the inside out, although not all grains will act the same way. Here cement can be seen filling in the voids which most likely occurred prior to the material being sampled. This procedure reduces the amount of intraparticle voids and reduces the amount of grain crushing. Price (1988) found that two things could occur when pores are cemented over. The pores could be covered, but the

voids on the inside left unfilled, causing the density and porosity of the sand to be lower and the particle more susceptible to grain crushing. The second possibility is that the pores and the voids are all filled. This would greatly increase the stiffness and strength of the sand, as well as greatly reducing the porosity and potential for grain crushing. It should be noted that grain crushing is still a factor at higher strains because the cementitious bond is formed from CaCO_3 , which as mentioned in Chapter 3, is much softer than silica or quartz.

Images from the thirty and sixty day specimens were taken at various magnifications to show the intergranular behavior as well as zooming in on the cementation bonds between the grains. This was found necessary because when very high magnifications are used, all that can be seen is the cementitious bond and not the grains attached by the bond. Much can be learned from both sets of pictures. Analyzing the pictures from a lower magnification can show how the bonds between grains are formed. Bonds are only formed between touching grains, and because of the high angularity of the grains, they are not touching in many places.

Figures 6.5-6.7 show the cementation developed after aging thirty days. The cementitious bonds were apparent throughout most of the specimen. Cementation can be seen coating individual grains as well as forming cohesive bonds between particles. The CaCO_3 cement has an appearance very similar to a smoothed finish concrete. Figure 6.8 show cementation occurring on many of the grains. The cement appears to remove some of the roughness of the particle. The cement on the grains is very 'patchy' and does not seem to negatively affect the angularity of the particles.

Figures 6.9-6.11 show the cementation developed after aging sixty days. The figures show the increase in cementation from the thirty day specimens. These figures show evidence of layering and strengthening of the cement bonds between grains. This layering is important because it shows that as the time of aging increases, the bonds between the grains have strengthened. This theory coincides with triaxial and cone penetration test data discussed in the previous chapters. The SEM helps us to see the voids still left and the small amount of intergranular connectivity caused by the angularity of the particles. The cement on the grains also shows evidence of increasing. With this being true, it would seem reasonable to assume the CaCO_3 used for the cement is coming from the grains and not from the already cemented areas.

6.3 EWA SAND IMAGING

Figures 6.12 -6.14 are a good representation of the Ewa sand. The grains are very angular like the Waikiki sand, but the porosity and outer layer of the sands is very different. The grains seemed to be coated over with grainy crystal-like structures overlying a center grain. As opposed to the Waikiki sand, the Ewa sand was harvested on land. This sand was probably formed during or before the Pleistocene period, which was about a million years ago. It is interesting to note the lack of pores on the grains.

Pictures of the thirty day aged specimens are shown in Figures 6.15-6.23. Each example of cementation was taken at magnifications of 200, 500, 1000, and 2000. The lower magnification pictures show the angularity of the particles and how bonds form from the connections of the grains. The higher magnifications focus in on the bond created between the grains of sand. Cemented bonds like those in the Waikiki sand are not present in the Ewa sand. It is clear that bonds between the sand have been formed,

but little evidence of cement is present. Semple (1988) suggested that in the absence of a cementing agent, the particles engage in a material exchange. From looking at the pictures taken by the SEM, it appears that a material exchange is the means of bonding for the Ewa sand as the bonds between the grains are of the same material, or same characteristics, as the grains themselves and show no evidence of precipitated CaCO_3 "cement."

Figure 6.15 shows the 200 times magnification of two grains of sand. The bonding is very clear in the middle section of the picture and at the bottom of the picture between the grains. These bonds are shown in Figures 6.16, 6.17, and 6.19. It is not apparent that cementation is occurring between the two grains shown in Figure 6.15. It appears the grains are touching, and one might assume cementation is occurring, but shadows discussed in the introduction of the chapter exist here and a clear grasp of what is occurring can not be obtained.

The light/shadow effect can also be seen in Figures 6.20 and 6.21. A small bond can be seen between these two grains and is shown in Figures 6.22 and 6.23. Again, this bond seems to closely resemble the bonds seen in Figures 6.15-6.19,

Sixty day images can be seen in Figures 6.23-6.25. They look very similar to that of the thirty day aged specimens. IN figures 6.23-6.25, the light/shadow effect clearly shows two grains that are close, but not touching with the exception of the bonds created between them. This specific trait was not seen in the Waikiki sand, although that is not to say it does not exist.

The sixty day images may not have cemented as well as they possibly could have. Upon removing the specimens after aging for oven drying, a bubble was detected in the

membrane in the sixty day specimen that may have reduced the effective confining pressure of the specimen. If it was a water bubble from saturation on the surface of the sand and not an air bubble, than the effective confining pressure would not be affected. The specimen's ability to cement seemed unharmed, although because of angularity and limited visibility, it is unclear whether the magnitude of cementation was affected because of this flaw.

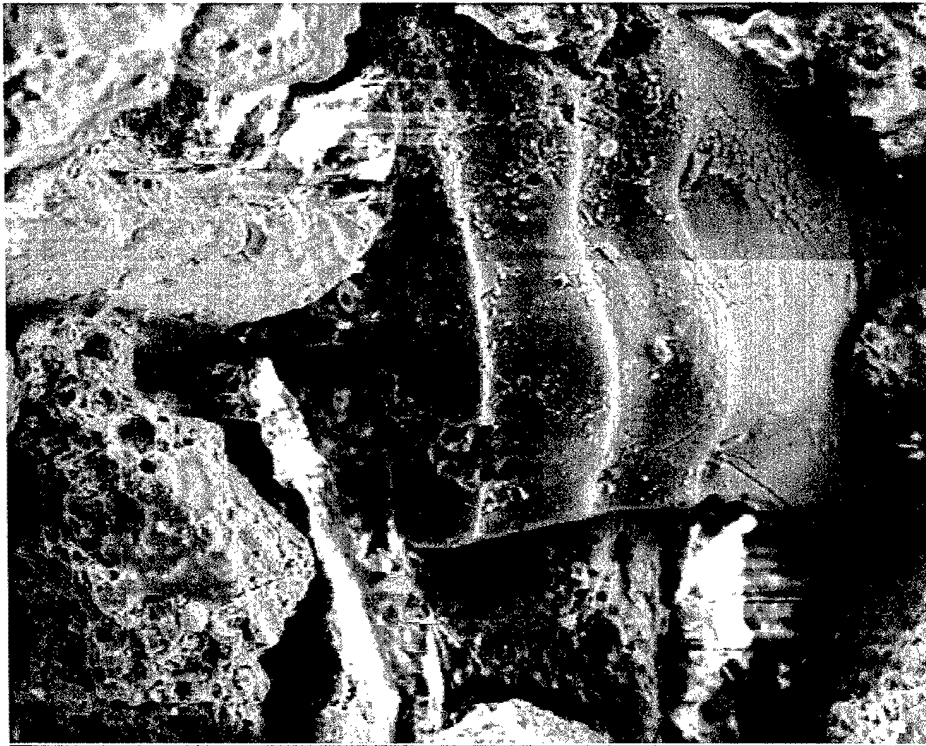


Figure 6.1 – Waikiki sand image at 200x magnification.

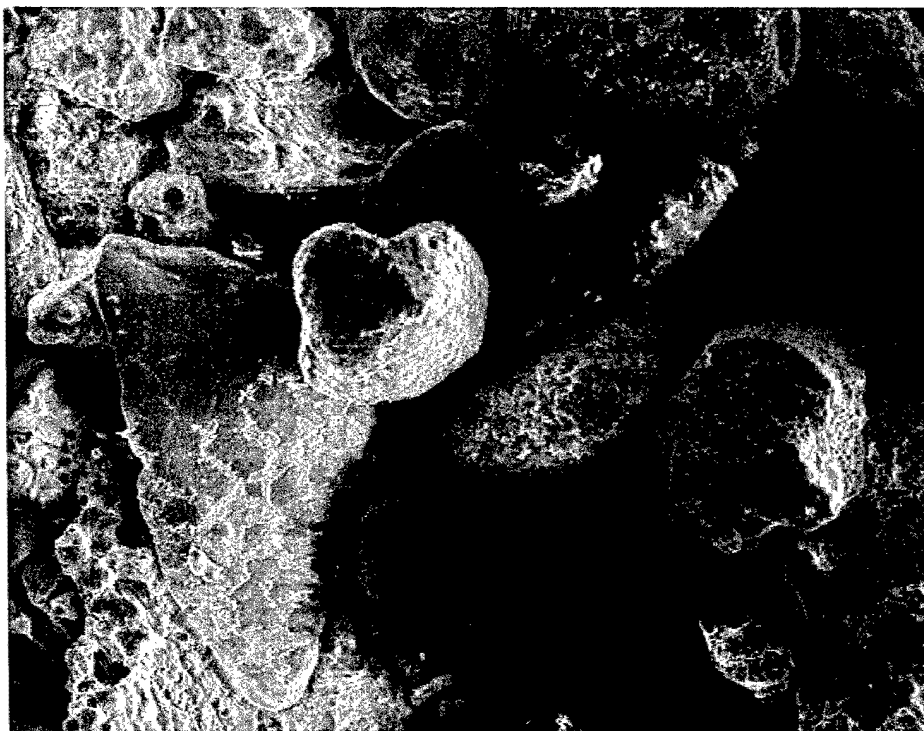


Figure 6.2 – Waikiki unaged sand at 100x magnification.

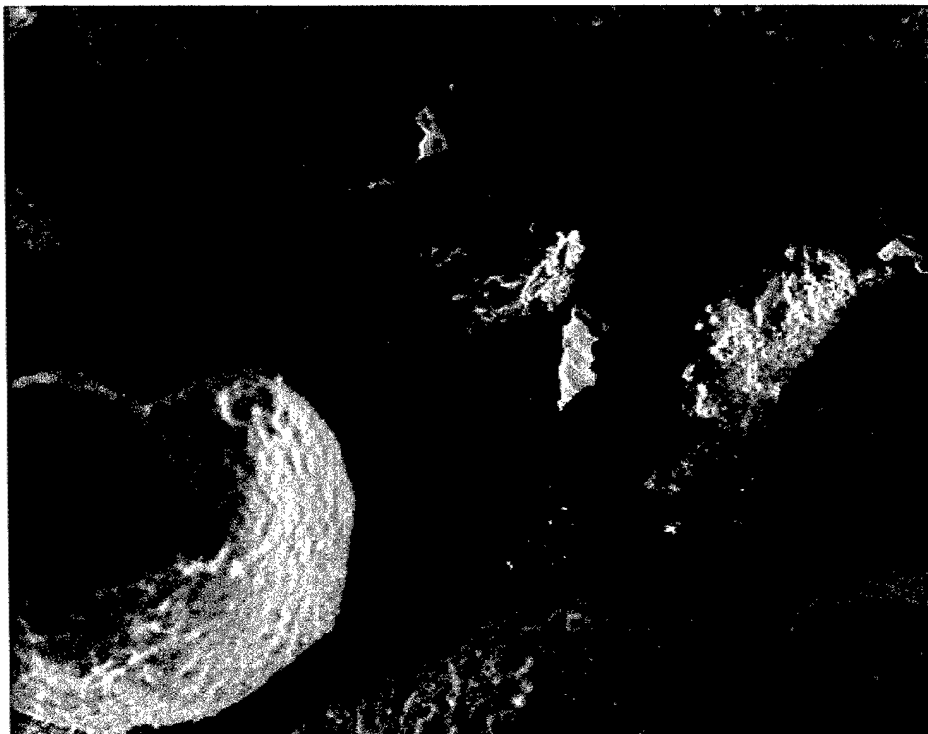


Figure 6.3 – Waikiki unaged sand at 200x magnification.

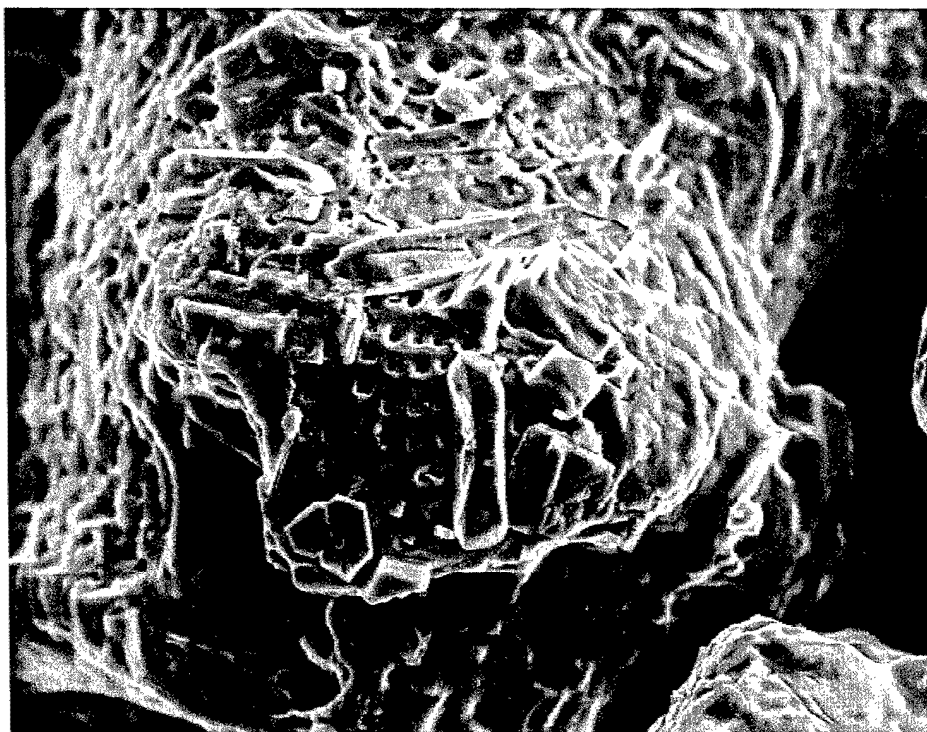


Figure 6.4 – Waikiki sand with cement filled pores at 500x magnification.

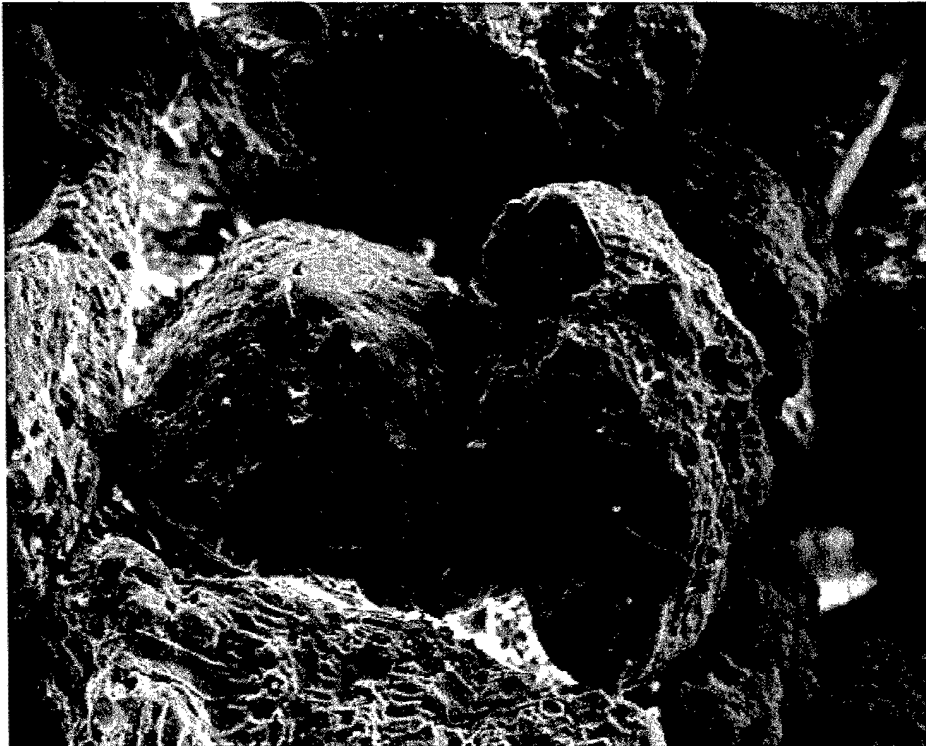


Figure 6.5 – Waikiki 30-Day cemented sand at 200x magnification.

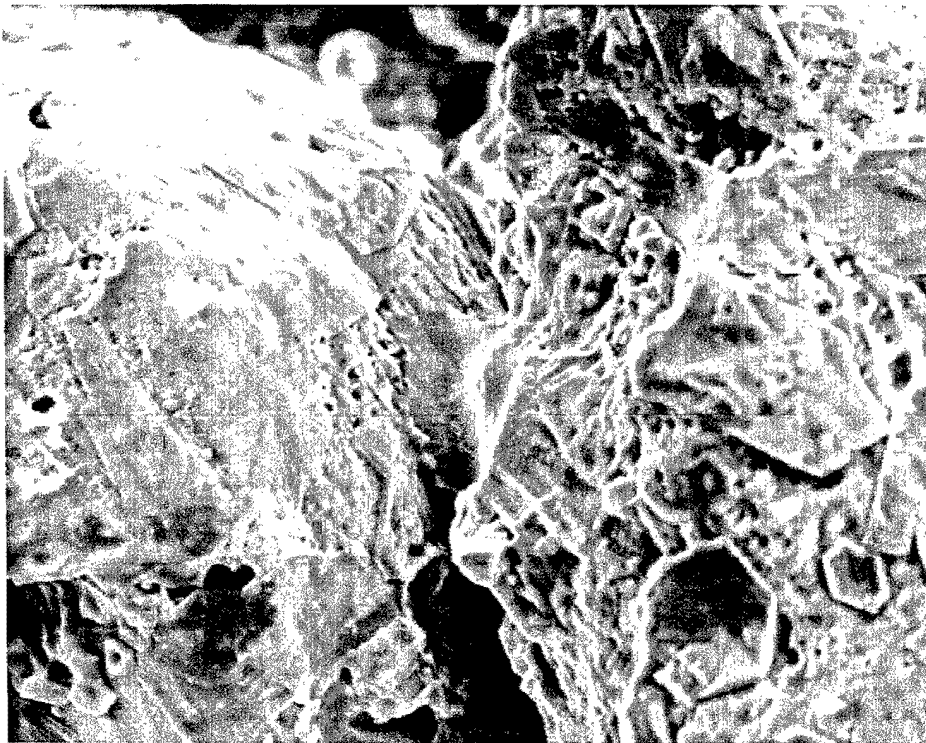


Figure 6.6 – Waikiki 30-Day cemented sand at 500x magnification.

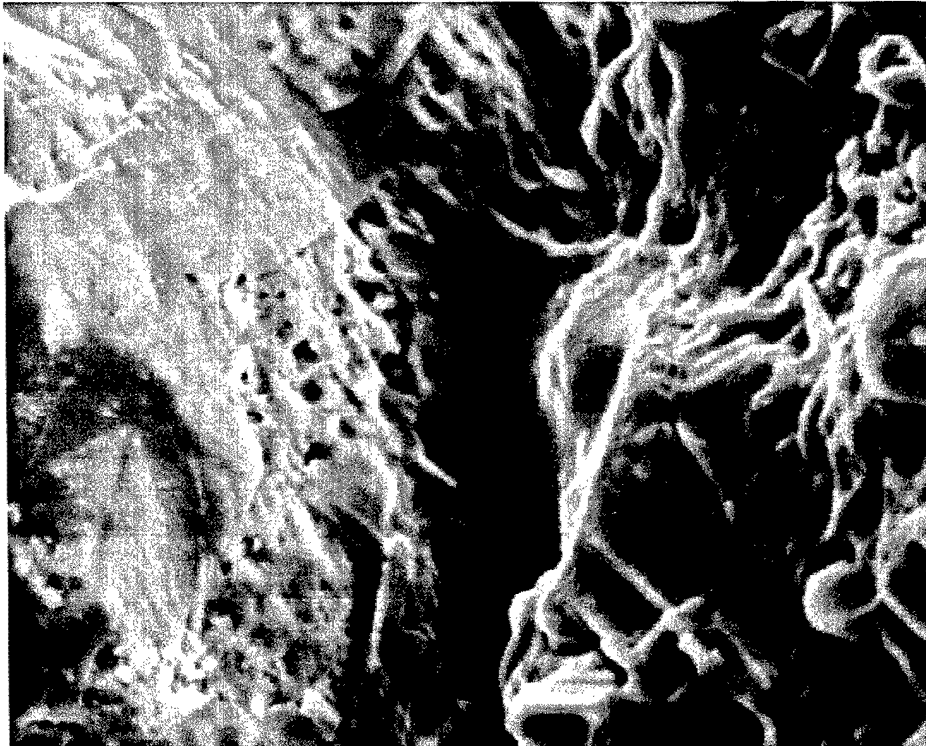


Figure 6.7 – Waikiki 30-Day cemented sand at 1000x magnification.

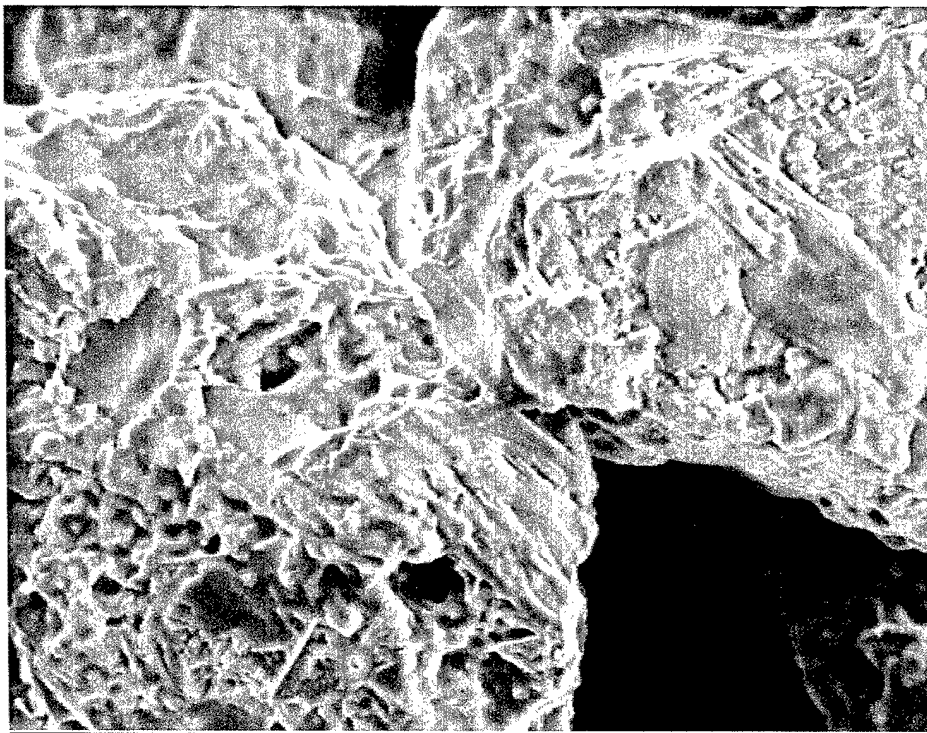


Figure 6.8 – Waikiki 30-Day cemented sand at 500x magnification.

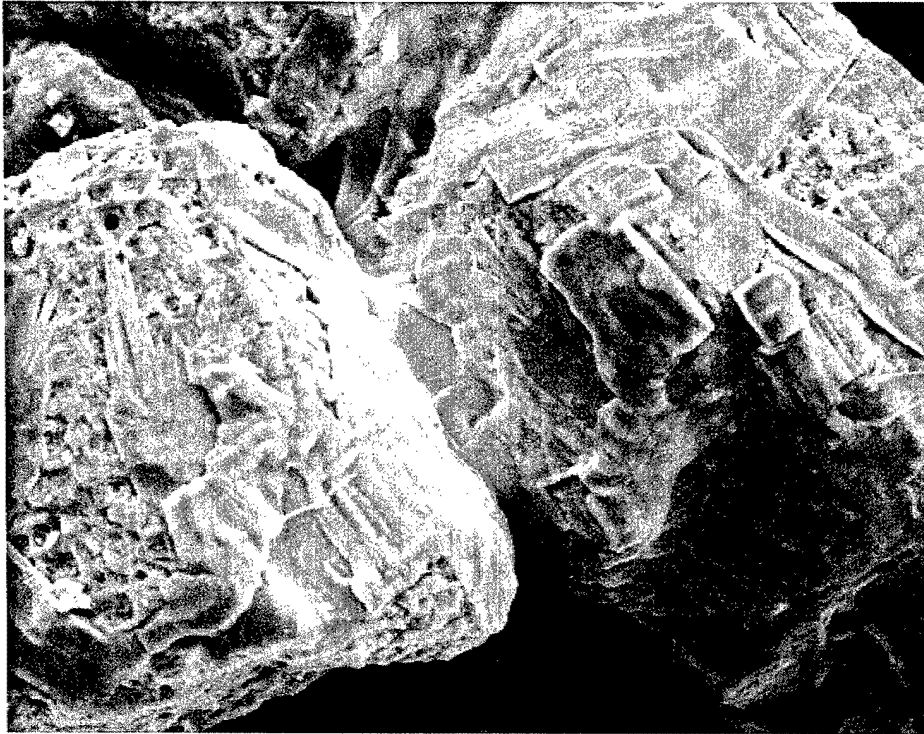


Figure 6.9 – Waikiki 60-Day cemented sand at 500x magnification.

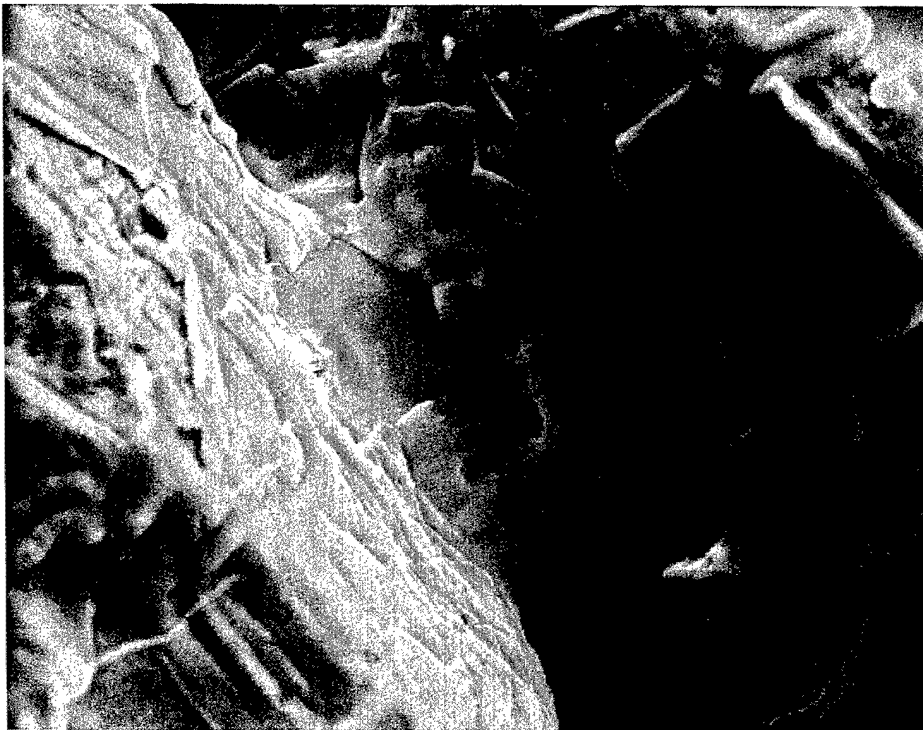


Figure 6.10 – Waikiki 60-Day cemented sand at 1000x magnification.



Figure 6.11 – Waikiki 60-Day cemented sand at 2000x magnification.



Figure 6.12 – Ewa unaged sand at 100x magnification.

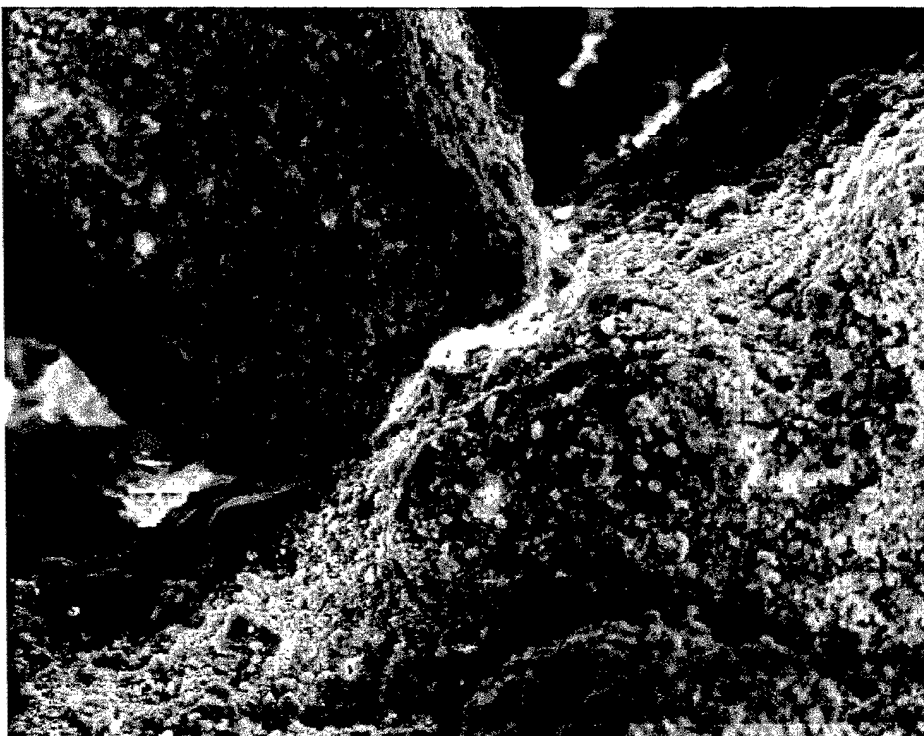


Figure 6.13 – Ewa unaged sand at 500x magnification.



Figure 6.14 – Ewa unaged sand at 1000x magnification.

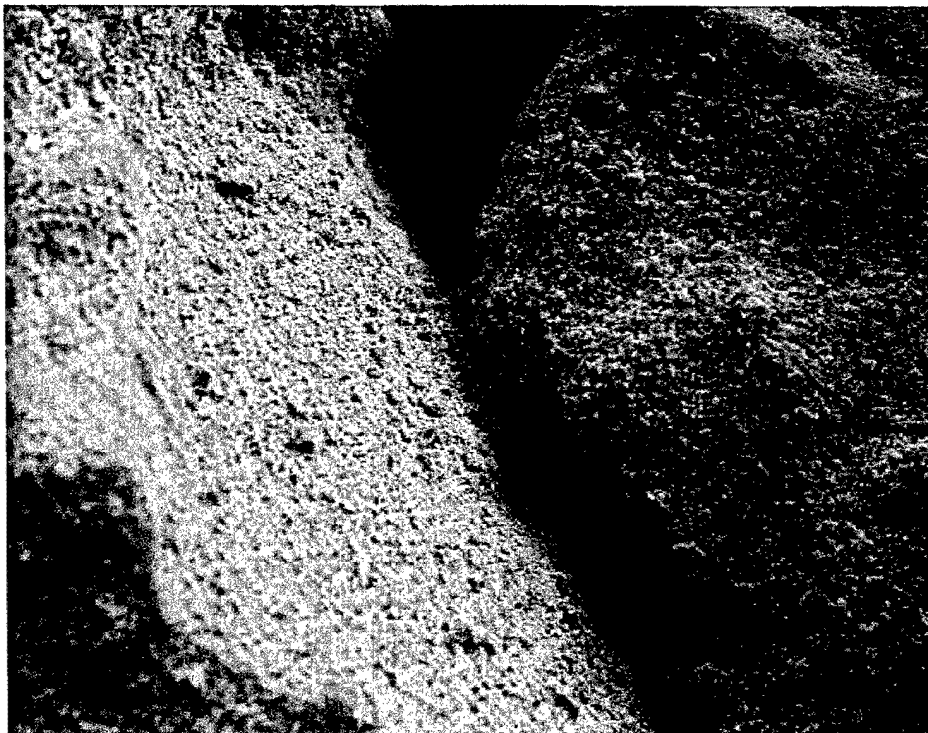


Figure 6.15 – Ewa 30-Day cemented sand at 200x magnification.

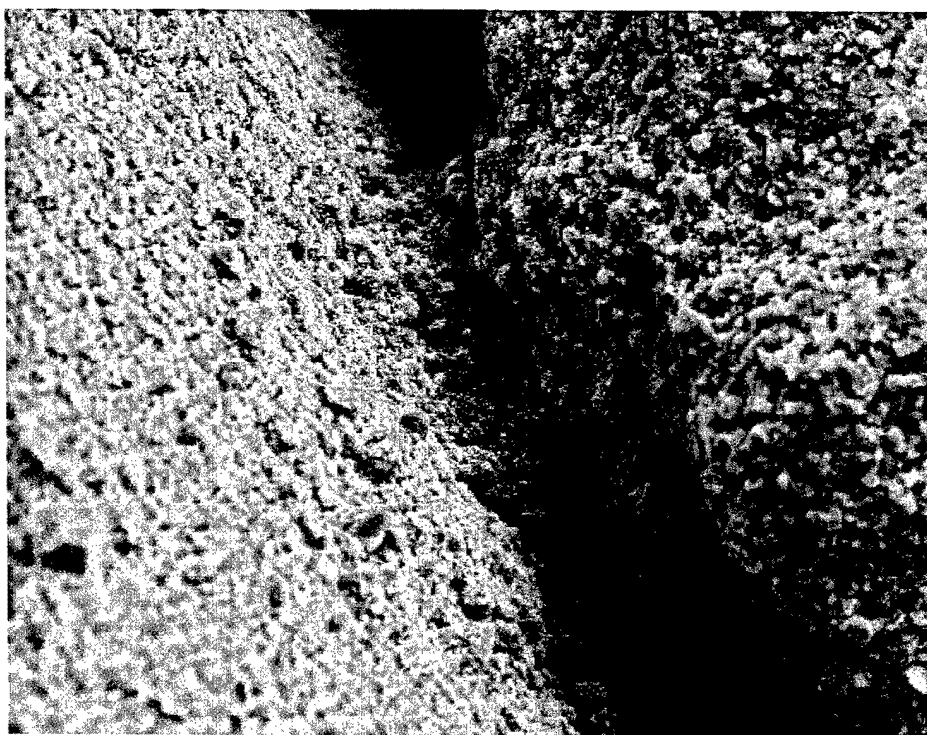


Figure 6-16 – Ewa 30-Day cemented sand at 500x magnification.

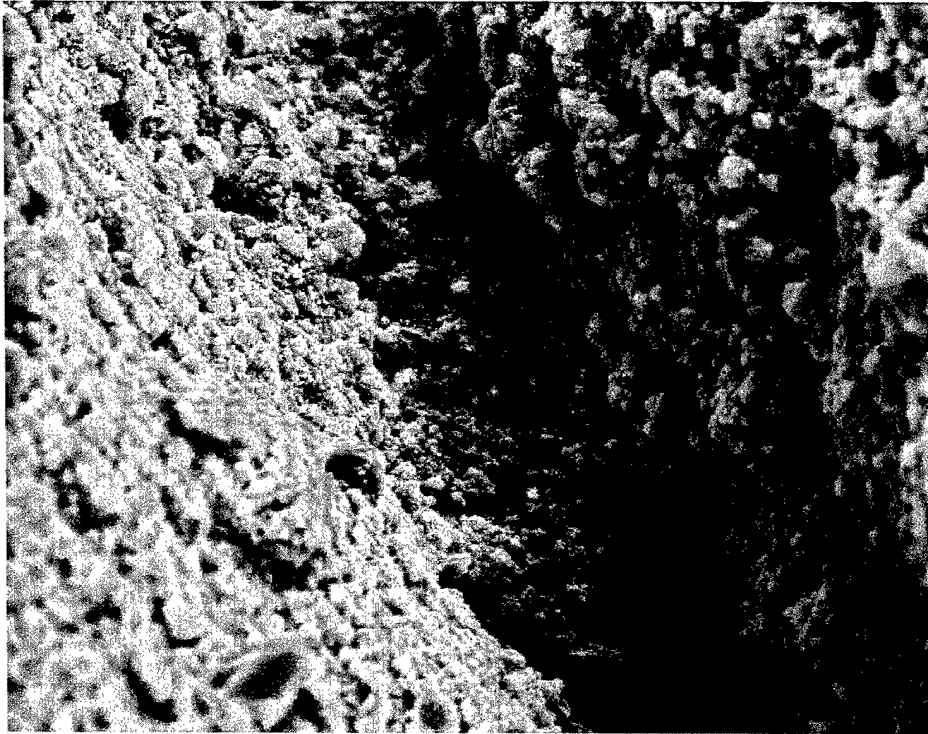


Figure 6-17 – Ewa 30 Day cemented sand at 1000x magnification

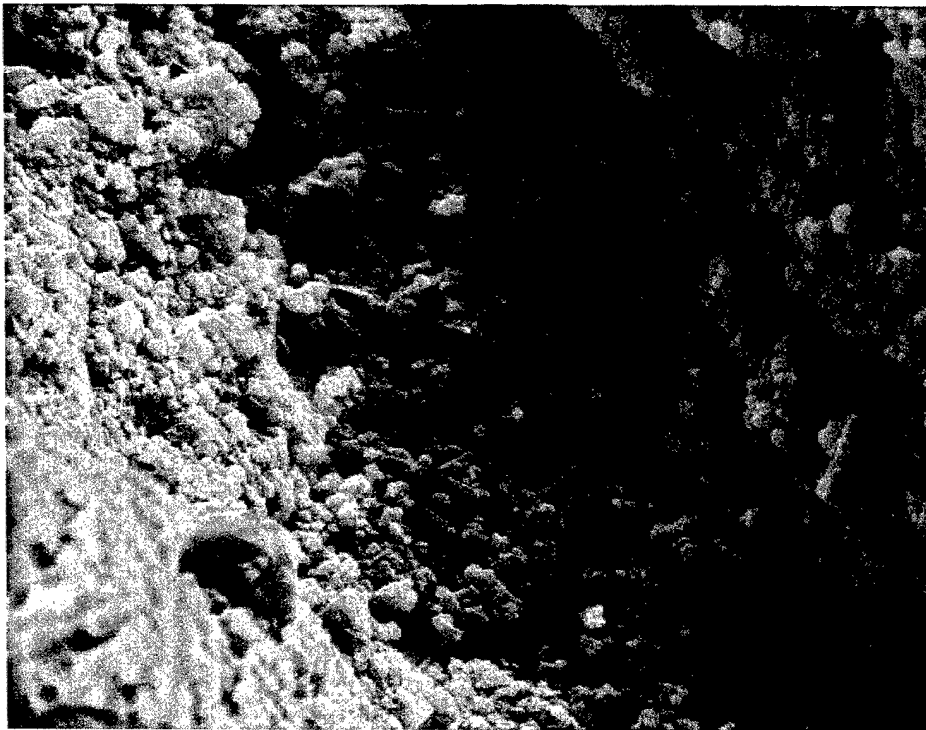


Figure 6-18 – Ewa 30-Day cemented sand at 2000x magnification.

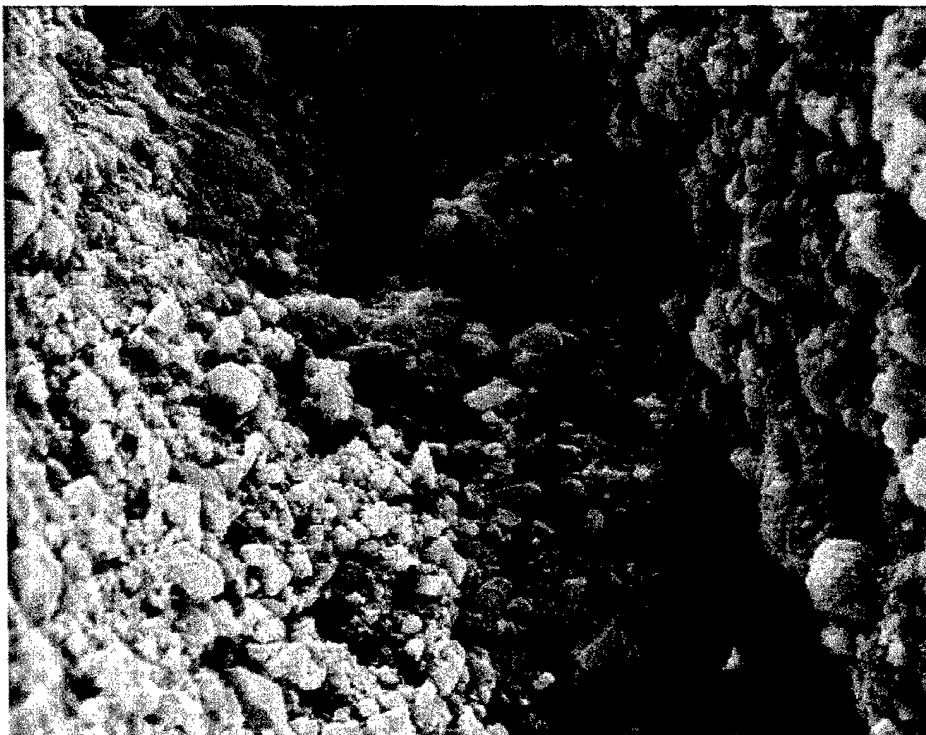


Figure 6-19 – Ewa 30 Day cemented sand at 2000x magnification.

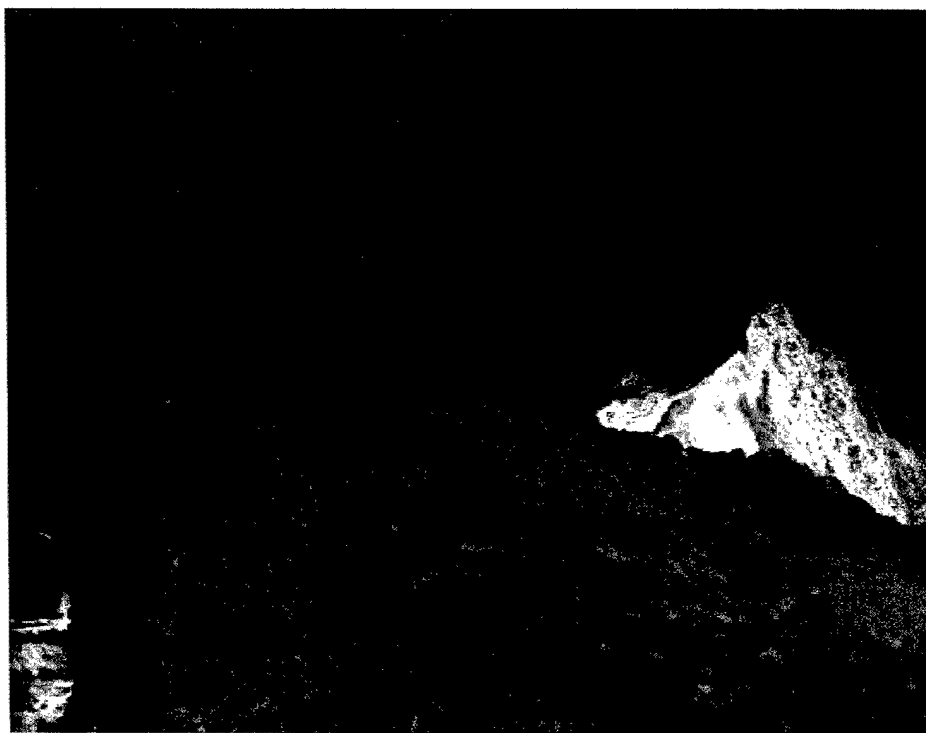


Figure 6-20 – Ewa 30-Day cemented sand at 200x magnification.



Figure 6-21 – Ewa 30-Day cemented sand at 500x magnification.

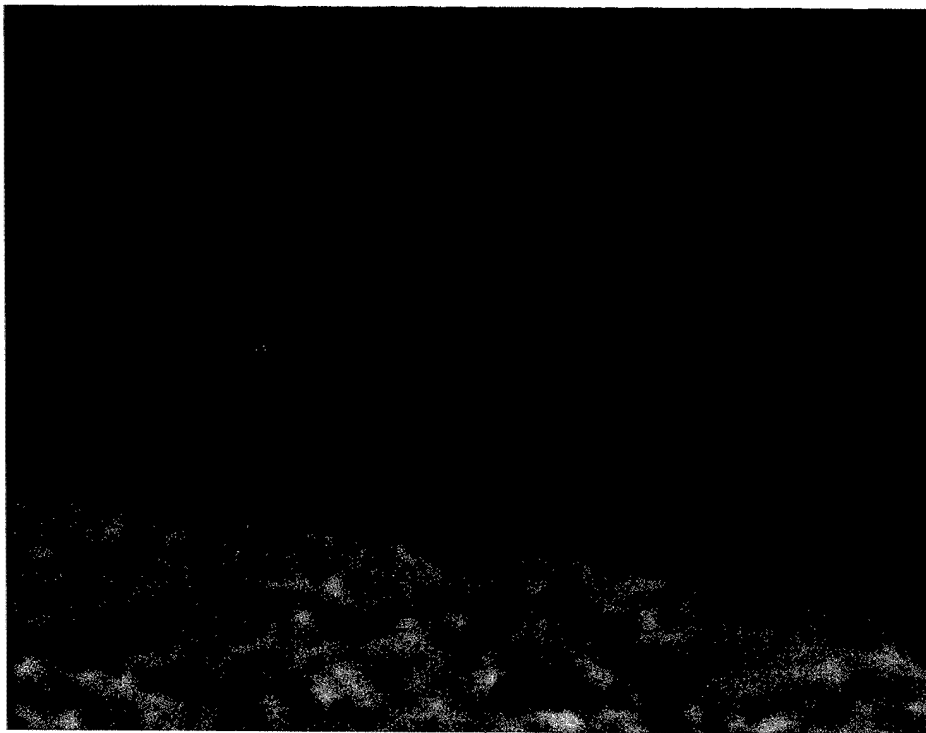


Figure 6-22 – Ewa 30-Day cemented sand at 1000x magnification.

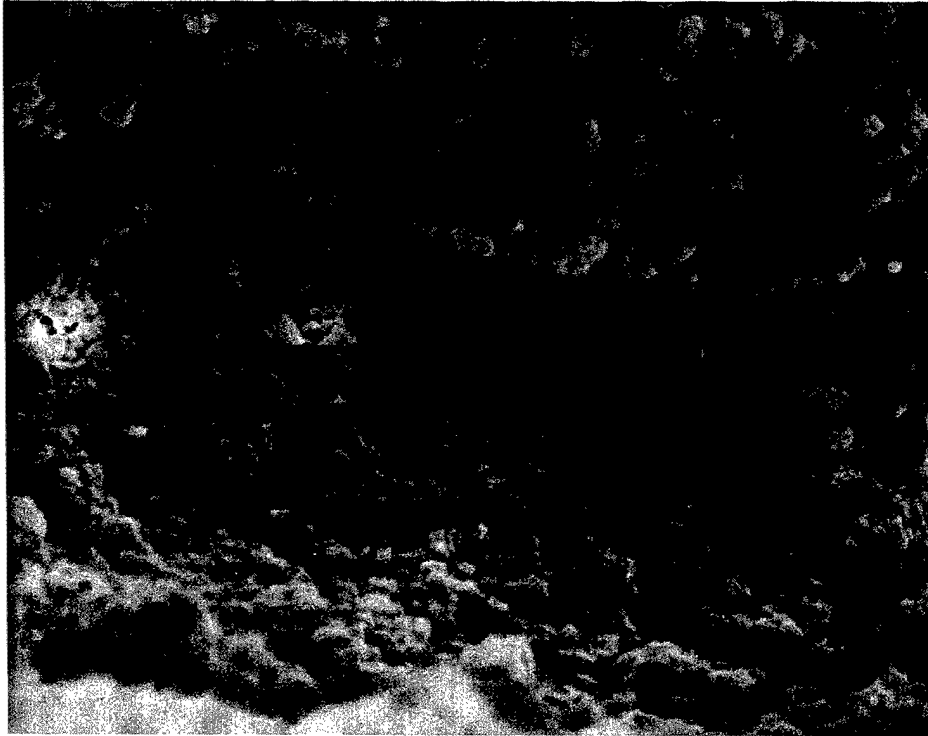


Figure 6-23 – Ewa 30-Day cemented sand at 2000x magnification.

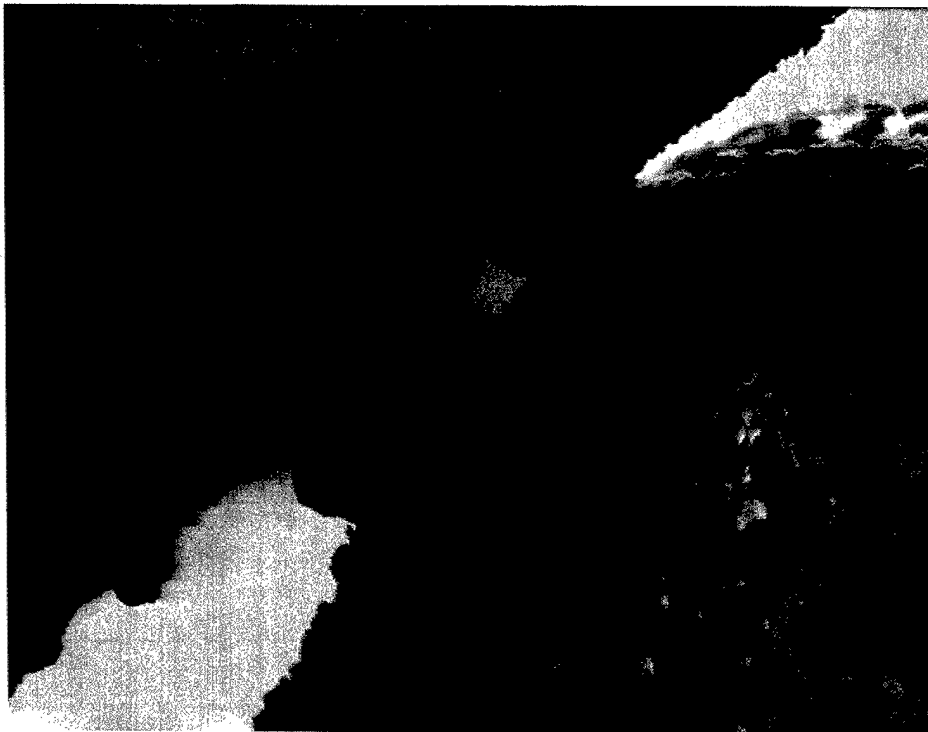


Figure 6-24 – Ewa 60-Day cemented sand at 1000x magnification.



Figure 6-25 – Ewa 60-Day cemented sand at 2000x magnification.

CHAPTER 7 SUMMARY AND CONCLUSIONS

7.1 CONCLUSIONS

Testing results are summarized in Tables 5 and 6. It was originally a surprise to see the coarser, Ewa sand have less strength than the finer, Waikiki sand. Generally coarser materials have higher strengths. The unexpected strength is attributed to the angularity and composition of the two sands. Although the Ewa sand is coarser, it has greater volume for intraparticle voids to occur, and therefore greater susceptibility to grain crushing. The fineness of the Waikiki sand makes it hard to notice the angularity of the particles, which were shown by the SEM to be more angular than the Ewa sand.

| TEST | EWA SAND | WAIKIKI SAND |
|-----------------|---|--|
| Static Triaxial | Very little increase in strength with aging | Increase in strength with aging |
| Cyclic Triaxial | Larger increase in liquefaction resistance | Significant increase in liquefaction resistance, but smaller than Ewa |
| CPT | No noticeable increase in tip resistance | Noticeable increase in tip resistance and possible evidence of cementation |
| SEM | Helpful in ID of grain characteristics and bonding mechanisms | Helpful in ID of grain characteristics and bonding mechanisms |
| Cement Bond | Grain-sharing or material exchange | Noticeable calcium carbonate cement bond |
| Angularity | Less angular | More Angular |

Table 5 - Summary of Test Results.

| Sand | Age | c | ϕ |
|---------|--------|-----------|--------|
| Waikiki | Unaged | 15 kPa | 39.4° |
| | 30-Day | 97.4 kPa | 39.7° |
| | 60Day | 125.5 kPa | 37.2° |
| Ewa | Unaged | 15 kPa | 36.9° |
| | 30-Day | 31.3 kPa | 36.9° |
| | 60Day | 37.5 kPa | 36.9° |

Table 6 – Summary of Static Test Results

While the greater angularity of the Waikiki sand appeared to have increased strength, it decreased the resistance to liquefaction. Based on the static results, the Ewa sand having a higher resistance to liquefaction was a surprise. At the same D_r , the angularity of the Waikiki particles resulted in less grain to grain contacts, which possibly limited the amount of cementation and the resistance to liquefaction. However the significant increase in liquefaction resistance after little increase in mini-cone and static triaxial testing was a surprise.

Cone tests were beneficial in showing the effects of light cementation in the Waikiki tests. Evidence of the cementation was seen in both the tip resistance and the sleeve friction. This was very useful in showing the increase in strength and reduction in sleeve friction coming from cementation. The lack of increase in tip resistance in the Ewa sand helped support the static test results. The static results showed a very small increase in the 30-day aged specimen, where the 60-day specimen had a larger increase, but also had a slightly higher density.

The SEM allowed a close look at the different types of bonding between grains. This was a very important step in advancing our understanding of natural, short term aging effects. Results from the SEM showed cementation in both sands at contact points between the grains. The Ewa sand displayed more grain sharing, whereas the Waikiki sand had a clear cement bond holding grains together. Cementation between two grains that were very close together, but not touching was seen in a specimen aged for 60 days. As stated in Chapter 2, Lee (1982) and Morioka (1999) both questioned whether the strength gain from aging was from cementation or other mechanical processes. The result of other mechanical processes causes more grain to grain contact, and may bring grains closer together. If left to age in an environment suitable for cementation, this would increase the strength through both mechanical and chemical processes.

The differences in types of cementation were seen through the SEM and may be the cause of the differences observed during testing of the two carbonate sands. The carbonate-cemented Waikiki sand displayed increased tip resistance, static strength and resistance to liquefaction with age and cementation. It also showed a reduction in sleeve friction values with age and cementation, all of which are traits of cemented sands. The Ewa sand showed relatively no increase in static strength and cone tip resistance, although it showed a large increase in resistance to liquefaction with age. The bonds formed by grain sharing may not be as strong as the carbonate cement bonds formed between the Waikiki sand grains, but are strong enough to resist the build up of pore pressures and increase resistance against liquefaction.

Examination of the vacuumed water during specimen preparation showed CaCO_3 being pulled from the specimen before a test was run. The dried material appeared to be

finer, although there was also evidence of a white powder in the pans after oven drying. Even though the particles had very high CaCO_3 contents, this change affects the density, cementation potential, and does not create a realistic environment for the calcareous material. In fact, this would suggest that the amount of cementation noted in this study may be conservative, and that in nature actual cementation may be higher.

7.2 FUTURE RESEARCH

The results of this research program have demonstrated that there are still many questions to be answered concerning calcareous sediments. Cementation and the degree of cementation leave many questions regarding the strength of calcareous sands. Many topics are being researched today, including different types of piles and their capacities in cemented sands, effects of terrigenous material in calcareous sediments, and many others.

Several things were intentionally not taken into account in this research. As mentioned in previous chapters, the test specimens were constructed in the laboratory and saturated with distilled water. The natural environment of calcareous sediments is in saline water at least partially saturated with calcite or aragonite. Also, because saturation with distilled water likely puts some of the calcite or aragonite back into solution, it is unclear how much was lost during the vacuum saturation period when several liters of distilled water were used in the deairing process. To limit the number of variables, CaCO_3 contents of both specimens were well above 90%, and only one density was used. The author proposes the following future research topics to further study the effects of cementation:

- A comparative study on the use of different saturation techniques to best represent the in situ environment of calcareous sediments. A comparison of

the effects of natural aging with salt water saturation, salt water with a calcite solution, and saturation with distilled water with a calcite or aragonite solution should be compared to distilled water. Temperature variation on specimens adds another dimension to this line of testing.

- A testing program at higher consolidation pressures utilizing the SEM to show the processes of cementation and grain crushing under higher confining stresses.
- Analysis of “undisturbed” lightly cemented specimens to compare the results of this report using SEM and static triaxial, cyclic triaxial and mini-cone tests.
- A comparative study on the cementation effects of terrigenous input into calcareous material.
- Further study on the effects of cementation on the reduction of skin friction in Calcareous sands.
- Focus on the cementation differences from calcareous material from different origins

The use of the SEM was shown to provide an important tool, and is recommended for all future testing with calcareous soils and cementation effects. Several methods of drying specimens should be examined to ensure oven drying does not distort images displayed in this paper. The SEM should be used after static and cyclic tests are run to see how the cement bonds react when the specimen fails. It should also be used after the cement bonds are broken to determine if the new grain structure becomes more angular or if the bond completely detaches from the grain.

Another question to be answered is whether the use of Portland cement or gypsum as an artificial cementing agent accurately depicts the cementation that would occur naturally over time? Clough (1989) said the use of Portland cement does represent the behavior of calcareous soils. Ismail et al. (1998) disagrees, stating that the use of Portland cement or gypsum adds a significant fraction of fines, which reduces the void ratio. The cementing process is generated from these fines, compared to naturally cemented sands forming calcium carbonate bonds at grain contact points as seen in pictures in Chapter 6. Portland cement also does not accurately depict the brittleness after cement bonds are broken. These problems should be looked into further, and should push future study in artificial cementation to look at more accurate methods of replicating cemented specimens.

7.3 SUMMARY

Carbonate sands have many differences from terrigenous sands. Cementation is one of many characteristics that separate the two. Cementation can vary in carbonate sands from cemented rock to completely uncemented soil, and even the types of cementation are different. Significant differences may exist between grain sharing and carbonate cemented bonds between grains. These differences affect the strength characteristics of the sand. Cementation was found to increase static strength, liquefaction resistance, and cone tip resistance. It was also found to lower the sleeve friction on the mini-cone.

Angularity not only has a lot to do with the strength characteristics, but also with cementation. SEM photography showed cement bonds forming between connected grain contacts. As angularity increases, there are less grain to grain contacts. It is unclear if

this reduces the cementation or if perhaps the cement bonds between those grains becomes stronger.

Use of the SEM is an important tool in the study of cementation. The clarity of cementation on grain to grain contacts was exceptional and adds a valuable asset to research project of this type. It showed differences in cementing between the two sands, as well as layering of cement on grains aged for 60 days. It appeared to verify Semple's (1988) statement that in the absence of a cementing agent, grains can bond together through material sharing. It can also be used to determine mineralogy of the grains and the cement bonds. It is suggested that the SEM be used to look at the bonds between specimens artificially cemented with Portland cement to determine if the cement is filling in voids or speeding up cementation at contact points.

The "naturally" cementing process as described in this study is not actually representative of the natural environment. Carbonate sands are found in salt water and possibly in a calcite or aragonite solution. Distilled water can take away some of the fines and calcium carbonate used to bond grains together without adding back in the same solution. Future research should be conducted to find a suitable way to replicate the cementation of calcareous soils in the laboratory to give the best possible answers to problems in the field.

REFERENCES

- Angemeer, J. and McNeilan, T. W. (1982). "Subsurface Variability—The key to Investigation of Coral Atoll," *Geotechnical Properties, Behavior, and Performance of Calcareous Soils*, ASTM Special Technical Publication 777, pp. 36-53.
- Beringen, F. L., Kolk, H.J., and Windle, D. (1982). "Cone Penetration and Laboratory Testing in Marine Calcareous Sediments," *Geotechnical Properties, Behavior, and Performance of Calcareous Soils*, ASTM Special Technical Publication 777, pp. 179-209.
- Campanella, R. G., Robertson, P. K., and Gillespie, D. (1986). "Seismic Cone Penetration Test," *Use of In Situ Tests in Geotechnical Engineering*, Geotechnical Special Publication No. 6, pp 116-130.
- Clough, W., Iwabuchi, J., Rad, N. R., and Kuppusamy, T. (1989). "Influence of Cementation on Liquefaction of Sands," *Journal of Geotechnical Engineering*, Volume 115, No.8, August 1989.
- Coop, M. R., and Atkinson, J. H. (1993). "The Mechanics of Cemented Carbonate Sands," *Geotechnique* 43, No. 1, pp. 53-67.
- Currie, P. K., Cuckson, J., and Jewell, R. J. "Testing of Chemically Stabilized Calcareous Material," *Engineering for Calcareous Sediments Volume 2*. Jewell and Korshid (eds.), Balkema, Rotterdam, pp. 587-595.
- Datta, M., Gulhati, S. K., and Rao, G. V., "Engineering Behavior of Carbonate Soils of India and Some Observations on Classification of Such Soils," *Geotechnical Properties, Behavior, and Performance of Calcareous Soils*, ASTM Special Technical Publication 777, pp. 113-140.
- Fahey, M. (1993). "Selection of Parameters for Foundation Design in Calcareous Soil," Research Report No. G1077. The University of Western Australia.
- Flynn, W. (1997). "A Comparative Study of Cyclic Loading Responses and Effects of Cementation on Liquefaction Potential of Calcareous and Silica Sands," Master's Thesis, Department of Civil Engineering, University of Hawaii.
- Huang, J. T. and Airey, D. W. (1991). "The Manufacture of Cemented Carbonate Soils," Research Report No. R631. The University of Sydney.
- Ismail, M.A., Joer, H. and Randolph, M. F. (1998). "Sample Preparation Technique for Artificially Cemented Soils," Research Report No. 1337. The University of Western Australia, Department of Civil Engineering, Geomechanics Group.

- Joer, H.A, Jewell, R.J., and Randolph, M.F. (1997). Cone Penetrometer Testing in Calcareous Sediments. Research Report No. G1289. The University of Western Australia.
- Lee, H. J. (1982). "Bulk Density and Shear Strength of Several Deep-Sea Calcareous Sediments," *Geotechnical Properties, Behavior, and Performance of Calcareous Soils*, ASTM Special Technical Publication 777, pp. 54-78.
- McClelland, Bramlette (1988). "Calcareous Sediments: an Engineering Enigma," *Engineering for Calcareous Sediments Volume 2*. Jewell and Korshid (eds.), Balkema, Rotterdam, pp. 777-784
- Morioka, B. T. and Nicholson, P. G. (1999). Evaluation of the Static and Cyclic Properties of Calcareous Sands in a Calibration Chamber Study," Department of Civil Engineering Research Report, University of Hawaii.
- Perlea, Vlad G. (2000). "Liquefaction of Cohesive Soils," *Soil Dynamics and Liquefaction 2000*. R. Y. S. Pak and J. Yamamura, Eds., pp. 58-76.
- Poulos, H. G. (1988). *Marine Geotechnics*. Unwin Hyman Ltd, London, UK, pp 74-76.
- Poulos, H. G. (1989). "The Mechanics of Calcareous Sediments." Research Report No. 595. The University of Sydney.
- Price, Graham P. (1988). "Fabrics of Calcareous Sediments at North Rankin 'A', Northwest Shelf," *Engineering for Calcareous Sediments Volume 2*. Jewell and Korshid (eds.), Balkema, Rotterdam, pp.367-376.
- Renfrey, G. E., Waterton, C. A. and van Gondever, P. (1988). Geotechnical Data used for Design of the North Rankin 'A' Platform Foundation," *Engineering for Calcareous Sediments Volume 2*. Jewell and Korshid (eds.), Balkema, Rotterdam, pp 409- 428.
- Rad, N. S. and Tumay, M. T. (1986). "Effect of Cementation on the Cone Penetration Resistance of Sand," *Use of In Situ Tests in Geotechnical Engineering*, Geotechnical Special Publication No. 6, pp 926-948.
- Rad, N. S. (1982). "Static and Dynamic Behavior of Cemented Sands," Thesis Submitted in Partial fulfillment of Ph.D. to Stanford University, Stanford, California.
- Seed, H. B. and Idriss, I. M. (1982). *Ground Motions and Soil Liquefaction During Earthquakes*, Earthquake Engineering Research Institute. El Cerrito, CA.

Semple, R. M. (1988). "The Mechanical Properties of Calcareous Sediments,"
Engineering for Calcareous Sediments Volume 2. Jewell and Korshid (eds.),
Balkema, Rotterdam, pp 807-836.

Stearns, H. T. (1966). *Geology of the State of Hawaii*. Pacific Books, Palo Alto,
California.